

© 2007 Sean Robert Nowling

CONFORMAL FIELD THEORY DESCRIPTIONS OF STRING  
INITIAL CONDITIONS AND QUANTUM ENTANGLEMENT  
ENTROPY

BY

SEAN ROBERT NOWLING

B.S., Purdue University, 2001

M.S., University of Illinois at Urbana-Champaign, 2004

DISSERTATION

Submitted in partial fulfillment of the requirements  
for the degree of Doctor of Philosophy in Physics  
in the Graduate College of the  
University of Illinois at Urbana-Champaign, 2007

Urbana, Illinois

Doctoral Committee:

Sheldon Katz, Chair  
Robert Leigh  
George Gollin  
John Stack

# Abstract

Although there has been much progress in string theory, most of the efforts have been focused on particle physics applications. To that end, string theory is usually studied with a non-compact four dimensional Minkowski manifold, while almost nothing is known about how to deal with time-dependence in string theory. Similarly, initial conditions in string theory remain largely out of reach. In part one of this thesis, a toy model for a big-bang like initial singularity will be constructed and a proposal will be made for the construction of initial conditions in string theory in the presence of cosmological singularities.

We shall review the construction of a  $\mathbb{Z}_2$  orbifold in closed string theory, with special attention to the differences between field theories and string theories in this background. Then we shall discuss the behavior of open string theories in such a background. While studying the allowed open string boundary interactions in the presence of a singularity, we will be led to novel cosmological initial conditions for closed strings. This part will close with a discussion about the late time effects expected from these initial conditions.

Quantum theories are filled with predictions which defy any classical analog. Perhaps the phenomenon which is most bizarre from a classical perspective is entanglement. This effect is the driving force behind the growing interest in quantum information. From entanglement, one is naturally led to the concept of entanglement entropy as a measure of the maximal amount of information which can be stored in a system. We shall begin the second part of this thesis by reviewing the role of entanglement entropy in quantum mechanics and in  $1 + 1$  dimensional quantum field theories. We shall then discuss entanglement entropy for Chern-Simons gauge theories, which is of direct interest in theoretical constructions of topological quantum computers.

*to Elizabeth, Mom, Dad, and Michael*

# Acknowledgements

I want to thank my wife Elizabeth, for keeping my spirits high, for always being supportive no matter how many dimensions I have traversed, and for always helping me to keep touch with the "real world." But most importantly, thank you for for being my greatest friend.

I would like to express my gratitude to my advisor Robert Leigh, for acquainting me with a wide view of theoretical physics, for always being available to talk about physics or anything else, and finally for patiently listening to my rambling ideas no matter how crazy they may have been.

I would like to thank my parents and brother, who started me on this path long ago and have always been supportive no matter how many neutrinos I might find. I would like to thank Grandma and Grandpa Nowling, Nanaw and Papaw Simpson, and all of my aunts and uncles for always encouraging my endeavors no matter how crazy they may have seemed.

I would like to thank thank my many instructors, both in and out of the classroom. I would like to thank Jerry Williams, the worlds greatest winner, for showing me the importance of optimism.

I would like to thank my many wonderful officemates: Vishnu Jejjala, Rahul Biswas, Josh Guffin, Floren Bora, Shiyong Dong, Nam Nguyen, and Juan Jottar. Thank you for being sounding boards, collaborators, and always being willing to help waste time.

Thank you to Eric Sharpe, Rich Corrado, and Mohammad Edalati for bringing your new ideas and perspectives.

Thank you to my collaborators Eduardo Fradkin, Esko Keskki-Vakkuri, and Shinsuke Kawai. A final extra thank you to Shiyong Dong for the use of her wonderful figures.

This work was supported by the United States Department of Energy under contract DE-FG02-91ER40709.

# Table of Contents

<b>List of Figures</b> . . . . .	<b>vii</b>
<b>Chapter 1 Introduction</b> . . . . .	<b>1</b>
1.1 String Theory . . . . .	1
1.1.1 Perturbative String Theory . . . . .	1
1.1.2 String Theory Near Singularities . . . . .	2
1.1.3 String Theory Near Cosmological Singularities . . . . .	3
1.2 Entanglement Entropy . . . . .	4
<b>Chapter 2 Closed String Description of a Time-dependent <math>\mathbb{Z}_2</math> Orbifold</b> . . . . .	<b>5</b>
2.1 Introduction and Summary . . . . .	5
2.2 Overview of $\mathbb{R}^{1,d}/\mathbb{Z}_2$ . . . . .	7
2.3 Backreaction in Quantum Field Theory . . . . .	10
2.4 The String Theory Calculation . . . . .	13
2.4.1 One-loop Graviton Tadpole . . . . .	14
2.4.2 The Generating Functional on $\mathbb{R}^{1,d-1}$ . . . . .	15
2.4.3 The Generating Functional on Orbifolds . . . . .	16
2.4.4 One-loop Graviton Tadpole on the Orbifold . . . . .	18
2.5 Chapter Summary . . . . .	20
<b>Chapter 3 Open Strings in <math>\mathbb{Z}_2</math> Background and Closed String Initial Conditions</b> . . . . .	<b>21</b>
3.1 Rolling Tachyon CFT in $\mathbb{Z}_2$ Background . . . . .	21
3.2 Boundary CFT of a Free Boson . . . . .	22
3.2.1 The Free Orbifold Theory . . . . .	24
3.2.2 Chan-Paton Factors . . . . .	25
3.3 Adsorption and Open String Partition Functions . . . . .	27
3.3.1 Boundary Deformations . . . . .	27
3.3.2 The Adsorption Method . . . . .	28
3.4 Fermionic Representation . . . . .	30
3.4.1 Fermionic Action . . . . .	30
3.4.2 Solutions to Fermionic EOM . . . . .	33
3.4.3 Boundary States at $R = \infty$ . . . . .	35
3.4.4 Projection to Generic Radii . . . . .	36
3.5 The $\mathbb{Z}_2$ Orbifold . . . . .	41
3.5.1 Self-dual Radius and Adsorption . . . . .	41
3.5.2 Fermionic Description of the Orbifold . . . . .	42
3.5.3 Summary of Open String Partition Functions . . . . .	45

<b>Chapter 4</b>	<b>S-branes in the Presence of a Time-Dependent Orbifold</b>	<b>47</b>
4.1	The Boundary State Interpretation	47
4.2	Back to the Lorentzian Signature	52
4.3	Conclusions and Outlook	56
<b>Chapter 5</b>	<b>Entanglement Entropies in Quantum Field Theories</b>	<b>58</b>
5.1	Entanglement	58
5.1.1	Entanglement Entropy	59
5.1.2	Field Theory Systems	60
5.2	<i>AdS/CFT</i> Description of Entanglement Entropy	65
5.2.1	<i>AdS/CFT</i>	65
5.2.2	Entanglement in $AdS_3$ Space	66
<b>Chapter 6</b>	<b>Entanglement Entropy in Chern-Simons Theories</b>	<b>69</b>
6.1	Introduction	69
6.2	Entanglement Entropy and Chern-Simons Gauge Theory	71
6.3	Explicit Entropy Computations	73
6.3.1	Surgery Properties	73
6.3.2	Entanglement Entropy on $S^2$ with One A-B Interface	77
6.3.3	Entanglement Entropy on $T^2$ with One Component A-B Interface	78
6.3.4	Entanglement Entropy on $S^2$ with Two-Component AB Interface	80
6.3.5	Entanglement Entropy on $T^2$ with Two-Component AB Interface	82
6.4	General Case	85
6.5	Conclusions	90
<b>Appendix A</b>	<b>Introduction to Conformal Field Theory and Chern-Simons Theory</b>	<b>92</b>
A.1	Conformal Field Theory	92
A.2	Basic Structure	92
A.3	Orbifolds	96
A.4	WZW Models	97
A.5	Boundary Conformal Field Theories	99
A.6	Chern-Simons Theory	101
A.7	Summary of Perturbative Renormalization	102
A.8	Connections with WZW Theories	102
<b>Appendix B</b>	<b>Tadpole Computations</b>	<b>105</b>
<b>Appendix C</b>	<b>Open String Partition Function Sums</b>	<b>108</b>
<b>Appendix D</b>	<b>Detailed Free Field Theory Entropy Calculations</b>	<b>110</b>
D.1	Free Boson	110
D.2	Free Fermion	112
D.3	Evaluation of Sums	114
<b>References</b>		<b>117</b>
<b>Author's Biography</b>		<b>124</b>

# List of Figures

2.1	The orbifold $\mathbb{R}^{1,1}/\mathbb{Z}_2$ . Also depicted are some identified points and resulting closed timelike curves. . . . .	7
2.2	Three possible time-arrows on the quotient $\mathbb{R}^{1,1}/\mathbb{Z}_2$ . . . . .	8
2.3	A view of the quotient spacetime (for 1+1 dimensions). Note the absence of the $x = 0$ axis for $t < 0$ . . . . .	9
2.4	Another view of the quotient spacetime (for 1+1 dimensions). Note the absence of the $t = 0$ axis for $x < 0$ . The $t = 0$ axis represents a “big bang” singularity—the beginning of the spacetime. . . . .	9
2.5	The CTC’s of Fig. 2.1 are not forward oriented in the quotient. . . . .	10
2.6	Correlator of point-split composite operator. The ‘short’ contractions, between $x$ and $x'$ are the usual short-distance ones, and should be subtracted. The ‘long’ contractions give rise to the Casimir energy. . . . .	12
4.1	The pre-Big Bang scenario (a), and the creation of two-branched Universe from the Big Bang, which is interpreted as a spacetime $\mathbb{Z}_2$ orbifold (b). . . . .	48
4.2	Untwisted closed string emission in the covering space. . . . .	54
4.3	The double HH contour in the covering space. . . . .	55
5.1	The field takes different values on either side of the cut in the $A$ region. . . . .	62
5.2	After gluing $\rho_A^n$ together the $A$ system lives on a circle of size $n\beta$ whereas the $n$ $B$ regions each live on circles of size $\beta$ . . . . .	63
5.3	The result of mapping the $n$ -sheeted geometry to a single sheet . . . . .	63
5.4	Boundary operators in $AdS_3/CFT_2$ . . . . .	67
6.1	A general $m$ -handled surface. Red lines are the Wilson loops. Different states are generated by the choice of Wilson line’s representation. . . . .	73
6.2	Shading implies a 3-d solid ball. This can be made by rotating a disk about an axis passing the origin, as shown at right. . . . .	77
6.3	The overall manifold is generated by four pieces of disks glued together one after another and rotated along the same axis as in Fig. 6.2. . . . .	78
6.4	The solid torus with A B regions indicated as on the LHS is topologically the same as a solid 3-ball with a solid torus “planted” in the A region. . . . .	79
6.5	The two red circles indicate the two cycles. . . . .	79
6.6	Two component interface on spatial sphere. The notation is the same as in Fig. 6.2. . . . .	80
6.7	The red lines form a cycle. . . . .	81

6.8	Two parts of the A region are connected through a disk, and when we glue $2n$ copies of A pairwise, they become $n$ two-spheres.	81
6.9	Two of the ways to cut torus using two interfaces. The RHS one is a solid torus with the surface cut into two pieces bearing the same topology. . . . .	82
6.10	The red line forms 3 cycles when connected with the 3 green lines.	83
6.11	Two solid balls connecting each other through two solid cylinders, with or without Wilson loop. . . . .	83
6.12	The two rows form two $S^3$ separately. They are connected through the region with the same colors along a $S^2$ tube. . . . .	84
6.13	A representative example of the general case. Here the A and B regions are each connected and are separated by a 3-component interface. In the case shown, A and B are connected. Wilson loops are shown in red for a choice of basis 1-cycles. . . . .	85
6.14	Inequivalent choices of cutting into A and B regions when there is a 3-component interface. They have 2, 1, 0, 0 cycles shared by A and B ( <i>i.e.</i> , in the set $\{c_k\}$ ). . . . .	86
6.15	The space shown in Fig. 6.14 after 'squeezing'. The components of C are connected to each other either by a $D^2$ or $D^2$ with a puncture. . . . .	86
6.16	A more complicated example, with a Wilson line cut into four pieces. . . . .	88
A.1	Cycles on a torus . . . . .	96

# Chapter 1

## Introduction

### 1.1 String Theory

The 20<sup>th</sup> century saw the emergence of two successful frameworks for theoretical physics. First was the development of general relativity, explaining most of the large scale properties of the universe. Second came the development of quantum theories, capable of explaining all known microscopic events.

In fact, it is the great success of these two theories which lies at the heart of one of the great mysteries in modern physics, why are these two theories individually successful when their marriage is an apparent disaster. Any direct quantization of gravity leads to a nonsensical theory with no regulator independent meaning.

However, the great successes of relativity gives us hope that it must, at least on large distances, be the correct effective theory. Using this as a guide, one seeks an appropriate ultraviolet completion of general relativity, which preserves the infrared behavior. Note that this theory need not be a field theory, despite the field theoretic character of general relativity. In fact, it just this role, as an ultraviolet completion, which string theory plays.

#### 1.1.1 Perturbative String Theory

Qualitatively, the extended nature of a string naturally smoothes out the singular ultraviolet behavior of "quantum general relativity." The resulting theory, in its current formulation, is not a quantum field theory with particle excitations, but a first quantized theory of strings.

String perturbation theory is formulated as a sum over 2 dimensional conformal field theories on Riemann surfaces of different genus:

$$Z \sim \sum_g Z_g \tag{1.1}$$

$$Z_g = \int [dX] e^{iS_p} \tag{1.2}$$

$$S_p = \frac{1}{4\pi\alpha'} \int d^2x h^{\alpha\beta} G_{\mu\nu}(X) \partial_\alpha X^\mu \partial_\nu X^\nu. \tag{1.3}$$

Here, the two dimensional surfaces describe the worldsheet swept out in space-

time by the propagating string. The fields  $X^\mu(x)$  describe the embedding of the string worldsheet into spacetime. The low energy spectrum of this theory includes a massless scalar (the dilaton), a massless symmetric and traceless two tensor (the graviton), and a massless 2-form (the Kolb-Ramond field). Supersymmetric generalizations of this theory also predict chiral fermions in the spacetime theory.

Shockingly, when the low energy scattering behavior of string theory is analyzed, we obtain an effective gravitational field theory with gauge fields, form fields, and chiral fermions. In fact, one may view the infinite set of higher string modes and effective couplings as providing the infinite number of terms necessary to define the nonrenormalizable quantum field theory of "general relativity." All this has led people to label string theory as a "theory of everything." It is important to emphasize that, while low energy string theory is consistent with a point particle field theoretic description, it is not a string field theory, whose quanta would necessarily describe the creation of strings in spacetime.

The above strings come in two classes, open and closed. Closed string theories contain gravitational physics, while open strings encode gauge degrees of freedom. When studying open string theories, one must impose boundary conditions at the worldsheet's edges. The study of allowed boundary conditions naturally leads one to study D-branes.

### 1.1.2 String Theory Near Singularities

The low energy effective action of string theory,

$$S_{ST} = \frac{1}{g_s^2 \alpha'} \int d^4x (R + \alpha' R^2 + \dots) + \frac{1}{\alpha'} \int d^4x (c_1 R + c_2 \alpha' R^2 + \dots) + \dots \quad (1.4)$$

is a double expansion, with powers of the string tension,  $\alpha'$ , corresponding to a curvature expansion in units of the string length, while the string coupling constant,  $g_s$ , counts the number of loops in the string worldsheet expansion. This picture is satisfactory if the classical curvature is large with respect to  $(\alpha')^{-1}$  and the energies are low enough so that amplitudes are dominated by diagrams containing a small number of loops.[1] However, near a classical cosmological singularity, it is not clear that the  $g_s$  expansion is reliable and the  $\alpha'$  expansion almost certainly fails. One must doubt the reliability of this type of low energy effective action. In fact there are known examples of static classically singular spacetimes, which are only sensible upon the inclusion of the full set of string theoretic modes.

Orbifolds are constructed as the quotient of a smooth spacetime by a discrete symmetry. If the quotient has fixed points, one is led to spacetime singularities. Typically, there is no sensible way of defining field theories in orbifold spacetimes. Fields at the singularity are described by multiple coincident fields in the covering space. The standard divergent short distance behavior of field theories

becomes problematic at an orbifold spacetime's singularity.

However, string theories often are sensible in such spacetimes. Even classically, one finds new string modes localized at the singularity, which improve the theory's behavior. These new modes, or twisted states, highlight purely stringy physics. This pattern extends to all known static singularities which are sensible within string theory. One always finds new string states localized at the classical singularity which "resolve" the singularity. [1]

### 1.1.3 String Theory Near Cosmological Singularities

The possibility of cosmological singularities provides new challenges which simply do not exist in static spacetimes. Because string theory is a first quantized theory, by construction, it is appropriate only when one is interested in scattering experiments. This assumes one may sensibly define asymptotic "in" and "out" states.

One immediately runs into a problem near cosmological singularities. Near the singularity, the gravitational physics is not expected to be weakly coupled. It does not seem that one can use a Fock space basis to describe the theory's states. If no single particle states may be defined at the singularity, one needs a prescription for how to define an S-matrix in this singular spacetime.

In the literature, a common approach is the "pre-big bang" construction, where one continues the spacetime to times earlier than the big bang. The difficulty with this approach is that it assumes one may correctly extrapolate to all physics before the singularity, a region which, a priori, one has no way to probe.

However, at least in the presence of a singularity formed from a time dependent reflection orbifold, one could use the notion of an  $S$  matrix inherited from the covering space. In the quotient space, this is like defining the theory by implementing late time boundary conditions. The whole construction is quite analogous to the "out-out" formalism described in [2]. In chapter 2 of this thesis we shall revisit this construction in detail, describing the propagation of first quantized strings in a time-dependent orbifold spacetime.

Given that one may consistently describe string propagation near cosmological singularities by choosing appropriate asymptotic conditions, there is another issue. How do we consistently source strings near the singularity? In string theory the role of a quantum source is played by D-branes, so one needs to find a description of spacelike branes, or S-branes, localized at the singularity. In chapters 3 and 4 of this thesis we shall explicitly construct the worldsheet description of S-branes. In the process, we shall be led to new conformal field theory boundary states describing a new family of "fractional S-branes." These branes play the role of string sources in the presence of a time-dependent orbifold singularity.

## 1.2 Entanglement Entropy

Quantum theories are filled with predictions which defy any classical analog. Perhaps the phenomenon which is most bizarre from a classical perspective is entanglement. This effect has its origin in the tensor product nature inherent in the Hilbert space of many body quantum mechanics. As a measure of the amount of entanglement, one is naturally led to the notion of the von Neumann entanglement entropy.

In field theory, interest in entanglement entropy began with attempts to determine the microscopic origin of the Bekenstein-Hawking black hole entropy formula,

$$S_{BH} \sim \frac{\text{Area}}{4G_N}. \quad (1.5)$$

Unfortunately, this hope has remained unrealized in practice. In higher dimension, the entanglement entropy is typically not a universal quantity, depending upon the choice of regulator.

An unrelated interest in entanglement entropy lies in the growing field of quantum information theory. In this context, entanglement naturally becomes a measure of the maximal amount of information which can be stored in a system.

We shall begin the second part of this thesis by reviewing the role of entanglement entropy in quantum mechanics and in  $1 + 1$  dimensional quantum field theories. We shall explicitly verify, in  $1 + 1$  dimensions that entanglement entropy may be a universal quantity.

We shall then discuss entanglement entropy for Chern-Simons gauge theories, which is of direct interest in studies of the fractional quantum Hall effect.

## Chapter 2

# Closed String Description of a Time-dependent $\mathbb{Z}_2$ Orbifold

### 2.1 Introduction and Summary

A technical obstacle in exploring string theory in time-dependent space-times is to find suitable backgrounds where string quantization is tractable. Early work includes [3, 4, 5, 6, 7, 8]. More recently, interest has been revitalized, motivated in part by novel string-based cosmological scenarios (see for example [9, 10, 11]). An obvious path to follow was to construct such backgrounds as time-dependent orbifolds of Minkowski space [12, 13, 14, 15, 16, 17, 18, 19] or anti-de Sitter space [20, 21, 22]. Further related work includes [23, 24, 25, 26, 27, 27, 28, 29, 30, 31, 32]. However, depending on how the orbifold identifications are defined, potentially dangerous issues may arise. The resulting time-dependent orbifolds can have regions with closed time-like curves (CTCs) or closed null curves (CNCs), or may not even be globally time-orientable. Therefore, one could choose to first make a list of desirable features for the orbifolds and then try to limit the study only to those backgrounds that possess those features. This sensible strategy was laid out and pursued by Liu, Moore and Seiberg [16, 17]. For orbifolds of type  $\mathbb{R}^{1,3}/\Gamma$  where  $\Gamma$  is a discrete subgroup of the Poincaré group, the list turned out to be very short containing only null brane theories. However, the null brane construction involves identifications by arbitrarily large boosts. This turns out to be another potential reason for instabilities, and it was argued by Horowitz and Polchinski [18] that such backgrounds become unstable after just a single particle is added, because on the covering space the particle can approach its infinitely many images with increasingly high momenta and produce a black hole. Additional discussion of potential problems can be found in [33, 17, 27].

If no field theory is well defined near orbifold singularities, it is important to understand if and/or why string theory actually has problems with these features. The reason for demanding that there be no regions containing closed time-like curves appears obvious. Classically, CTCs violate causality, and quantum mechanically, coherence and unitarity come into question. It has been conjectured by Hawking [34] that the laws of physics prevent CTCs from appearing if they do not exist in the past. The arguments in support of this chronology protection conjecture (CPC) are usually based on general relativity

plus matter at the classical or semiclassical level. A recent summary can be found in [35]. Essential features are that perturbations can keep propagating around a CTC so that backreaction accumulates, or quantum effects can lead the matter stress tensor to diverge at the boundary of the CTC region, leading to infinite backreaction. However, the trouble with CTCs and CNCs seems to arise from propagation along them, rather than merely from their existence. It is not clear if the two are equivalent. For example, the model studied in [12] involves CTCs and CNCs, but it was argued that they do not necessarily pose a problem in quantum mechanics if one can project to a subspace of states which do not time evolve along the CTCs and CNCs. Another desirable feature on the list was time-orientability. This was included to avoid problems in defining an S-matrix, and problems associated with the existence of spinors [36, 37, 38]. However, the consequences of a lack of time-orientability have not yet been subject to extensive investigation and are thus less well understood. From the point of view of local physics, one might wonder if the whole Universe could be globally time-nonorientable, but in such a way that the global feature could only be detected by meta-observers and never be revealed by local experiments. The orbifold studied in [12] is an example of a spacetime which is globally time-nonorientable. In any case, its structure appears to allow for a definition of an S-matrix for local experiments.

To summarize, there are many reasons to investigate the chronology protection conjecture and time-nonorientability. We also note that recently the former topic has been investigated from other points of view in the context of string theory and holography [39, 40, 41, 42, 43]. The  $\mathbb{R}^{1,d}/\mathbb{Z}_2$  orbifold, obtained by identifying points  $X$  with reflected points  $-X$ , provides a simple model which incorporates both issues. Some comments were made in passing in [12]. In this chapter we perform a more detailed investigation.

The orbifold is also relevant for the elliptic interpretation of de Sitter space ( $dS$ ) [44, 45, 46, 47]. A  $d$ -dimensional de Sitter space is a time-like hyperboloid embedded in  $\mathbb{R}^{1,d}$ . The  $\mathbb{Z}_2$  reflection on  $\mathbb{R}^{1,d}$  induces an antipodal reflection on the  $dS$  spacetime. The elliptic de Sitter space  $dS/\mathbb{Z}_2$  is then defined by identifying the reflected antipodal points.

The identification leads to various problems in quantum field theory. Previous studies of the elliptic  $dS$  spacetime have discussed problems in defining a global Fock space in the global patch; however, it was possible to construct QFT and a Fock space by restricting to the static patches of observers at the (identified) north and south poles. The same problem is encountered in trying to formulate QFT on  $\mathbb{R}^{1,d}/\mathbb{Z}_2$ . Moreover, there is a question of whether the orbifold is an unstable background. One can present a quick semiclassical derivation of the stress energy and find that it diverges; for example in the case of a massless scalar field one obtains a divergence in the lightcone emanating from the origin.

We also study the backreaction at one-loop level in string theory. We cal-

culate the one-loop graviton tadpole in the  $\mathbb{R}^{1,d}/\mathbb{Z}_2$  background, and show that the answer is the same as if the background were just  $\mathbb{R}^{1,d}$ ! While the answer first appears puzzling, it is very analogous to what happens in Euclidian orbifolds. This leads one to believe string theory in this singular space-time is sensible, while any straight forward field theory analysis fails. In [48] a field theory description was found, but it required the introduction of a "copy" set of fields. This was taken to be consistent with the analysis of  $dS/\mathbb{Z}_2$ , where the zero curvature limit has been identified with two copies of Minkowski space [47].

We have organized the chapter as follows. In Section 2.2, we review some features of the time-dependent orbifold background introduced in [12], and focus on some novel features of these orbifolds. In particular, we point out that a choice of time orientation must be made. In Section 2.3, we review the (naïve) analysis of the gravitational back reaction in this geometry. In Section 2.4, we ask if string theory can do better, and present similar calculations in string theory (complementary calculations in a different formalism are shown in D). We find that the result differs significantly from the naïve QFT analysis.

## 2.2 Overview of $\mathbb{R}^{1,d}/\mathbb{Z}_2$

Let us first review some features of the  $\mathbb{R}^{1,d}/\mathbb{Z}_2$  orbifold [12]. We begin with the covering space  $\mathbb{R}^{1,d}$  and identify the time and space coordinates under the reflection

$$(t, x^a) \sim (-t, -x^a) . \quad (2.1)$$

The resulting orbifold is a space-time cone, depicted in Figure 2.1 for  $d = 1$ . Points in the opposite quadrants (I and III, and II and IV) are identified. Orbifolds that act purely spatially are familiar and are certainly well under-

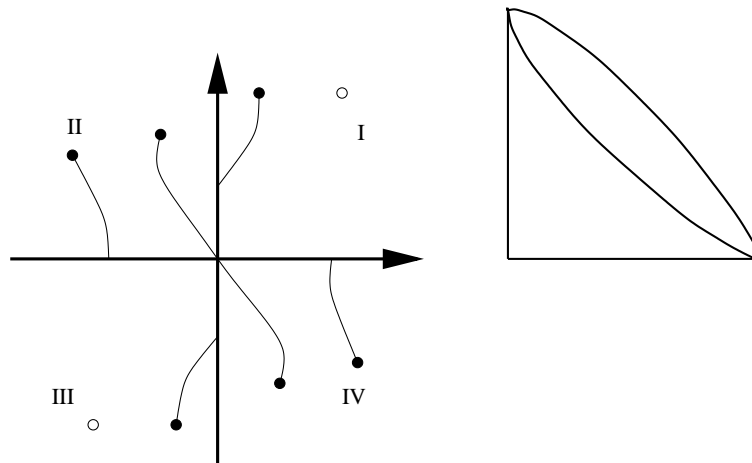


Figure 2.1: The orbifold  $\mathbb{R}^{1,1}/\mathbb{Z}_2$ . Also depicted are some identified points and resulting closed timelike curves.

stood. New problems arise when the identification involves the time direction; for example it is not guaranteed that the string spectrum will be free from tachyons and ghosts. Ref. [12] investigated bosonic and type II superstrings on  $\mathbb{R}^{1,d}/\mathbb{Z}_2 \times \mathbb{R}^n$ , with  $n$  additional spacelike directions added to bring the total spacetime dimension to 26 or 10. It was shown, using a Euclidean continuation, that although the background is time-dependent and quantization had to be done in the covariant gauge, the physical spectrum did not contain any negative norm states (ghosts), at least in a range of  $d$ . The superstring spectrum did not contain any tachyons and the one-loop partition function vanishes for the superstring.

In the case of the orbifold (2.1), we must ask how various quantities descend from the covering space to the orbifold. In particular,  $\partial/\partial t$  is manifestly not invariant under the group action, and so does not define a time's arrow, or time-like Killing vector, in the quotient. Thus, this orbifold leaves ambiguous the direction on which time flows in the quotient – we must manually make a choice of direction of time-flow.

Furthermore, the natural time orientation bundle on the covering space does descend to the quotient space, but (omitting the singularity at the origin) the class  $w_1(L)$  is non-trivial. Thus the image of  $L$  on the quotient is not time-orientable. Although locally we can choose a perfectly sensible notion of time orientation, this is not possible globally.

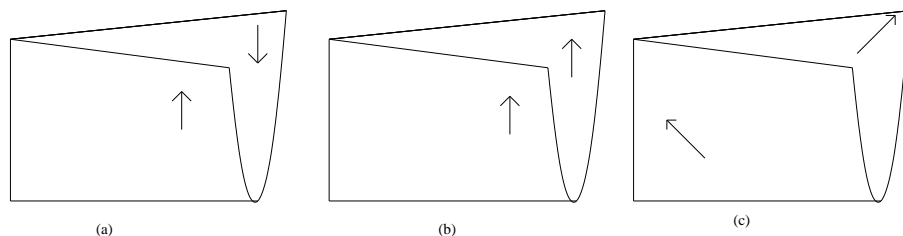


Figure 2.2: Three possible time-arrows on the quotient  $\mathbb{R}^{1,1}/\mathbb{Z}_2$ .

To illustrate, let us consider the case of  $\mathbb{R}^{(1,1)}/\mathbb{Z}_2$ . The obvious choice of time's arrow on the covering space  $\mathbb{R}^{1,1}$ , namely  $\partial/\partial t$ , is not invariant under the group action, a property which manifests itself in the observation that by picking different fundamental domains for the group action on the cover, the time's arrow in those fundamental domains restricts to a different time's arrow on the quotient.

In Fig. 2.2 we have shown three possible time-arrows that one can construct on  $\mathbb{R}^{1,1}/\mathbb{Z}_2$ . The left-most case corresponds to taking the fundamental domain to be regions I and IV, the middle case corresponds to taking the fundamental domain to be regions I and II, and the right-most case corresponds to taking the fundamental domain to be one side of a wall of the lightcone through the origin. In each case, omitting the origin, the time-orientation line bundle on

the quotient is not orientable ( $w_1(L) \neq 0$ ), hence each choice of time's arrow depicted in figure 2.2 has zeroes – in case (a), along the left vertical crease, and in case (b), along the bottom horizontal crease. Note that in each case it would also be possible to choose a reverse time orientation (reversed arrows). Then *e.g.* Fig. 2.2(b) would depict a “big crunch” rather than a “big bang.”

In Figure 2.3, we have drawn the quotient space corresponding to Fig. 2.2(a). In this case, there are asymptotic regions for both  $t \rightarrow \pm\infty$ . However, there is a topology change of constant  $t$  slices at  $t = 0$ . Another choice for the quotient

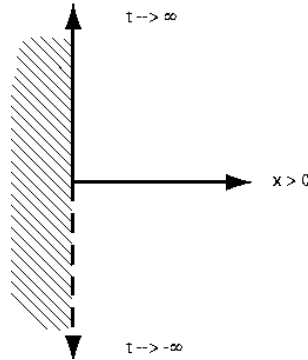


Figure 2.3: A view of the quotient spacetime (for 1+1 dimensions). Note the absence of the  $x = 0$  axis for  $t < 0$ .

space, corresponding to Fig. 2.2(b), is shown in Fig. 2.4. In this case, there is no asymptotic region corresponding to  $t \rightarrow -\infty$ . Instead, we have a “big

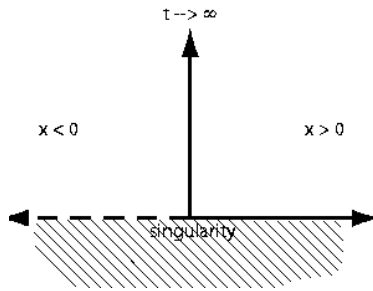


Figure 2.4: Another view of the quotient spacetime (for 1+1 dimensions). Note the absence of the  $t = 0$  axis for  $x < 0$ . The  $t = 0$  axis represents a “big bang” singularity—the beginning of the spacetime.

bang” singularity at  $t = 0$ . It is interesting to contemplate the properties of quantum field theory on such a spacetime. It is of even more interest to ponder the role of string theory. We will return to a more thorough discussion of these issues in a later section.

Let us also discuss the closed time-like curves in this geometry. In the covering space, with the natural choice of Minkowski time orientation, there are non-trivial forward oriented closed time-like curves. Examples are shown in

Fig. 2.1. It is clear from the figure that there are CTC's which begin at any spacetime point.

Consider however these curves in the quotient space (let us refer to the choice of time-orientation in Fig. 2.2(a) to be definite). In going to the quotient we make a choice of (local) time orientation which is not compatible with the time orientation of the covering space. As a result (and this is true for any choice), the CTC's that we identified in the covering space are *not forward oriented* in the quotient. The examples given in Fig. 2.1 are redrawn in the quotient in Fig. 2.5. In fact, the only CTC in the quotient must begin and end on the

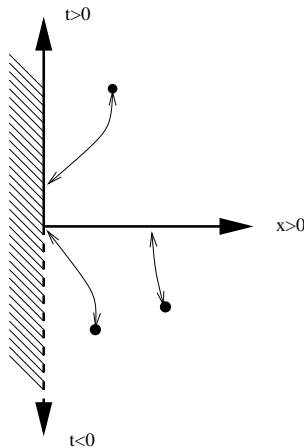


Figure 2.5: The CTC's of Fig. 2.1 are not forward oriented in the quotient.

singular axis (the curve can be constructed by a limiting procedure.)

Let us quickly review this discussion. In the Lorentzian orbifold, a choice of time orientation must be made in the quotient.<sup>1</sup> This gives rise to physically inequivalent spacetimes that are singular along an axis. The singularity is associated with an undefined time orientation. Whereas there were oriented CTC's through every point in the covering space, (almost) all of these are not forward oriented in the quotient. Next, we will consider quantum field theory on this background; we focus on the issue of back-reaction.

### 2.3 Backreaction in Quantum Field Theory

Here we give a short review of the standard QFT calculation for the vacuum expectation value (vev) of the stress tensor, which in general leads to a divergence hinting at an instability of the background. Later, we will contrast this with a calculation in string theory.

The gravitational backreaction from the renormalized stress energy of a

<sup>1</sup>It is not clear how this choice should be encoded in string theory.

quantum field may be evaluated semi-classically

$$G_{\mu\nu} = -8\pi G_N \langle T_{\mu\nu} \rangle_{ren}. \quad (2.2)$$

Here the subscript refers to the fact that one subtracts off the usual vacuum energy contribution — the curvature is well-defined if there are no divergences other than the usual flat space short distance singularities. In more detail [35], one defines the renormalized stress tensor starting from the two-point correlation function  $G(x, y)$  written in Hadamard form as a sum over geodesics  $\gamma$  from  $x$  to  $y$ . The expectation value of the point-split stress tensor can then be defined as

$$\langle T_{\mu\nu}(x, y, \gamma_0) \rangle = D_{\mu\nu}(x, y, \gamma_0)G(x, y), \quad (2.3)$$

where  $\gamma_0$  denotes the trivial geodesic from  $x$  to  $y$  which collapses to a point as  $y \rightarrow x$ , and  $D_{\mu\nu}(x, y, \gamma_0)$  is the second order differential operator associated with the action of the particular field in scrutiny. The renormalized stress energy  $\langle T_{\mu\nu}(x) \rangle_{ren}$  is defined by discarding the universal divergent piece arising from the contribution of the trivial geodesic to the Green function. That is, one replaces in (2.3) the Green function by the renormalized Green function, defined with the trivial geodesic excluded from the sum over geodesics:

$$G(x, y) = \sum_{\gamma} \dots \rightarrow G_{ren}(x, y) = \sum_{\gamma \neq \gamma_0} \dots, \quad (2.4)$$

and then removing the point-splitting regularization from (2.3) by taking the limit  $\lim_{y \rightarrow x}$ .

Let us then consider the  $\mathbb{R}^{1,1}/\mathbb{Z}_2$  orbifold and *e.g.* the stress energy of a free massless scalar field. The field decomposes into left- and right-movers. Let us focus on the right-movers only. The right-moving component of the stress tensor is

$$T_{uu}(u) =: \partial_u \phi(u) \partial_u \phi(u) :, \quad (2.5)$$

where  $u = t - x$ . To proceed as in the above, we start from the Minkowski space two-point correlation function

$$G(u, u') \sim -\ln(u - u'), \quad (2.6)$$

associated with the trivial geodesic from  $(u, v)$  to  $(u', v')$ . On the orbifold, the points  $(u, v)$  are identified with  $(-u, -v)$  and  $(u', v')$  identified with  $(-u', -v')$ . This gives arise to three additional geodesics (Fig. 2.6), so the two point function on the orbifold would be

$$G_{orb}(u, u') = G(u, u') + G(u, -u') + G(-u, u') + G(-u, -u'). \quad (2.7)$$

Subtracting off the trivial universal divergence, we then obtain the renormalized

stress energy

$$\begin{aligned} \langle \tilde{T}_{uu}(u) \rangle_{ren} &= \lim_{u' \rightarrow u} \partial_u \partial_{u'} \{ -\ln(u - u') - \ln(u + u') \}_{ren} \\ &= \lim_{u' \rightarrow u} \frac{1}{(u + u')^2} = \frac{1}{4u^2}. \end{aligned} \quad (2.8)$$

However, the result is divergent on the null line  $u = 0$ . The problem arises from the non-trivial geodesics which can also become zero length (see Fig. 2.6). A similar calculation for the left-movers yields a divergence at  $v = 0$ . Hence one concludes that the orbifold is potentially unstable. Similar calculations can be done in higher dimensions.

However, upon closer inspection the above argument has some puzzling features. If we want to associate the two-point function (2.7) with a field operator, the operator should be symmetric under the  $u \rightarrow -u$   $\mathbb{Z}_2$  reflection. A naive way to impose the invariance is to consider

$$\tilde{\phi}(u) = \frac{1}{\sqrt{2}}(\phi(u) + \phi(-u)). \quad (2.9)$$

Formally, one can check that the renormalized expectation value (2.8) is that of the  $\mathbb{Z}_2$  invariant field operator, with the four contributions associated with 'short' and 'long' contractions. However, this construction has various prob-

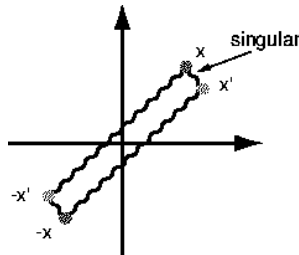


Figure 2.6: Correlator of point-split composite operator. The 'short' contractions, between  $x$  and  $x'$  are the usual short-distance ones, and should be subtracted. The 'long' contractions give rise to the Casimir energy.

lems. The most cumbersome one is that the  $\mathbb{Z}_2$  invariant field operator (2.9) has the mode expansion

$$\tilde{\phi}(u) = \sqrt{2} \int d\omega (a_\omega + a_\omega^\dagger) \cos(\omega u) \quad (2.10)$$

so it is not clear what exactly is meant by the naive notion of particles and vacuum. The problem of constructing a global Fock space is also well known from investigations of elliptic de Sitter space  $dS/\mathbb{Z}_2$  [44, 45, 46, 47]. In the above, the problem has been lifted onto  $\mathbb{R}^{1,d}/\mathbb{Z}_2$ , where the  $dS/\mathbb{Z}_2$  can be embedded.

Actually, it was argued in [48] that the  $\mathbb{Z}_2$  identification requires identifying a particle with positive energy at  $(t, x)$  with a particle with negative energy

at  $(-t, -x)$ . Particles of the latter kind cannot be created with  $a_\omega^\dagger$ . A quick look at the mode expansion of  $\phi(-u)$  might give a false impression that this would happen, but really  $\phi(-u)$  is just the field operator  $\phi$  evaluated at point  $-u$  rather than a new operator with the creation and annihilation operators acting in a different way. Another problem is that the usual prescription calls us to evaluate commutators of field operators at equal time. On the orbifold covering space this becomes problematic, since “equal time” now corresponds to times  $t$  and  $-t$ . For these reasons we should take a step back and reconsider the formulation of field theory on the  $\mathbb{R}^{1,d}/\mathbb{Z}_2$  orbifold. However, we will first examine if the divergence of the stress tensor persists in string theory. The result that we find will provide additional motivation to reconsider the formulation of field theory.

## 2.4 The String Theory Calculation

Our next goal is to calculate the backreaction on the orbifold at one-loop level in string theory. In practice, this is done by calculating the one-loop graviton tadpole.

If we write the metric tensor as  $g_{\mu\nu}(x) = \eta_{\mu\nu} + 2\kappa h_{\mu\nu}(x)$ , the vev of the stress tensor may be written [49]

$$\langle T_{\mu\nu} \rangle = -i \frac{\delta}{\delta g^{\mu\nu}} \ln Z_{EFT}^{2nd} |_{h^{\mu\nu}=0} = -\frac{i}{2\kappa} \frac{\delta Z_{1st}}{\delta h^{\mu\nu}} |_{h^{\mu\nu}=0} . \quad (2.11)$$

In the above, we used the relation between the vacuum amplitudes in the second quantized and first quantized formalism,  $Z_{2nd} = e^{Z_{1st}}$ , to replace the effective field theory action  $\ln Z_{EFT}^{2nd}$  by the point particle partition function  $Z_{1st}$ .

Now we replace point particles by strings. At one-loop level [50]

$$Z_{1-loop}^{ST}[g] = \int \frac{d\tau d\bar{\tau}}{4\tau_2} Z(\tau) = \int \frac{d\tau d\bar{\tau}}{4\tau_2} \int_{T^2} \mathcal{D}X e^{i\frac{\tau}{2} \int d^2w g_{\mu\nu}(X) \partial X^\mu \bar{\partial} X^\nu} . \quad (2.12)$$

This is then inserted in (2.11).<sup>2</sup> Suppressing the integral over  $\tau$ , we have

$$Z_{1-loop}^{ST} = \int \mathcal{D}X e^{i\frac{\tau}{2} \int d^2w \eta_{\mu\nu} \partial X^\mu \bar{\partial} X^\nu} \times \left\{ 1 + i \frac{g_{str}}{\alpha'} \int d^2w h_{\mu\nu}(X) \partial X^\mu \bar{\partial} X^\nu + \dots \right\} . \quad (2.13)$$

Now Fourier expand the perturbation,

$$h_{\mu\nu}(X) = \int \frac{d^{D+1}k}{(2\pi)^{D+1}} e_{\mu\nu}(k) e^{ik \cdot X} \quad (2.14)$$

and introduce

$$V_{\mu\nu}(k) = \partial X^\mu \bar{\partial} X^\nu e^{ik \cdot X} , \quad (2.15)$$

---

<sup>2</sup>This is somewhat reminiscent of a recent calculation in [51].

then

$$Z_{1-loop}^{ST}[g] = Z_{1-loop}^{ST}[\eta] + i \frac{g_{str}}{\alpha'} \int \frac{d^{26}k}{(2\pi)^{D+1}} \int d^2w e_{\mu\nu}(k) \langle V^{\mu\nu}(k; w) \rangle + \dots \quad (2.16)$$

We then get

$$\langle T^{\mu\nu}(x) \rangle = \frac{1}{4\pi\alpha'} \int \frac{d^{D+1}k}{(2\pi)^{D+1}} \int d^2w \langle V^{\mu\nu}(k; w) \rangle e^{-ik \cdot x} \quad (2.17)$$

the relation between the Fourier transformed tadpole and the stress tensor.

Note that in Minkowski space, one obtains

$$\langle V^{\mu\nu}(k) \rangle = - \left( \frac{g_{str}}{4\pi\tau_2} \right) \frac{\delta^{(D+1)}(\sqrt{\alpha'}k)}{V_{D+1}} \eta^{\mu\nu} Z_{1-loop} , \quad (2.18)$$

so that

$$\langle T_{\mu\nu} \rangle \sim \frac{1}{\alpha'^{13} V_{26}} Z_{1-loop} \times \eta_{\mu\nu} \quad (2.19)$$

which is of the right form for the stress tensor of a cosmological constant  $\Lambda \sim Z_{1-loop}$ .

On  $\mathbb{Z}_2$  orbifolds, the story is essentially similar. What is different in the string graviton tadpole calculation is that a) the relevant vertex operator must be  $\mathbb{Z}_2$  invariant: it is the sum of vertex operators carrying  $k$  and  $-k$  in the directions of the orbifold, and b) a priori there are contributions from the twisted sector strings. The fact a) suggests that the Fourier transform of the tadpole will be the sum

$$\langle T_{\mu\nu}(X) \rangle + \langle T_{\mu\nu}(-X) \rangle, \quad (2.20)$$

where  $X$  are the coordinates along the orbifold directions. This could be obtained from the effective action by including the functional differentiation  $\delta/\delta h_{\mu\nu}(-X)$ . We will return to these issues when we discuss the reformulation of QFT. Let us first proceed with the calculation of the tadpole.

### 2.4.1 One-loop Graviton Tadpole

Now we proceed to give some of the details of the calculation of the one-loop graviton tadpole in string theory described above. Our calculations are based on the functional method. We begin with a brief review of the latter, following [50]. As it turns out, an immediate difference with tadpole calculations on Euclidean orbifolds is in kinematics and in appropriate choice of polarization of vertex operators. We have also performed the same calculations in the oscillator formalism. It also turns out that there are some interesting subtleties and differences with the standard discussion; detailed notes may be found in the appendix.

We should note that in the string computations, one usually performs a Wick rotation in both spacetime and worldsheet, necessary for formal convergence. If

the target space is time-dependent, the standard techniques of analytic continuation may not be applicable.<sup>3</sup> In the context of the  $\mathbb{R}^{1,d}/\mathbb{Z}_2$  orbifold, the issue was already noted in [12]. In the present chapter, we simply adopt the same strategy as in [12], namely we formally continue the worldsheet to Euclidean signature in the calculations to obtain an expression for the tadpole. As well, we will encounter zero-mode integrations whose values are defined by a space-time Euclidean continuation. The result is apparently well-defined and in a later section, we search for a field theory formalism that is compatible with the low-energy limit. In that section, propagation on the orbifold will be essentially shown to be an identification of forward and backward propagation on the covering space  $\mathbb{R}^{1,d}$ . This may also explain why the formal analytic continuation prescription continues to work in the calculations of this section.

### 2.4.2 The Generating Functional on $\mathbb{R}^{1,d-1}$

Following [50], the generating functional is

$$Z[J] = \langle \exp\{i \int d^2w J_\mu(w, \bar{w}) X^\mu(w, \bar{w})\} \rangle . \quad (2.21)$$

In order to perform the functional integrals, we introduce a complete set eigenmodes  $X_I$  of the Laplacian  $\nabla^2$  on the toroidal worldsheet,

$$\begin{aligned} \nabla_w^2 X_I(w, \bar{w}) &= -\omega_I^2 X_I(w, \bar{w}) \quad , \\ \int d^2w X_I(w, \bar{w}) X_J(w, \bar{w}) &= \delta_{IJ} \end{aligned} \quad (2.22)$$

and expand the string embedding coordinates in the eigenmodes,

$$X^\mu(w, \bar{w}) = \sqrt{4\pi^2\alpha'} \sum_I x_I^\mu X_I(w, \bar{w}) . \quad (2.23)$$

We also denote

$$J_{\mu,I} = \sqrt{4\pi^2\alpha'} \int d^2w J_\mu(w, \bar{w}) X_I(w, \bar{w}) . \quad (2.24)$$

We then integrate out the expansion coefficients  $x_I^\mu$  by completing the squares in the generating functional and performing the resulting Gaussian integrals. In particular, the integrals will include zero mode contributions from  $x_0^\mu$ . The result in  $d$  target space dimensions is

$$Z[J] = N[J_0] [\det'(-\nabla_w^2)]^{-d/2} e^{-\frac{1}{2} \int d^2w \int d^2w' J(w) \cdot G'(w, w') \cdot J(w')} , \quad (2.25)$$

where  $N[J_0]$  is the zero mode contribution

$$N[J_0] = i(2\pi)^d \delta^{(d)}(J_0) , \quad (2.26)$$

---

<sup>3</sup>See *e.g.* [52] for a proposal to modify the standard approach.

(with  $i$  coming from the Wick rotation  $x_I^0 \equiv ix_I^d$ ), the determinant factor is

$$\det'(-\nabla_w^2) \equiv \prod_{I \neq 0} \omega_I^2, \quad (2.27)$$

and  $G'(w, w')$  is the Green function

$$G'(w, w') = \sum_{I \neq 0} \frac{2\pi\alpha'}{\omega_I^2} X_I(w) X_I(w'). \quad (2.28)$$

The latter satisfies the differential equation

$$-\frac{1}{2\pi\alpha'} \nabla_w^2 G'(w, w') = g^{-1/2} \delta^{(2)}(w - w') - X_0^2, \quad (2.29)$$

where  $X_0$  is the zero mode of the Laplacian on the torus. The functional determinant (2.27) gives the torus partition function,

$$Z_{T^2}[0] = V_d [\alpha' X_0^2 \det'(-\nabla_w^2)]^{-d/2} \quad (2.30)$$

### 2.4.3 The Generating Functional on Orbifolds

Next we generalize this to the case of the orbifold. For comparison, we will consider two related types of orbifolds:

A) The Euclidean orbifold  $\mathbb{R}^{1,d} \times \mathbb{R}^{25-d}/\mathbb{Z}_2$

B) The Lorentzian orbifold  $\mathbb{R}^{1,d}/\mathbb{Z}_2 \times \mathbb{R}^{25-d}$ .

To streamline the notation, we will denote the total number of orbifold directions in both cases as  $d_o$ . We split the coordinates  $X$  and the components of the source  $J$  into those along the orbifolded ( $o$ ) and un-orbifolded ( $u$ ) directions. The generating functional takes the form

$$Z[J] = \sum_{g=0}^1 \sum_{h=0}^1 \langle \exp\{i \int J_o \cdot X_o + i \int J_u \cdot X_u\} \rangle_{gh} \quad (2.31)$$

including the sum over the untwisted ( $g = 1$ ) and twisted ( $g = 0$ ) sectors, with ( $h = 0$ ) and without ( $h = 1$ ) the  $\mathbb{Z}_2$  reflection, for string oscillations in the orbifolded directions. We then again expand  $X^\mu$  in the eigenmodes of  $\nabla^2$ , but now the eigenvalues and -modes will be different in the orbifolded directions for each sector, due to the different (anti)periodic boundary conditions. After integrating over the eigenmode coefficients, the functional takes the form

$$\begin{aligned} Z[J] &= \frac{N_u[J_0]}{N_u[0]} Z_u[0] e^{-\frac{1}{2} \int d^2 w \int d^2 w' J_u(w) \cdot J_u(w') G'(w, w')} \\ &\times \sum_{gh} \frac{N_{o,gh}[J_0]}{N_{o,gh}[0]} Z_{o,(g,h)}[0] e^{-\frac{1}{2} \int d^2 w \int d^2 w' J_o(w) \cdot J_o(w') G'_{(g,h)}(w, w')}. \end{aligned} \quad (2.32)$$

In the above,  $N_u[J_0]$ ,  $N_{o,(g,h)}[J_0]$  are the zero mode contributions (we have formally multiplied and divided by  $N[0]$  recognizing that  $Z$  includes such a factor.) In the orbifolded directions, there are zero modes only in the untwisted sector without the  $\mathbb{Z}_2$  reflection, and none in the other sectors because  $X$  satisfies an antiperiodic boundary condition in at least one of the toroidal worldsheet directions. Thus, for  $J = k\delta^{(2)}(w - w')$ ,

$$\frac{N_{o,(1,1)}[J_0]}{N_{o,(1,1)}[0]} = \frac{1}{V_{d_o}} \delta^{(d_o)}(k) ; N_{o,(g,h)}[k] = 1 \text{ for } (g, h) \neq (1, 1) . \quad (2.33)$$

The factors  $Z_u[0]$ ,  $Z_{o,(g,h)}$  are the partition function contributions from the directions transverse to and parallel with the orbifold, including the four untwisted and twisted  $(g, h)$ -sectors. Explicitly [12],

$$\begin{aligned} Z_{o,(1,1)} &= \frac{V_{d_o}}{2} \left| \frac{1}{\sqrt{\tau_2} \eta^2(\tau)} \right|^{d_o} \\ Z_{o,(g,h)} &= \left| \frac{\eta(\tau)}{\theta_{gh}(\tau)} \right|^{d_o}, \quad (g, h) \neq (1, 1) \end{aligned} \quad (2.34)$$

There are four different Green functions, corresponding to the different periodicities on the toroidal worldsheet. The doubly periodic one is [50]

$$G'_{(1,1)}(w, w') \equiv G'(w, w') = -\frac{\alpha'}{2} \ln \left| \theta_{11} \left( \frac{w - w'}{2\pi} \middle| \tau \right) \right|^2 + \pi \alpha' X_0^2 [\text{Im}(w - w')]^2, \quad (2.35)$$

and the other ones with at least one antiperiodic direction are

$$\begin{aligned} G'_{(1,0)}(w, w') &= -\frac{\alpha'}{2} \ln \left| \frac{\theta_{11}(\frac{w-w'}{4\pi}|\tau)\theta_{10}(\frac{w-w'}{4\pi}|\tau)}{\theta_{00}(\frac{w-w'}{4\pi}|\tau)\theta_{01}(\frac{w-w'}{4\pi}|\tau)} \right|^2 \\ G'_{(0,1)}(w, w') &= -\frac{\alpha'}{2} \ln \left| \frac{\theta_{11}(\frac{w-w'}{4\pi}|\tau)\theta_{01}(\frac{w-w'}{4\pi}|\tau)}{\theta_{10}(\frac{w-w'}{4\pi}|\tau)\theta_{00}(\frac{w-w'}{4\pi}|\tau)} \right|^2 \\ G'_{(0,0)}(w, w') &= -\frac{\alpha'}{2} \ln \left| \frac{\theta_{11}(\frac{w-w'}{4\pi}|\tau)\theta_{00}(\frac{w-w'}{4\pi}|\tau)}{\theta_{01}(\frac{w-w'}{4\pi}|\tau)\theta_{10}(\frac{w-w'}{4\pi}|\tau)} \right|^2. \end{aligned} \quad (2.36)$$

In  $n$ -point amplitudes, one also encounters self-contractions which require renormalization. A simple prescription is to subtract the divergent part  $-\frac{\alpha'}{2} \ln |w - w'|^2$  from the Green functions and define their renormalized versions. The renormalized version of  $G'_{11}$  is [50]

$$G'_{(1,1),ren}(w, w) = -\frac{\alpha'}{2} \ln \left| \frac{\theta'_1(0|\tau)}{2\pi} \right|^2. \quad (2.37)$$

After some manipulations, the renormalized versions of the other Green functions also turn out to simplify considerably to the following simple forms:

$$G'_{(g,h),ren} = -\frac{\alpha'}{2} \ln |\theta_{gh}(0|\tau)|^4 \quad (2.38)$$

for  $(g, h) \neq (1, 1)$ .

#### 2.4.4 One-loop Graviton Tadpole on the Orbifold

Consider then the one-loop graviton tadpole on the orbifold. The vertex operator for a state which is not projected out by the  $\mathbb{Z}_2$  reflection must be symmetric under  $X \rightarrow -X$ , hence the relevant massless tadpole on the orbifold is

$$\begin{aligned} & \langle V_{\mu\nu}(k_o, k_u) + V_{\mu\nu}(-k_o, k_u) \rangle \\ &= \frac{2g_{str}}{\alpha'} \langle \partial X^\mu \bar{\partial} X^\nu e^{ik_o \cdot X_o + ik_u \cdot X_u} + \partial X^\mu \bar{\partial} X^\nu e^{-ik_o \cdot X_o + ik_u \cdot X_u} \rangle \end{aligned} \quad (2.39)$$

The momentum must satisfy the on-shell condition  $k^2 = -m^2 = 0$ . Now there are some immediate choices to be done where the Euclidean and Lorentzian orbifolds **A** and **B** differ. In string theory one often considers Euclidean orbifolds as a way of compactifying extra dimensions. Therefore one is usually interested in states which only propagate and carry polarization in the non-orbifolded noncompact directions, and the momentum and the polarization are chosen to be entirely transverse to the orbifold, with  $k^2 = k_u^2 = -m^2$ . However, in the Lorentzian orbifold one must also include momentum components in orbifold directions in order to satisfy the on-shell condition. Furthermore, in the Lorentzian case, in order to compare with the quantum field theory calculation of Section 2.3, we choose the polarization to be along the orbifold directions<sup>4</sup>.

We evaluate the tadpole by first performing a point splitting and then functional differentiation of the generating functional,

$$\begin{aligned} & \langle \partial X^\mu(w, \bar{w}) \bar{\partial} X^\nu(w, \bar{w}) e^{ikX(w, \bar{w})} \rangle = \\ & (-i)^2 \lim_{w_1, w_2 \rightarrow w} \partial_{w_1} \bar{\partial}_{w_2} \frac{\delta}{\delta J_\mu(w_1)} \frac{\delta}{\delta J_\nu(w_2)} \langle e^{i \int d^2 w' J_\lambda(w') X^\lambda(w')} \rangle \end{aligned} \quad (2.40)$$

evaluated at  $J(w') = k \delta^{(2)}(w' - w)$ . Before the functional differentiation, for the generating functional we substitute the integrated form (2.32). We will also substitute the on-shell condition  $k^2 = 0$ .

In the case where the polarizations are in the unorbifolded directions, the

---

<sup>4</sup>Another reason why this is the interesting case is to view the orbifold as a cosmological toy model. If one would make the model truly  $d + 1$ -dimensional, the extra dimensions would need to be compactified. The massless gravitons would carry polarization in the non-compact orbifold directions.

functional differentiation and the on-shell condition gives

$$\begin{aligned} \langle \partial X^\mu(w) \bar{\partial} X^\nu(w) e^{ikX} \rangle &= \frac{N_u[k]}{N_u[0]} Z_u[\tau] \left( \sum_{g,h} Z_{o,(g,h)}[\tau] \right) \\ &\times \lim_{w_1, w_2 \rightarrow w} \left[ \eta^{\mu\nu} \partial_{w_1} \bar{\partial}_{w_2} G'(w_1, w_2) - k^\mu k^\nu \partial_{w_1} G'(w_1, w) \bar{\partial}_{w_2} G'(w_1, w) \right] \end{aligned} \quad (2.41)$$

whereas when the polarizations are in orbifolded directions, the corresponding result is

$$\begin{aligned} \langle \partial X^\mu(w) \bar{\partial} X^\nu(w) e^{ikX} \rangle &= \frac{N_u[k]}{N_u[0]} Z_u[\tau] \times \sum_{g,h} \frac{N_{o,(g,h)}[k]}{N_{o,(g,h)}[0]} Z_{o,(g,h)}[\tau] \\ &\times \lim_{w_1, w_2 \rightarrow w} \left[ \eta^{\mu\nu} \partial_{w_1} \bar{\partial}_{w_2} G'_{(g,h)}(w_1, w_2) - k^\mu k^\nu \partial_{w_1} G'_{(g,h)}(w_1, w) \bar{\partial}_{w_2} G'_{(g,h)}(w_1, w) \right]. \end{aligned} \quad (2.42)$$

In both cases, the Green function will need to be replaced by their renormalized versions. We can already see that the expressions are quite different. Let us simplify them further. First, we can use the equation (2.29) to simplify the double derivatives of the Green functions. First, since  $G'(w_1, w_2) = G'(w_1 - w_2)$ ,

$$\partial_{w_1} \bar{\partial}_{w_2} G'(w_1, w_2) = -\partial_{w_1} \bar{\partial}_{w_1} G'(w_1, w_2). \quad (2.43)$$

On the other hand, the equation (2.29) evaluates to

$$\partial_w \bar{\partial}_w G'(w, w') = -\pi \alpha' \delta^2(w - w') + \frac{\pi \alpha'}{2} X_0^2. \quad (2.44)$$

The first term on the right hand side originates from the short distance divergence  $G'(w_1, w_2) \sim \ln |w_1 - w_2|^2$  of the Green function, which we subtract off when we renormalize the Green functions. The latter then satisfy the equation

$$\partial_{w_1} \bar{\partial}_{w_2} G'_{ren}(w_1, w_2) = -\frac{\pi \alpha'}{2} X_0^2. \quad (2.45)$$

Similar results hold for the renormalized Green functions  $G'_{(g,h),ren}$ . Since a zero mode  $X_0$  exists only in the doubly periodic  $(g, h) = (1, 1)$  sector, the double derivatives  $\partial \bar{\partial} G'_{gh,ren}$  vanish in all the other three sectors.

Next, we examine the first derivatives of the renormalized Green functions. A short calculation shows that in all cases the Green functions have a short distance behavior of the type

$$\partial G'_{(g,h)}(w, w') \approx_{w \rightarrow w'} -\frac{\alpha'}{2} (w - w')^{-1} + C_{(g,h)}(\tau) (w - w') + \mathcal{O}((w - w')^3) \quad (2.46)$$

where  $C_{(g,h)}(\tau)$  are rational functions of derivatives of theta functions at  $(0|\tau)$ . A similar formula is found for the antiholomorphic derivative  $\bar{\partial} G'_{(g,h)}$ . There is only one divergent term, due to the self-contraction of  $X$  with  $\partial X$ . The renormalization prescription again removes the divergent term, so the renormalized (derivatives of) Green function vanish in the limit  $w \rightarrow w'$ . Hence these terms

will not contribute to the graviton tadpole.

Substituting all the normalization and partition function factors, the final results are

$$\langle V^{\mu\nu}(k) + V^{\mu\nu}(-k) \rangle_{1-loop} = -\frac{g_{str}}{4\pi\tau_2} \frac{\delta^{(d_u)}(k)}{V_u} Z_u[\tau] \times \sum_{g,h} \frac{N_{o,(g,h)}[k]}{N_{o,(g,h)}[0]} Z_{o,(g,h)}[\tau] \eta^{\mu\nu}. \quad (2.47)$$

for polarizations in the unorbifolded directions, and

$$\langle V^{\mu\nu}(k) + V^{\mu\nu}(-k) \rangle_{1-loop} = -\frac{g_{str}}{4\pi\tau_2} \frac{\delta^{(26)}(k)}{V_{26}} Z_u(\tau) Z_{o,(1,1)}[\tau] \eta^{\mu\nu}. \quad (2.48)$$

for polarizations in the orbifolded directions. By analogy, one would then expect this tadpole to vanish for the superstring.

Equation (2.47) is the standard result one would find in flat space. In the case of the Lorentzian orbifold, we would like to think of spacetime as the orbifolded directions, while the unorbifolded directions are perhaps compactified. Thus in the Lorentzian orbifold, it is appropriate to consider (2.48). At first sight, this result looks rather surprising, as it is precisely the same as for a graviton in the usual  $\mathbb{R}^{1,25}$  target space.

This is in direct conflict with the field theory calculation of the previous section, but we have already noted the problems of principal with that calculation. In the light of the string theory analysis, we must search for a field theory description that can be consistent with these results. A key observation is that the string calculation involved strings with  $k$  and  $-k$ , opposite spacelike momentum *and* energy. Indeed, in [48] it was proposed that the string theory computation indicated that the proper field theory limit of this orbifold string theory possesses a doubled Hilbert space. The time evolution for the fields in this doubled Hilbert space are taken to have opposite orientation.

## 2.5 Chapter Summary

In this chapter we discussed a time-dependent  $\mathbb{Z}_2$  orbifold of Minkowski space. Numerous issues about the definition of time's orientation were discussed, leading a naive definition of field theory to fail. However, closed string theory is well defined upon this spacetime, having finite 1-loop corrections to the vacuum energy and the graviton tadpoles. Given that closed string theory is sensible in this spacetime, it is natural to move on to open string theory, which we shall do in the next chapter. En route we shall naturally be led to a family of spacelike branes which model closed string initial conditions in the presence of a cosmological singularity.

## Chapter 3

# Open Strings in $\mathbb{Z}_2$ Background and Closed String Initial Conditions

### 3.1 Rolling Tachyon CFT in $\mathbb{Z}_2$ Background

In the previous chapter we discussed a closed string construction of a time-dependent space-time via a  $\mathbb{Z}_2$  orbifold. In this chapter we shall investigate open strings in the presence of both the orbifold and marginal boundary deformations. By allowing boundary deformations, we probe the space of allowed open string boundary conditions (the set of consistent open string theories). These are interesting CFT's in their own right, being nontrivial examples of solvable interacting field theories. In addition, using the duality between open string loop diagrams and closed string tree diagrams, we may view the associated boundary states as setting stringy initial conditions to space-time. In a later chapter we shall use these conformal field theory results to discuss gravitational particle production in space-times with cosmological singularities.

The  $c = 1$  conformal field theory on worldsheets with boundary is known to have a boundary interaction

$$-\frac{\lambda}{2} \int_{\partial\Sigma} ds e^{iX/\sqrt{\alpha'}} + h.c.$$

which is exactly marginal. This theory was originally studied at self-dual radius ( $X \in S^1_{R=\sqrt{\alpha'}}$ ) by Callan et al [53], where the marginality was established. Although there is renormalization of  $\lambda$  in perturbation theory, due to operator products of  $e^{iX/\sqrt{\alpha'}}$  with  $e^{-iX/\sqrt{\alpha'}}$ , it is possible to absorb these divergences and obtain an RG-stationary coupling. At self-dual radius, the operators of the theory organize themselves into multiplets of an  $\widehat{SU(2)}_1$  current algebra, and this structure plays an important organizing rôle in the analysis.

A complementary analysis of this theory, at infinite radius, was later provided by Polchinski and Thorlacius [54]. By introducing auxiliary bosonic fields, it is possible to re-write the theory in terms of free fermions with a quadratic boundary interaction. This essentially constitutes a regularization of the theory (different than the one noted above) and is tractable because the action is quadratic in fermions (from the bulk worldsheet point of view, there are mass terms with  $\delta$ -function support—these are both classically and quantum mechanically marginal).

In this chapter, we will consider the extension of this theory to other backgrounds, including a  $\mathbb{Z}_2$  reflection orbifold, as well as circles of arbitrary rational radius. We were led into this work by considerations of S-brane solutions [55, 56, 51] in Lorentzian orbifold backgrounds [12, 48]. In the following chapter (see also [57, 58]), we use the results of the present chapter; following a Wick rotation, to discuss ‘fractional S-branes,’ objects which may be of importance in cosmological orbifold backgrounds.

Our calculations will be formulated and presented directly in the open string channel. Passing these results to the closed string channel then allows for the determination of boundary states<sup>1</sup>. Away from self-dual radius, we must formulate the theories of interest in the fermionic picture. In particular, this was originally formulated at infinite radius. For the orbifold theory, it is necessary to carefully consider various subtleties of the fermionic construction. As a result, we have organized this chapter as follows. In Section 3.2, we set up notation and discuss some standard boundary states of the undeformed theory. We also discuss the effect of orbifolds in free string theories. Then, in Section 3.3, we review the standard bosonic treatment of the bosonic theory at self-dual radius. In Section 3.4 we then review the fermionic construction of the infinite radius deformed theory. As we have mentioned above, there are a number of subtleties involved in extending this analysis to the orbifold theory, and thus we take the liberty of going into some detail in this review. In this section we also review how the corresponding boundary states can be written in terms of a projection operator acting on  $\widehat{SU(2)}_1$  Ishibashi states. We then discuss how finite radius theories may be constructed in the fermionic picture. In constructing these, there are both classical and quantum consistency conditions in the fermionic path integral to which we must pay attention. Doing so gives rise in the end to boundary states that can be written using projection operators, and these boundary states transform in a simple way under T-duality. In Section 3.5, we construct the orbifold theory in the fermionic description. In so doing, we introduce a number of consistency checks to ensure that the results are correct.

## 3.2 Boundary CFT of a Free Boson

### Unorbifolded Free Boson

In order to set notation and collect some known results, we first consider the undeformed boundary conformal theory on a circle of radius  $R$ . Free open bosonic string theory, with action  $\frac{1}{4\pi\alpha'} \int d^2\sigma \sqrt{-h} h^{ab} \partial_a X \partial_b X$ , on a strip  $\sigma \in (0, r), \tau \in (0, \ell)$ , has mode expansion

$$\hat{X}(\sigma, \tau) = \hat{x} + \frac{2\pi\alpha'}{r} \tau \hat{p} + i\sqrt{2\alpha'} \sum_{\substack{n \in \mathbb{Z} \\ n \neq 0}} \frac{1}{n} \hat{\alpha}_n \cos\left(\frac{\pi n \sigma}{r}\right) e^{-i\pi n \tau / r}$$

---

<sup>1</sup>For related work on boundary states on deformed boundary conformal field theory on the orbifold, see also [59].

where we have assumed Neumann boundary conditions at  $\sigma = 0, r$ . The spectrum of  $\hat{p}$  is determined by the compactification radius,  $spectrum(\hat{p}) = \mathbb{Z}/R$ . With this normalization, the vertex operator  $e^{ikX}$  has conformal dimension  $\Delta = \alpha' k^2$ .

If we compute the NN annulus amplitude (the open string partition function with Neumann boundary conditions on each boundary), we may obtain information on the Neumann boundary state of the closed string channel. This is

$$\mathcal{A}_{NN} = \frac{1}{\eta(q)} \sum_n q^{\alpha' n^2 / R^2} . \quad (3.1)$$

We use the notation  $q = e^{-\pi t}$ ,  $t = \ell/r$ . This may be re-written as

$$\mathcal{A}_{NN} = \frac{R}{\eta(q)} \int dp q^{\alpha' p^2} \sum_m e^{2\pi i p R m} , \quad (3.2)$$

which can be understood as explicitly implementing the shift orbifold to finite radius within the infinite radius theory. This form will be important later.

In the present NN case, at finite radius, it is also possible to introduce a Wilson line, and we record the result [60] here

$$\mathcal{A}_{NN}(\Delta\theta) = \frac{1}{\eta(q)} \sum_n q^{\alpha' (n/R + \Delta\theta/2\pi R)^2} . \quad (3.3)$$

By Poisson resummation, with notation  $\tilde{q} = e^{-2\pi/t}$ , we find

$$\mathcal{A}_{NN}(\Delta\theta) = \frac{R}{\sqrt{2\alpha'} \eta(\tilde{q}^2)} \sum_{m \in \mathbb{Z}} (\tilde{q}^2)^{m^2 R^2 / 4\alpha'} e^{-im\Delta\theta} . \quad (3.4)$$

In this channel, following the discussion in A.1 and [61] we identify boundary states via

$$\mathcal{A}_{NN}(\Delta\theta) \equiv \langle N, \theta | \Delta(\tilde{q}) | N, \theta + \Delta\theta \rangle \quad (3.5)$$

with  $\Delta(\tilde{q})$  the closed string propagator. We may write the boundary state in oscillator form as [60]

$$|N, \theta\rangle = 2^{-1/4} e^{\sum_k \alpha_k \tilde{\alpha}_k} |0\rangle_{Fock} \otimes \sum_{n \in \mathbb{Z}} e^{in\theta} \left| \frac{nR}{\sqrt{\alpha'}}, -\frac{nR}{\sqrt{\alpha'}} \right\rangle$$

In this form, it is clear that the Neumann boundary state has zero momentum,<sup>2</sup> and is at fixed  $\tilde{X} \equiv X_L - X_R$ .

Note that at self-dual radius,  $R = \sqrt{\alpha'}$ , the conformal dimensions are square integers. In fact, there is an  $\widehat{SU}(2)$  current algebra that classifies the spectrum

<sup>2</sup>We record the Dirichlet boundary state at self-dual radius

$$|D, x\rangle \sim 2^{-1/4} e^{-\sum_k \alpha_k \tilde{\alpha}_k} |0\rangle_{Fock} \otimes \sum_n e^{-inx/\sqrt{\alpha'}} \left| \frac{n}{\sqrt{\alpha'}}, \frac{n}{\sqrt{\alpha'}} \right\rangle$$

(see e.g. [62]). In this case, (3.4) can be rewritten [63]

$$\mathcal{A}_{NN}(\Delta\theta) = \frac{1}{\sqrt{2}} \sum_{j=0,1/2,1,\dots} \chi_{j^2}^{Vir}(\tilde{q}^2) \chi_j^{SU(2)}(e^{-2i\Delta\theta J_0^3}) \quad (3.6)$$

with  $SU(2)$  characters

$$\chi_j^{SU(2)}(g) = Tr_j \mathcal{D}^{(j)}(g) , \quad (3.7)$$

where  $\mathcal{D}^{(j)}(g)$  is the matrix representing the  $SU(2)$  element  $g$  in representation  $j$ , and Virasoro characters

$$\chi_{j^2}^{Vir}(\tilde{q}^2) = \frac{\tilde{q}^{2j^2} - \tilde{q}^{2(j+1)^2}}{\eta(\tilde{q}^2)} . \quad (3.8)$$

Using the normalization of Ishibashi states

$$\langle\langle j, m, n | \Delta(\tilde{q}) | j', m', n' \rangle\rangle = \chi_{j^2}^{Vir}(\tilde{q}^2) \delta_{jj'} \delta_{mm'} \delta_{nn'} \quad (3.9)$$

we obtain the boundary state in the  $\widehat{SU(2)}$  basis

$$|N, \theta\rangle \simeq 2^{-1/4} \sum_{j=0,1/2,1,\dots} \sum_{m,n=-j}^j \mathcal{D}_{m,n}^{(j)}(e^{-2i\theta J_0^3}) |j, -m, n\rangle . \quad (3.10)$$

### 3.2.1 The Free Orbifold Theory

The  $\mathbb{Z}_2$  orbifold is implemented in the open string sector, apart from Chan-Paton factors, by a projection operator  $\frac{1}{2}(1 + g)$ . The first 1 term is proportional to the results of the last subsection and gives rise to untwisted boundary states. The  $g$  term will give rise to twisted boundary states. Note that at finite radius, there are two fixed orbifold points at  $x = 0$  and  $x = \pi R$ ; correspondingly, there are two discrete Wilson lines at  $\theta = 0, \pi$  that are fixed by the orbifold.

At self-dual radius, we find

$$Z_{g;NN} \equiv Tr g q^{L_0 - 1/24} \quad (3.11)$$

$$= \frac{1}{\eta(q)} \sum_{n \in \mathbb{Z}} (-1)^n q^{n^2} \quad (3.12)$$

$$= \frac{1}{\sqrt{2}} \frac{1}{\eta(\tilde{q}^2)} \sum_{m \in \mathbb{Z}} (\tilde{q}^2)^{(m-1/2)^2/4} . \quad (3.13)$$

Writing a boundary state for the twisted states only is complicated by the presence of two fixed points. In a later section, we will show how the lowest lying twisted modes contribute to the boundary states.

It is interesting to note that, at the self-dual radius, the orbifold partition function is T-dual to an unorbifolded partition function at twice the self-dual radius [64]. In making this equivalence we exchange the  $J^3$  current at twice the self-dual radius with the  $J^1$  current of the self-dual radius theory. Consider

again the orbifold partition function

$$Z_{NN} = \frac{1}{2} \text{Tr} (1 + g) q^{L_0 - 1/24} = \frac{1}{\eta(q)} \sum_{n \in \mathbb{Z}} q^{n^2} \left( \frac{1 + (-1)^n}{2} \right). \quad (3.14)$$

Clearly,  $n$  must be even, and we can re-write this as

$$Z_{NN} = \frac{1}{\eta(q)} \sum_{n \in \mathbb{Z}} q^{4n^2} \quad (3.15)$$

which indeed is the partition function at radius  $R = \sqrt{\alpha'}/2$ . After rewriting it in the closed string channel, and T-dualizing to radius  $\tilde{R} = 2\sqrt{\alpha'}$ , we find the Dirichlet boundary state with zero modes

$$|D, x\rangle \sim \sum_{m \in \mathbb{Z}} e^{-imx_0/2\sqrt{\alpha'}} \left| \frac{m}{2\alpha'}, \frac{m}{2\alpha'} \right\rangle. \quad (3.16)$$

For different discrete values of  $x_0$ , we have boundary states which correspond to fractional brane states in the orbifold theory. This implies a relationship between fractional branes in the self-dual radius theory, and D-branes at twice the self-dual radius [59]. We will elaborate this in section 4.3.1. If we allow for the possibility of branes centered at differing positions in the twice self-dual theory, we find

$$Z_{R=2R_{s.d.}}^{DD} = \frac{1}{\eta(q)} \sum_{n \in \mathbb{Z}} q^{(2n + \Delta x_0/2\pi\sqrt{\alpha'})^2}. \quad (3.17)$$

### 3.2.2 Chan-Paton Factors

With multiple branes, the above computation is only trivially modified. The boundaries attain an extra discrete index labeling the map of the worldsheet boundary onto a D-brane. The role of Chan-Paton indices become especially important in the context of orbifolds.

The novel feature of Euclidean orbifold theories is the existence of fractional branes, localized at the orbifold fixed points. In this section we review the role of Chan-Paton indices in the construction of branes in the non-compact Euclidean  $\mathbb{R}^D/\mathbb{Z}_2$  orbifold models (with a single fixed point). The route we will take is to deduce the fractional brane boundary states from the open string partition function with Chan-Paton indices. This formalism will be carried over later to the case of deformed boundary states, and to Lorentzian signature.

Begin with a D-brane which is pointlike in the directions of the orbifold. An open string in the covering space then sees two D-branes, at  $X$  and  $-X$ . Consequently there are 4 types of open strings which are labeled by the branes upon which they end, summarized by the Chan-Paton matrix

$$\lambda = \begin{pmatrix} D0 - D0 & D0 - D0' \\ D0' - D0 & D0' - D0' \end{pmatrix}. \quad (3.18)$$

The  $\mathbb{Z}_2$  action exchanges the brane and image brane, in the above basis the group elements are represented by

$$\gamma(e) = \begin{pmatrix} 1 & 0 \\ 0 & 1 \end{pmatrix}, \quad \gamma(g) = \begin{pmatrix} 0 & 1 \\ 1 & 0 \end{pmatrix}. \quad (3.19)$$

At the fixed point, the representation is reducible, and it is useful to work in a different basis where

$$\gamma(e) = \begin{pmatrix} 1 & 0 \\ 0 & 1 \end{pmatrix}, \quad \gamma(g) = \begin{pmatrix} 1 & 0 \\ 0 & -1 \end{pmatrix}. \quad (3.20)$$

Fractional branes are associated with the irreducible one-dimensional representations. In the closed string language, they are described by boundary states which we denote by  $|D, \alpha\rangle_{frac}$ , with  $\alpha = \pm$ .

Now consider the open string partition function, corresponding to an annulus diagram. Take the open string to be suspended between two fractional branes at the same fixed point, with labels  $\alpha, \beta$ . This is encoded in the partition function by inserting appropriate projection operators  $P_\alpha, P_\beta$  for each boundary into the Chan-Paton traces. They impose the projection into the two irreducible representations, and are given by

$$P_+ = \begin{pmatrix} 1 & 0 \\ 0 & 0 \end{pmatrix}, \quad P_- = \begin{pmatrix} 0 & 0 \\ 0 & 1 \end{pmatrix}. \quad (3.21)$$

The projection operators are then inserted into the open string partition function as follows:

$$\begin{aligned} Z_{DD}^{\alpha, \beta} &= \frac{1}{2} \left( ([\text{tr } P_\alpha \gamma(e)][\text{tr } P_\beta \gamma(e)^{-1}] \text{Tr } e^{-\beta H} \right. \\ &\quad \left. + [\text{tr } P_\alpha \gamma(g)][\text{tr } P_\beta \gamma(g)^{-1}] \text{Tr } g e^{-\beta H} \right) \\ &= \frac{1}{2} (\text{Tr } e^{-\beta H} + \epsilon_{\alpha\beta} \text{Tr } g e^{-\beta H}), \end{aligned} \quad (3.22)$$

with  $\epsilon_{\pm, \pm} = 1$  and  $\epsilon_{\pm, \mp} = -1$ . Cardy's condition then relates the one-loop open string partition function to the tree level closed string exchange between fractional brane boundary states,

$$Z_{DD}^{\alpha, \beta} \rightarrow {}_{frac}\langle D, \alpha | \Delta(\tilde{q}) | D, \beta \rangle_{frac}. \quad (3.23)$$

It is natural to isolate the untwisted  $|\cdot\rangle_U$  and twisted  $|\cdot\rangle_T$  sector boundary states, normalized as

$${}_U\langle D | \Delta | D \rangle_U = \text{Tr } e^{-\beta H}, \quad {}_T\langle D | \Delta | D \rangle_T = \text{Tr } g e^{-\beta H}. \quad (3.24)$$

From (3.22), we then read off the fractional boundary states as linear combina-

tions

$$|D, \alpha\rangle_{frac} = A_\alpha |D\rangle_U + B_\alpha |D\rangle_T \quad (3.25)$$

with the coefficients

$$A_\pm = \frac{1}{\sqrt{2}}, \quad B_\pm = \pm \frac{1}{\sqrt{2}}. \quad (3.26)$$

In other words, the two fractional states are

$$|D, \pm\rangle = \frac{1}{\sqrt{2}} (|D\rangle_U \pm |D\rangle_T) . \quad (3.27)$$

The regular representation is the direct sum of irreducible representations, associated to  $P_+ + P_-$ . Thus, the regular D-brane is identified with  $|D_o\rangle = |D, +\rangle_{frac} + |D, -\rangle_{frac} = \sqrt{2}|D\rangle_U$ . One can check that this correctly accounts for the factors of two and such that occur in the analysis away from the fixed points.

The calculations in the following sections will actually involve deformations away from Neumann-Neumann amplitude. However, because varying the strength of the deformation parameter smoothly interpolates between Neumann and Dirichlet boundary conditions, the Chan-Paton structures can be treated in essentially the same manner as discussed above.

### 3.3 Adsorption and Open String Partition Functions

#### 3.3.1 Boundary Deformations

In the context of rolling tachyons, the generic boundary perturbation of interest is of the form

$$S_\lambda = \int_{\partial\Sigma} ds \left[ \lambda_+ e^{X^0(s)/\sqrt{\alpha'}} + \lambda_- e^{-X^0(s)/\sqrt{\alpha'}} \right] \quad (3.28)$$

where  $X^0$  is the time-like target space coordinate. Classically (using the correlators of the undeformed theory), this perturbation is marginal, that is  $d_{cl} = 1$ . For  $\lambda_\pm = \frac{1}{2}\lambda e^{\mp X_0^0/\sqrt{\alpha'}}$ , this is related to the “full S-brane” [55] centered at  $X_0^0$ , while for  $\lambda_- = 0$ , we have the “half S-brane” [51]. The full S-brane corresponds to a process where a carefully fine-tuned initial closed string configuration time evolves to form an unstable D-brane which then decays to a final state of closed strings [65, 66, 67, 68]. The whole process is centered around the time  $X_0^0$  and is time reflection invariant about it, as evident from writing the deformation in the form

$$S_\lambda = \lambda \int_{\partial\Sigma} ds \cosh[(X^0(s) - X_0^0)/\sqrt{\alpha'}], \quad (3.29)$$

in particular the initial state of closed strings is a time reflection image of the final state. By Wick rotating  $X^0 = iX$ , it becomes

$$S_\lambda = -\lambda \int_{\partial\Sigma} ds \cos[(X(s) - X_0)/\sqrt{\alpha'}], \quad (3.30)$$

which is a known exactly marginal deformation [53]. In practise, computations in the background (3.29) are first performed in the Euclidean signature with (3.30), and the results are then Wick rotated back to the Lorentzian signature. In the rest of the present chapter, we will disregard any relation to rolling tachyons, and simply consider the Euclidean theory.

One could absorb the parameter  $X_0$  into the definition of the origin of time. However, for a given worldsheet with multiple boundaries, there can be a distinct deformation for each boundary component. For example, if we consider the annulus, we will consider a boundary deformation of the form

$$S_{int} = -\lambda \int_{\partial\Sigma_1} ds \cos\left(\frac{X - X_0^{(1)}}{\sqrt{\alpha'}}\right) - \tilde{\lambda} \int_{\partial\Sigma_2} ds \cos\left(\frac{X - X_0^{(2)}}{\sqrt{\alpha'}}\right) \quad (3.31)$$

where  $\partial\Sigma_j$  are the boundary components. This is essentially a Chan-Paton structure. Indeed in the presence of multiple branes,  $\lambda$  and  $\tilde{\lambda}$  would be replaced by matrices, and the annulus would include overall traces for each boundary component. A priori, there is no need to take the cosines to be centred at the same point on different boundaries, and the difference cannot be absorbed to the choice of the time origin.

In the orbifold  $\mathbb{R}^{1,d}/\mathbb{Z}_2$  the  $\mathbb{Z}_2$  acts by  $(X^0, X^1, \dots, X^d) \rightarrow -(X^0, X^1, \dots, X^d)$  [12, 48]. After Wick rotation  $X^0 = iX$ , we obtain a Euclidean orbifold  $\mathbb{R}^{d+1}/\mathbb{Z}_2$ , where  $\mathbb{Z}_2$  acts by  $(X, X^1, \dots, X^d) \rightarrow -(X, X^1, \dots, X^d)$ . The full S-brane deformation is invariant under the orbifold identifications, if we choose it to be centered around  $X^0 = 0$ . In the Euclidean signature, for worldsheets with multiple boundaries, if we allow for distinct deformations at each boundary component  $\partial\Sigma_j$ , we would then need each of them to be centered around  $X = 0$  (i.e., set  $X_0^{(j)} = 0$ , but the associated parameters  $\lambda_j$  can be independent of one another. Wick rotation back to Lorentzian signature is subtle, because of the issues with the branching of time's arrow. This will be discussed in Ref. [58].

### 3.3.2 The Adsorption Method

Let us begin with the theory at self-dual radius  $R_{sd} = \sqrt{\alpha'}$ . One way to understand this case is known as ‘adsorption’ [60]. This method highlights the close relationship with the Kondo problem of condensed matter physics. In that situation we think of the deformation as the  $U(1)$  charge current for a free fermionic theory.

We can study this theory by replacing the boson  $\hat{X}$  on the strip by an ‘unfolded’ chiral boson  $\hat{\phi}$  on  $\sigma \in (-r, r)$ ,  $\tau \in (0, \ell)$ , where  $\sigma = -r$  is identified

with  $\sigma = +r$  (this is a torus in the  $w = i\tau + \sigma$  plane, with modular parameter  $\ell/2r$ ). To do so, we identify  $\phi(\sigma, \tau) = X_L(i\tau + \sigma)$  for  $\sigma > 0$ , and  $\phi(\sigma, \tau) = X_R(i\tau - \sigma)$  for  $\sigma < 0$ . It is most natural to quantize this boson by taking  $\sigma$  as the 'time' direction; we simply have a periodic boundary condition in the  $\tau$ -direction, and we obtain the mode expansion

$$\hat{\phi}(w) = \hat{\phi}_0 + \frac{\pi\alpha' w \hat{p}}{\ell} + i\sqrt{\frac{\alpha'}{2}} \sum_{\substack{n \in \mathbb{Z} \\ n \neq 0}} \frac{1}{n} \hat{\alpha}_n e^{-2\pi n w / \ell} . \quad (3.32)$$

At self-dual radius, the theory reduces to a chiral  $\widehat{SU(2)}$  current algebra, with currents

$$\begin{aligned} J^\pm &= e^{\pm i\phi / \sqrt{\alpha'}} \\ J^3 &= i\partial\phi / \sqrt{\alpha'} , \end{aligned} \quad (3.33)$$

where  $J^\pm = (J^1 \pm J^2) / \sqrt{2}$ . The basic strategy will be to make use of the  $\widehat{SU(2)}$  current algebra relations,

$$\mathcal{H}_0 \propto : (J^3(\sigma))^2 : = \frac{1}{3} : \bar{J}^2(\sigma) : = : (J^1(\sigma))^2 : . \quad (3.34)$$

For simplicity we will focus on the situation with a single boundary deformation, taking the form

$$\lambda \int_0^\ell d\tau J^1(i\tau + 0) = \ell \lambda J_0^1 . \quad (3.35)$$

In detail, the partition function becomes:

$$\begin{aligned} Z_\lambda &= Tr \left( e^{\frac{1}{2\pi} \int_{-r}^0 d\sigma \int_0^\ell d\tau : (J^1(\sigma, \tau))^2 :} e^{i\lambda \int_0^\ell d\tau J^1(\tau + i0)} \right. \\ &\quad \left. e^{1/2\pi \int_0^r d\sigma \int_0^\ell d\tau : (J^1(\sigma, \tau))^2 :} \right) . \end{aligned} \quad (3.36)$$

Here the boundary deformation takes the form of an operator insertion at the fixed "time"  $\sigma = 0$ . Using the explicit mode expansions, we obtain

$$\begin{aligned} Z_\lambda &= Tr \left( e^{-\frac{r}{t\pi} \cdot ((J_0^1)^2 + 2 \sum_{n=1}^\infty J_{-n}^1 J_n^1)} e^{i\lambda J_0^1} \right) \\ &= \frac{1}{\eta(\tilde{q}^2)} \sum_{n \in \mathbb{Z}} (\tilde{q}^2)^{n^2/4} e^{\pi i \lambda n} , \quad \left( \tilde{q} = e^{-2\pi/t}, t = \ell/r \right) . \end{aligned} \quad (3.37)$$

Because we quantized using  $\sigma$  as "time" we obtain an answer in the closed string channel. We should perform a Poisson resummation to write the partition function in the open string channel,

$$Z_\lambda = \sum_{m \in \mathbb{Z}} \frac{q^{(m+\lambda/2)^2}}{\eta(q)} , \quad (q = e^{-\pi t}, t = \ell/r) . \quad (3.38)$$

## 3.4 Fermionic Representation

Having studied the orbifold theory at self-dual radius, we consider now other radii. At infinite radius, the renormalized bosonic theory may also be represented using a ‘free’ fermionic picture [54, 69]. We will take the liberty in this section of discussing this construction in detail. Although many aspects have been discussed in the literature, certain subtle points will be needed later in the chapter when we apply the construction to orbifold theories.

The boundary interaction involves open string tachyonic vertex operators,  $e^{\pm iX/\sqrt{\alpha'}}$ . We should first study how this is represented in terms of the “doubled” chiral boson living on  $\sigma \in [-r, r]$ . When fermionizing we will quantize using  $\tau$  as the time direction and the mode expansion of section 3.2, in contrast with the previous section. With  $\hat{p}$  conjugate to  $\hat{x}$ , this vertex operator may be written:

$$e^{ik\hat{X}(\tau,0)/\sqrt{\alpha'}} = e^{i2k\hat{\phi}(\tau)/\sqrt{\alpha'}} \quad (3.39)$$

$$e^{ik\hat{X}(\tau,r)/\sqrt{\alpha'}} = e^{i2k\hat{\phi}(\tau+r)/\sqrt{\alpha'}} e^{-i\pi\sqrt{\alpha'}k(2\hat{p}+k/\sqrt{\alpha'})}. \quad (3.40)$$

In particular, when  $k = \pm 1$  the vertex operator at  $\sigma = r$  becomes

$$e^{\pm i\hat{X}(\tau,r)/\sqrt{\alpha'}} = -e^{\pm i2\hat{\phi}(\tau+r)/\sqrt{\alpha'}} e^{\mp i2\pi\sqrt{\alpha'}\hat{p}}. \quad (3.41)$$

Thus the boundary interaction is

$$S_{int} = -\lambda \int_{\sigma=0} ds \cos(2\phi(s)/\sqrt{\alpha'}) + \frac{\tilde{\lambda}}{2} \int_{\sigma=r} ds \left( e^{i2\phi(s)/\sqrt{\alpha'}} e^{-i2\pi\sqrt{\alpha'}p} + e^{-i2\phi(s)/\sqrt{\alpha'}} e^{i2\pi\sqrt{\alpha'}p} \right) \quad (3.42)$$

### 3.4.1 Fermionic Action

Here we want to find a fermionization appropriate for the boundary interaction. A convenient (but not unique) way to proceed is to mix in a second boson,  $Y$ . In [54] the second boson was viewed as auxiliary. However, in the context of string theory we may use one of the spatial directions as the second boson. It will be necessary to introduce co-cycles in order for the algebraic properties to be faithfully reproduced. As  $X$  was related to a chiral boson  $\phi$ , we may relate  $Y$  to a chiral boson  $\chi$ . It is possible to take

$$\psi_1 = e^{i(\chi-\phi)/\sqrt{\alpha'}} e^{i\pi ap} \equiv e^{i\phi_1} e^{i\pi ap}, \quad \psi_2 = e^{i(\chi+\phi)/\sqrt{\alpha'}} e^{i\pi bp} \equiv e^{i\phi_2} e^{i\pi bp}, \quad (3.43)$$

where  $a$  and  $b$  are real parameters. As before  $p$  is conjugate to  $x$ . We have chosen to write the fermion cocycles in terms of the  $X$  zero modes so that the interaction is independent of the field,  $Y$ . We can introduce  $p_\phi = 2p$ , conjugate to  $\phi_0$ . Similarly we may introduce  $p_\chi$ , conjugate to  $\chi_0$ .  $\chi$  has a mode expansion

similar to that of  $\phi$ .

The values of  $a$  and  $b$  may be constrained by demanding anticommutativity. This leads to the condition  $\frac{b+a}{2\sqrt{\alpha'}} \in 2\mathbb{Z} + 1$ . As in [54], we will choose  $a = 0$  and  $b = -2\sqrt{\alpha'}$ .

Recall that in the doubling we have

$$\phi(\tau, r) = \phi(\tau, -r) + \pi\alpha' p_\phi . \quad (3.44)$$

Similarly,

$$\chi(\tau, r) = \chi(\tau, -r) + \pi\alpha' p_\chi . \quad (3.45)$$

Defining parameters  $\zeta_i$ , these periodicity conditions correspond to boundary conditions on the fermions

$$\psi_i(r) = -e^{2\pi i\zeta_i} \psi_i(-r) . \quad (3.46)$$

The  $\zeta_i$  correspond to the fractional (in units of  $\sqrt{\alpha'}$ ) parts of the momenta. From the fermionization map, we may relate the  $\zeta_i$  to the momenta  $p_\phi$  and  $p_\chi$  (mod  $\mathbb{Z}$ )

$$\zeta_1 = \frac{\sqrt{\alpha'}}{2} (p_\chi - p_\phi) ; \quad \zeta_2 = \frac{\sqrt{\alpha'}}{2} (p_\chi + p_\phi) . \quad (3.47)$$

We will find it convenient to define  $\zeta_\pm = \frac{1}{2} (\zeta_1 \pm \zeta_2)$ . We then have

$$\zeta_+ = \frac{\sqrt{\alpha'}}{2} p_\chi , \quad \zeta_- = -\frac{\sqrt{\alpha'}}{2} p_\phi . \quad (3.48)$$

Given the fermionization, the interaction becomes

$$\begin{aligned} S_{int} &= -\frac{\lambda}{2} \int_\Sigma \left( \psi_1^\dagger \psi_2 e^{i\pi\sqrt{\alpha'} p_\phi} + \psi_2^\dagger \psi_1 e^{-i\pi\sqrt{\alpha'} p_\phi} \right) \delta(\sigma) \\ &\quad + \frac{\tilde{\lambda}}{2} \int_\Sigma \left( \psi_1^\dagger \psi_2 + \psi_2^\dagger \psi_1 \right) \delta(\sigma - r) . \end{aligned} \quad (3.49)$$

Unfortunately, the first term of  $L_{int}$  anti-commutes with the fermion fields. However, it is possible to write an equivalent expression for the partition function that has a fermion number projection operator inserted (specifically,  $(1 + (-1)^{F_1+F_2})/2$ ), while adjusting the allowed values of  $\zeta_\pm$ . In terms of this way of writing the partition function, the physical states have even fermion number, and we can with impunity modify the interaction by multiplying the first term in  $L_{int}$  by  $(-)^F$ . These changes have no effect on the energy spectrum, but now the modified fermionic interaction commutes with the fermionic fields. This adjustment is required for the fermionization to make sense algebraically, and should be understood as part of the fermionization map.

Defining

$$\Psi = \begin{pmatrix} \psi_1 \\ \psi_2 \end{pmatrix}, \quad (3.50)$$

we may write the full Lagrangian as<sup>3</sup>

$$L = \frac{1}{2\pi} \int_{-\pi}^{\pi} d\sigma \Psi^\dagger (\partial_\tau - \partial_\sigma + i\mathbf{N}_1 \delta(\sigma) - i\mathbf{N}_2 \delta(\sigma - \pi)) \Psi, \quad (3.51)$$

where we have defined matrices

$$\mathbf{N}_1 = \pi\lambda \begin{bmatrix} 0 & w \\ \bar{w} & 0 \end{bmatrix}, \quad \mathbf{N}_2 = \pi\tilde{\lambda} \begin{bmatrix} 0 & 1 \\ 1 & 0 \end{bmatrix}. \quad (3.52)$$

The factor  $w$  is  $e^{\sqrt{\alpha'} \pi i p_\phi (-)^F}$ . For fixed values of  $\zeta_\pm$ ,  $w$  takes the form  $e^{-2\pi i \zeta_- (-)^F}$ .

If we wish to study the partition function of this theory, we need to diagonalize the Hamiltonian of the system. Following [54, 69], we may Fourier transform in the  $\tau$  direction

$$\Psi(\tau, \sigma) = \int \frac{d\nu}{2\pi} e^{-i\nu\tau} \tilde{\Psi}_\nu(\sigma). \quad (3.53)$$

Inserting this into the equation of motion gives constraints on the allowed values of  $\nu$ ,

$$(-i\nu - \partial_\sigma + i\mathbf{N}_1 \delta(\sigma) - i\mathbf{N}_2 \delta(\sigma - \pi)) \tilde{\Psi}_\nu(\sigma) = 0. \quad (3.54)$$

Integrating, we find

$$\tilde{\Psi}_\nu(\pi) = e^{-2\pi i \nu} e^{-i\mathbf{N}_2} e^{i\mathbf{N}_1} \tilde{\Psi}_\nu(-\pi). \quad (3.55)$$

In this notation, the boundary conditions give also

$$\tilde{\Psi}_\nu(\pi) = -e^{2\pi i(\zeta_+ + \sigma_3 \zeta_-)} \tilde{\Psi}_\nu(-\pi). \quad (3.56)$$

To solve this equation we must demand that  $\tilde{\Psi}_\nu(-\pi)$  be proportional to an eigenvector of

$$\mathcal{N} \equiv e^{-i\mathbf{N}_1} e^{i\mathbf{N}_2} e^{2\pi i \sigma_3 \zeta_-} = \begin{pmatrix} \bar{w} \left( \cos(\pi\lambda) \cos(\pi\tilde{\lambda}) + w \sin(\pi\lambda) \sin(\pi\tilde{\lambda}) \right) & iw \left( \cos(\pi\lambda) \sin(\pi\tilde{\lambda}) - w \sin(\pi\lambda) \cos(\pi\tilde{\lambda}) \right) \\ i\bar{w} \left( \cos(\pi\lambda) \sin(\pi\tilde{\lambda}) - \bar{w} \sin(\pi\lambda) \cos(\pi\tilde{\lambda}) \right) & w \left( \cos(\pi\lambda) \cos(\pi\tilde{\lambda}) + \bar{w} \sin(\pi\lambda) \sin(\pi\tilde{\lambda}) \right) \end{pmatrix}. \quad (3.57)$$

The condition (3.55,3.56) also fixes  $\nu$  up to integer shifts. The eigenvalues of  $\mathcal{N}$  are  $e^{\pm 2\pi i \alpha}$ , where

$$\sin \pi \alpha = \left( \sin^2 \left( \frac{\pi}{2} (\lambda - \tilde{\lambda}) \right) \cos^2 (\pi \zeta_-) + \cos^2 \left( \frac{\pi}{2} (\lambda + \tilde{\lambda}) \right) \sin^2 (\pi \zeta_-) \right)^{1/2}. \quad (3.58)$$

After renaming the values of  $\nu$  which satisfy the equations of motion to  $\omega$ , we

---

<sup>3</sup>Henceforth we are setting  $r = \pi$  in the range of  $\sigma$ .

have the energy eigenvalues (for  $\Psi$ ),

$$\nu \equiv \omega_n^\pm = n - \frac{1}{2} - \zeta_+ \mp \alpha . \quad (3.59)$$

We will define

$$\Delta_\pm = \zeta_+ \pm \alpha(\zeta_-) . \quad (3.60)$$

We write the corresponding eigenvectors as

$$u(\pm\alpha) \equiv \begin{pmatrix} u_1^{(\pm)} \\ u_2^{(\pm)} \end{pmatrix} . \quad (3.61)$$

### 3.4.2 Solutions to Fermionic EOM

Next we present some notes on the structure of the Fock spaces. Our reason for discussing this in so much detail is that the energy eigenstate basis is not the natural one in the orbifold theory that we consider later in the chapter. We may write the matrix which moves us between the 1 – 2 basis and the basis in which  $\mathcal{N}$  is diagonal

$$U = \begin{pmatrix} u_1^{(+)} & u_2^{(+)} \\ u_1^{(-)} & u_2^{(-)} \end{pmatrix} \equiv \begin{pmatrix} \eta \cos \theta & -\xi \sin \theta \\ \xi^* \sin \theta & \eta^* \cos \theta \end{pmatrix} . \quad (3.62)$$

When acting on the fermionic variables, we should enlarge this to

$$\hat{U} = \begin{pmatrix} u_1^{(+)} & u_2^{(+)} & 0 & 0 \\ u_1^{(-)} & u_2^{(-)} & 0 & 0 \\ 0 & 0 & (u_1^{(+)})^* & (u_2^{(+)})^* \\ 0 & 0 & (u_1^{(-)})^* & (u_2^{(-)})^* \end{pmatrix} , \text{ when acting on } \begin{pmatrix} \psi_1 \\ \psi_2 \\ \psi_1^\dagger \\ \psi_2^\dagger \end{pmatrix} . \quad (3.63)$$

With the vectors  $u(\pm\alpha)$ , we may write a general solution to the equation of motion,

$$\begin{aligned} \tilde{\Psi}_{\omega_n^\pm}(\sigma) &= e^{-i\omega_n^\pm \sigma} b_{n,\pm} (1|_{[-\pi,0)} + e^{i\mathbf{N}_1}|_{[0,\pi)} + e^{-i\mathbf{N}_2} e^{i\mathbf{N}_1}|_{\sigma=\pi}) u(\pm\alpha) \\ &\equiv e^{-i\omega_n^\pm \sigma} b_{n,\pm} u(\omega_n^\pm; \sigma) . \end{aligned} \quad (3.64)$$

The field  $\Psi(\tau, \sigma)$  then has the mode expansion

$$\Psi(\tau, \sigma) = \sum_{\pm} \sum_{n \in \mathbb{Z}} e^{-i\omega_n^\pm(\tau+\sigma)} b_{n,\pm} u(\omega_n^\pm; \sigma) . \quad (3.65)$$

The  $b_{n,\pm}$  are essentially the values of the excitations at the  $\sigma = -\pi$  boundary. Similarly, the conjugate field is written

$$\tilde{\Psi}_{\omega_n^\pm}^\dagger(\sigma) = e^{+i\omega_n^\pm \sigma} \bar{b}_{n,\pm} \bar{u}(\omega_n^\pm; \sigma) . \quad (3.66)$$

By demanding that the pieces of  $\Psi$  and  $\Psi^\dagger$  which vanish as they approach the origin in the complex  $z$  plane be proportional to creation operators, we can interpret

$$b_{n,\pm} = \begin{cases} \text{annihilation operator for } n > \frac{1}{2} + \Delta_\pm \\ \text{creation operator for } n < \frac{1}{2} + \Delta_\pm \end{cases} \quad (3.67)$$

with  $\bar{b}_{n,\pm}$  as the conjugate operators with opposite action.

The normal ordered Hamiltonian is

$$\begin{aligned} :H: &= i \int d\sigma : \Psi^\dagger \partial_\tau \Psi : \\ &= \sum_{\pm} \sum_{n \in \mathbb{Z}} \omega_n^\pm : \bar{b}_{n,\pm} b_{n,\pm} : \\ &\equiv \sum_{\pm} \left( \sum_{n \geq 1/2 + \Delta_\pm} \omega_n^\pm \bar{b}_{n,\pm} b_{n,\pm} - \sum_{n < 1/2 + \Delta_\pm} \omega_n^\pm b_{n,\pm} \bar{b}_{n,\pm} \right) \\ &\equiv \sum_{\pm} \left( \sum_{n \geq 1/2 + \Delta_\pm} \omega_n^\pm \bar{b}_{n,\pm} b_{n,\pm} + \sum_{n > 1/2 - \Delta_\pm} \bar{\omega}_n^\pm b_{1-n,\pm} \bar{b}_{1-n,\pm} \right) \end{aligned} \quad (3.68)$$

with

$$\begin{aligned} \omega_n^\pm &= n - 1/2 - \Delta_\pm , \\ \bar{\omega}_n^\pm &= n - 1/2 + \Delta_\pm . \end{aligned} \quad (3.69)$$

The vacuum of the Fock space, for given boundary conditions, then has the structure

$$|vac\rangle = \left[ \prod_{n > \frac{1}{2} + \Delta_+} |n, +\rangle \prod_{\bar{n} > \frac{1}{2} - \Delta_+} \overline{|\bar{n}, +\rangle} \prod_{n' > \frac{1}{2} + \Delta_-} |n', -\rangle \prod_{\bar{n}' > \frac{1}{2} - \Delta_-} \overline{|\bar{n}', -\rangle} \right]_{(\zeta_+, \zeta_-)} \quad (3.70)$$

**Deformed Partition Function:** With the projection onto states of even total fermion number, (before integrating) the partition function takes the form:

$$\begin{aligned} Z(\zeta_-, \zeta_+) &= \frac{1}{2} \sum_{\epsilon = \pm} \prod_{\rho = \pm} \left( \left( q^{\frac{(\zeta_+ + \rho\alpha)^2}{2} - \frac{1}{24}} \prod_n \left( 1 + \epsilon q^{n-1/2-\zeta_+ - \rho\alpha} \right) \right. \right. \\ &\quad \left. \left. \times \left( 1 + \epsilon q^{n-1/2+\zeta_+ + \rho\alpha} \right) \right) \right) \\ &= \sum_{m_-, m_+ \in \mathbb{Z}} \frac{q^{(\zeta_+ + m_+)^2 + (\alpha + m_-)^2 - \frac{1}{12}}}{\prod_n (1 - q^n)^2} . \end{aligned} \quad (3.71)$$

and

$$Z = \int_0^1 d\zeta_+ \int_0^1 d\zeta_- Z(\zeta_+, \zeta_-) . \quad (3.72)$$

The ranges of the  $\zeta_{\pm}$  integrations have been carefully chosen, given the fermion number projection, to cover the original open string momentum space once. The  $Y$  system factors out (recall  $p_Y \leftrightarrow \zeta_+$ , and  $\alpha$  is independent of  $\zeta_+$ ):

$$Z = Z_Y \cdot \int_0^1 d\zeta_- \sum_{m_- \in \mathbb{Z}} \frac{q^{(\alpha+m_-)^2}}{\eta(q)} . \quad (3.73)$$

For comparison with other computations we can write this result in the closed string channel, via Poisson resummation,

$$Z = Z_Y \cdot \int_0^1 d\zeta_- \frac{1}{\sqrt{2}} \sum_{\tilde{j}=0, \frac{1}{2}, 1, \dots} \chi_{\tilde{j}^2}^{Vir}(\tilde{q}^2) \chi_{\tilde{j}}^{SU(2)}(e^{4\pi i \alpha J^3}) . \quad (3.74)$$

### 3.4.3 Boundary States at $R = \infty$

By observing the fermionized partition function, we can write a boundary state which correctly reproduces the open string partition function. Using the formula (3.9) we can write the partition function as an overlap of boundary states projected to infinite radius,

$$\langle B(\tilde{\lambda}; R = \sqrt{\alpha'}) | P_{\infty} \Delta(\tilde{q}^2) P_{\infty} | B(\lambda; R = \sqrt{\alpha'}) \rangle , \quad (3.75)$$

where

$$|B(\lambda; R = \sqrt{\alpha'}) \rangle = \sum_{j=0, 1/2, 1, \dots} \sum_{m, n} \varphi^j \mathcal{D}_{m, n}^{(j)}(e^{2\pi i \lambda J_0^1}) |j, -m, n \rangle . \quad (3.76)$$

Note that there is a possible phase  $\varphi$  here that is undetermined by the annulus computation; we will retain it for now. The projection to infinite radius is defined as [63]

$$P_{\infty} |B(\lambda; R = \sqrt{\alpha'}) \rangle = \int_0^1 d\zeta_- \sum_{j=0, 1/2, 1, \dots} \varphi^j \sum_{m, n} \mathcal{D}_{m, n}^{(j)}(e^{+2\pi i \zeta_- J_0^3} e^{2\pi i \lambda J_0^1} e^{+2\pi i \zeta_- J_0^3}) |j, -m, n \rangle . \quad (3.77)$$

Since  $P_{\infty}$  is a projection operator, one may show that this boundary state is consistent with the form of  $Z_{\lambda, \tilde{\lambda}}$ . We may also show that this is equivalent to the standard expression [53]

$$P_{\infty} |B(\lambda; R = \sqrt{\alpha'}) \rangle = \sum_{j=0, 1/2, 1, \dots} \varphi^j \sum_m \mathcal{D}_{-m, m}^{(j)}(e^{2\pi i \lambda J_0^1}) |j, m, m \rangle , \quad (3.78)$$

where it is manifest that the winding modes have been projected out by the infinite radius limit.

Let us also check various limits of  $\lambda$ . First, take  $\lambda = 0$ , which should give us the Neumann state:

$$P_\infty |B(0; R = \sqrt{\alpha'})\rangle = \sum_{j=0,1/2,1,\dots} \varphi^j |j, 0, 0\rangle, \quad (3.79)$$

where we have used<sup>4</sup>  $\mathcal{D}_{m,n}^{(j)}(\mathbb{I}) = \delta_{m,n}$ . This is the expected result.

For  $\lambda = 1/2$ :

$$P_\infty |B(1/2; R = \sqrt{\alpha'})\rangle = \sum_{j=0,1/2,1,\dots} \sum_m \varphi^j \mathcal{D}_{-m,m}^{(j)}(e^{i\pi J_0^1}) |j, m, m\rangle \quad (3.80)$$

and one finds  $\mathcal{D}_{-m,m}^{(j)}(e^{i\pi J_0^1}) = e^{i\pi j}$ . Thus we have

$$P_\infty |B(1/2; R = \sqrt{\alpha'})\rangle = \sum_{j=0,1/2,1,\dots} \varphi^j e^{i\pi j} \sum_m |j, m, m\rangle. \quad (3.81)$$

By rewriting this expression in oscillator variables, it becomes clear that it corresponds to an *array* of point-like D-branes separated by a distance  $2\pi\sqrt{\alpha'}$ ; that is, it is proportional to [56]

$$\sum_{s \in \mathbb{Z}} \delta(x - (\pi/2 + 2\pi s)\sqrt{\alpha'}),$$

if we set the phase  $\varphi$  to one. In fact,  $\varphi$  simply corresponds to the freedom to translate the array of branes.

### 3.4.4 Projection to Generic Radii

The fermionic calculation considered above is, strictly speaking, valid at infinite radius. The bosonic calculation is on the other hand valid at self-dual radius. With some care, we can in fact do the fermionic calculation at any (rational) radius. To our knowledge, this has not been described before from the open string point of view. In the boundary state formalism, there is a proposal [63, 70], given by introducing suitable projection operators. By carefully considering the open string calculation, we will be able to explicitly display the meaning of these projection operators, and the limits of applicability of the fermionic picture.

To see that there is a potential problem in the fermionic theory, consider the fermion boundary conditions. Recall that  $\zeta_-$  is the fractional part of what was

---

<sup>4</sup>In the notation used here, the general formula is

$$\mathcal{D}_{mn}^{(j)} \begin{pmatrix} a & b \\ c & d \end{pmatrix} = \sum_k \frac{[(j+m)!(j-m)!(j+n)!(j-n)!]^{1/2}}{k!(j-m-k)!(j+n-k)!(m-n+k)!} a^{j+n-k} b^{m-n+k} c^k d^{j-m-k}.$$

open string momentum in the bosonic picture. At finite radius, the open string momentum is quantized in units of  $1/R$ , and thus one might expect that one could obtain the annulus amplitude by restricting the values of  $\zeta_-$  appropriately [54]. However, this only has limited applicability, to the case of integer radius (in units of  $\sqrt{\alpha'}$ ). One can easily show that this procedure fails for any other radius.

In the fermionic picture this can be seen from the boundary conditions: if the radius is not an integer, then  $\zeta_- = 1$  is not equivalent to  $\zeta_- = 0$ , and this means that the fermionization does not make sense. This has roots in the fact that in the bosonic picture, the boundary operator  $e^{iX/\sqrt{\alpha'}}$  is not single-valued at generic radius, and thus the deformed theory does not exist. It is easy to repair this however, at least at rational radius, as we will now show.

Indeed, we may think of the finite radius theory as a shift orbifold, and define the theory by introducing a projection operator into open-string correlators of the form

$$P_{(R)} = \sum_{m \in \mathbb{Z}} e^{2\pi i \hat{P} m R} , \quad (3.82)$$

where  $\hat{P}$  is the momentum operator. In the undeformed theory, this implements the projection to finite radius correctly. In the deformed theory, the boundary operator

$$S_\lambda = \frac{1}{2} \int_{\partial\Sigma} ds \left[ \lambda e^{iX(s)/\sqrt{\alpha'}} + h.c. \right] \quad (3.83)$$

undergoes a transformation

$$S_\lambda \rightarrow \frac{1}{2} \int_{\partial\Sigma} ds \left[ \lambda e^{2\pi i R/\sqrt{\alpha'}} e^{iX(s)/\sqrt{\alpha'}} + h.c. \right] \quad (3.84)$$

under the shift  $X \rightarrow X + 2\pi R$ . Thus, if we insert  $P_{(R)}$  into the path integral, it does not commute with the action precisely, and so the theory is not well-defined. It is easy to see how to repair this however; essentially, in the deformed BCFT, we must include a non-trivial action in Chan-Paton corresponding to the shift. We may define a new theory by simply averaging the infinite radius theory over the values of  $\lambda$  in the image of all possible shifts. If we write  $R = (M/N)\sqrt{\alpha'} \equiv r\sqrt{\alpha'}$ , then we would have for the annulus amplitude

$$\mathcal{A}_{R;\lambda,\tilde{\lambda}} \equiv \frac{1}{N^2} \sum_{n=0}^{N-1} \sum_{\tilde{n}=0}^{N-1} Tr(P_{(R)} q^{L_0-1/24} e^{S_{\lambda e^{2\pi i n r}} + S_{\tilde{\lambda} e^{2\pi i \tilde{n} r}}}) . \quad (3.85)$$

This theory has the interpretation of the Chan-Paton space for each boundary being extended to be  $N$ -component, each with a complex deformation parameter  $\lambda e^{2\pi i n r}$ , for  $n = 0, 1, \dots, N-1$ . Note that at integer radius ( $N = 1$ ), this modification has no effect.

We emphasize that the expression (3.85) is an infinite radius calculation, expressed in the bosonic language. It is natural, because of the insertion, to

evaluate it in momentum space. In this case, eq. (3.85) differs from previous computations in two ways: first, there is a momentum dependent phase factor, and secondly, for any given  $m, n, \tilde{n}$ , there are effectively complex values of the boundary deformation parameters. Since we are at infinite radius, we may fermionize. In so doing, we find a generalization of the previous result: the important parameter  $\alpha$  now takes the form

$$\sin^2 \pi \alpha = \sin^2 \frac{\pi}{2} (|\lambda| - |\tilde{\lambda}|) + \sin^2 \pi \zeta_- \cos \pi |\lambda| \cos \pi |\tilde{\lambda}| + \sin^2 \pi (n - \tilde{n}) r \sin \pi |\lambda| \sin \pi |\tilde{\lambda}| \quad (3.86)$$

depending in general on  $|\lambda|, n, |\tilde{\lambda}|, \tilde{n}, \zeta_-$ .

We recall that the open string momentum was split into an integer  $\ell$  and  $\zeta_- \in [0, 1)$ . Thus, we obtain

$$\mathcal{A}_{R;\lambda,\tilde{\lambda}} = \frac{1}{N^2 \eta(q)} \sum_{m,\ell \in \mathbb{Z}} \sum_{n=0}^{N-1} \sum_{\tilde{n}=0}^{N-1} \int_0^1 d\zeta_- e^{2\pi i \zeta_- m r} e^{2\pi i \ell m r} q^{(\ell+\alpha)^2} \quad (3.87)$$

with  $\alpha$  now given by eq. (3.86), which is the generalization of previous results to complex couplings. Note that it is encoding the fact that  $|\lambda|$  and  $|\tilde{\lambda}|$  have been renormalized (in the fashion given by Ref. [53]) but the phases  $n, \tilde{n}$  are essentially not renormalized.<sup>5</sup> Thus the result is a function of  $|\lambda|, n; |\tilde{\lambda}|, \tilde{n}$  but *not* just of  $\lambda, \tilde{\lambda}$ .

It is important to realize that what we have done here is to resolve the classical problem of finite radius. In going to the fermionic representation however, there is a potential quantum problem as well – that is, the fermionic measure may not be well-defined in the presence of the projection operator. Indeed, the translation operator corresponds precisely to a chiral  $\mathbb{Z}_{2N}$  transformation on the fermions, and thus the measure is not invariant, transforming by a  $\mathbb{Z}_N$  phase. This may be repaired by introducing an array of Wilson lines, as

$$\mathcal{A}_{R;\lambda,\tilde{\lambda}}^{fermionic} = \frac{1}{N^2 \eta(q)} \sum_{m,\ell \in \mathbb{Z}} \sum_{n=0}^{N-1} \sum_{\tilde{n}=0}^{N-1} \int_0^1 d\zeta_- e^{2\pi i \zeta_- m r} e^{2\pi i \ell m r} q^{(\ell+\alpha)^2} \sum_{k=0}^{N-1} e^{-2\pi i m k / N} . \quad (3.88)$$

The idea is that the action of the projection operator on the fermionic measure leads to a  $\mathbb{Z}_N$  phase, which can be absorbed by a shift to another Wilson line. Thus, we obtain a well-defined fermionic theory by summing over such Wilson lines. It is important to note here that what is being said is that consistent fermionic theories can be defined only if we include the array of Wilson lines. The bosonic theory exists in the absence of the Wilson line array, but we have no way to compute in the deformed theory, away from self-dual radius. Note further that the Wilson line array appears only for fractional radii (i.e.,  $N \neq 1$ ); the integer radius cases work just fine without it.

<sup>5</sup>The reason for this dichotomy is that the renormalization comes from the collision of  $J_+$  and  $J_-$  insertions, each of which is accompanied by  $|\lambda|$ , but opposite phases. Thus the powers of  $|\lambda|$  build up, but the phases tend to cancel and do not renormalize.

Now what the array of Wilson lines does is force  $m = Ns$ , for  $s \in \mathbb{Z}$ . We then obtain

$$\begin{aligned}
\mathcal{A}_{R;\lambda,\tilde{\lambda}}^{fermionic} &= \frac{1}{N^2\eta(q)} \sum_{s,\ell \in \mathbb{Z}} \sum_{n=0}^{N-1} \sum_{\tilde{n}=0}^{N-1} \int_0^1 d\zeta_- e^{2\pi i \zeta_- Ms} q^{(\ell+\alpha)^2} \\
&= \frac{1}{MN^2\eta(q)} \sum_{\ell \in \mathbb{Z}} \sum_{n=0}^{N-1} \sum_{\tilde{n}=0}^{N-1} \int_0^1 d\zeta_- \sum_{k' \in \mathbb{Z}} \delta(\zeta_- - k'/M) q^{(\ell+\alpha)^2} \\
&= \frac{1}{MN^2\eta(q)} \sum_{\ell \in \mathbb{Z}} \sum_{n,\tilde{n}=0}^{N-1} \sum_{k'=0}^{M-1} q^{(\ell+\alpha(\zeta_- = k'/M))^2} . \tag{3.89}
\end{aligned}$$

For later use, we note that this can be manipulated into the form

$$\frac{1}{MN\eta(q)} \sum_{\ell \in \mathbb{Z}} \sum_{k=0}^{N-1} \sum_{k'=0}^{M-1} q^{(\ell+\beta(\zeta_- = k'/M))^2} \tag{3.90}$$

where

$$\cos 2\pi\beta = \cos \pi|\lambda| \cos \pi|\tilde{\lambda}| \cos 2\pi\zeta_- + \sin \pi|\lambda| \sin \pi|\tilde{\lambda}| \cos 2\pi k/N \tag{3.91}$$

This formula is a direct consequence of (3.86).

Let us consider a few special cases. First, the NN amplitude should be recovered by taking  $\lambda, \tilde{\lambda} \rightarrow 0$ . In this case,  $\alpha = \zeta_-$ , independent of  $n, \tilde{n}$ , and so we find

$$\frac{1}{M\eta(q)} \sum_{\ell \in \mathbb{Z}} \sum_{k'=0}^{M-1} q^{(\ell+k'/M)^2} = \frac{1}{M\eta(q)} \sum_{\ell \in \mathbb{Z}} q^{\ell^2/M^2} \tag{3.92}$$

which may be recognized as the NN amplitude at radius  $R$ , with the array of Wilson lines. Note also that

$$\mathcal{A}_{R;1,0} = \frac{1}{M\eta(q)} \sum_{\ell \in \mathbb{Z}} q^{(\ell/M+1/2)^2} . \tag{3.93}$$

Next let us consider the ND case, obtained by  $\lambda = 1/2, \tilde{\lambda} = 0$ . Here, we obtain  $\alpha = 1/4$ , independent of  $n, \tilde{n}$ , as well as  $\zeta_-$  and thus

$$\mathcal{A}_{R;1/2,0} = \frac{1}{\eta(q)} \sum_{l \in \mathbb{Z}} q^{(\ell+1/4)^2} . \tag{3.94}$$

Finally consider the DD case, obtained via  $\lambda = \tilde{\lambda} = 1/2$ , whence  $\alpha = (n - \tilde{n})r$ . Thus, we find

$$\mathcal{A}_{R;1/2,1/2} = \frac{1}{N^2\eta(q)} \sum_{\ell \in \mathbb{Z}} \sum_{n,\tilde{n}=0}^{N-1} q^{\ell+(n-\tilde{n})r} . \tag{3.95}$$

It is possible to show that the sum over  $n, \tilde{n}$  can be written as

$$\mathcal{A}_{R;1/2,1/2} = \frac{1}{N\eta(q)} \sum_{\ell \in \mathbb{Z}} \sum_{k=-j}^j q^{(N\ell+kM)^2/N^2} \quad (3.96)$$

where  $j = \lfloor N/2 \rfloor$ . This is

$$\mathcal{A}_{R;1/2,1/2} = \frac{1}{N\eta(q)} \sum_{\ell \in \mathbb{Z}} q^{\ell^2/N^2} \quad (3.97)$$

which is the correct result for an array of  $M$  D-branes, located at integer multiples of  $\sqrt{\alpha'}/N$ . This is the expected result [56], with branes located at extrema of the boundary potential. It is clear that this array of D-branes is T-dual to the array of Wilson lines at  $\lambda = \tilde{\lambda} = 0$ . For generic values of  $\lambda, \tilde{\lambda}$ , we interpolate smoothly between the two arrays, again as should be expected. The absence of the fermionic anomaly mentioned above corresponds to the recovery of T-duality in the annulus amplitude.

### Boundary States at Radius $r$

These finite radius annulus amplitudes may be transformed into the closed string channel. The result is consistent with boundary states given (from closed channel reasoning) by Gaberdiel and Recknagel [63]. They are written via projection operators acting on the self-dual radius result (here we have made a requisite translation into our conventions)

$$\begin{aligned} |B(\lambda; R)\rangle &= P_M^+ P_N^- \sum_{j \in 0, 1/2, \dots} \sum_{m, \tilde{m} = -j}^j \varphi^j \mathcal{D}_{m\tilde{m}}^j \left( e^{2\pi i \lambda J^1} \right) |j, -m, \tilde{m}\rangle \quad (3.98) \\ &\equiv \frac{1}{\sqrt{MN}} \sum_{\ell=0}^{M-1} \sum_{k=0}^{N-1} \sum_{j \in 0, 1/2, \dots} \sum_{m, \tilde{m} = -j}^j \varphi^j \\ &\quad \times \mathcal{D}_{m\tilde{m}}^j \left( e^{2\pi i (\frac{\ell}{M} + \frac{k}{N}) J^3} e^{2\pi i \lambda J^1} e^{2\pi i (\frac{\ell}{M} - \frac{k}{N}) J^3} \right) |j, -m, \tilde{m}\rangle. \end{aligned}$$

Using this boundary state, one obtains the following for the open string partition function,

$$\frac{1}{MN} \sum_{l=0}^{M-1} \sum_{k=0}^{N-1} \sum_{n \in \mathbb{Z}} \frac{q^{(n+\beta(\lambda, \tilde{\lambda}; \ell, k))^2}}{\eta(q)}. \quad (3.99)$$

Here  $\beta$  satisfies

$$2 \cos(2\pi\beta(\lambda, \tilde{\lambda}; \ell, k)) \equiv \text{Tr}_{r_{1/2}} \left( e^{-2\pi i \tilde{\lambda} J^1} e^{2\pi i (\frac{\ell}{M} + \frac{k}{N}) J^3} e^{2\pi i \lambda J^1} e^{2\pi i (\frac{\ell}{M} - \frac{k}{N}) J^3} \right). \quad (3.100)$$

One may show that the set of values of  $\beta$  is equivalent to the set of  $\alpha$ 's in eq. (3.89). This result is equivalent to the open string result, as long as the array of Wilson lines is included. Note that this is important, because the boundary

states proposed transform in a simple way under T-duality. Without the Wilson lines, T-duality is not implemented by flowing from  $\lambda = 0$  to  $\lambda = 1/2$ .

### 3.5 The $\mathbb{Z}_2$ Orbifold

We will now consider the orbifold action in the BCFT (3.31). For the annulus computation, this is implemented by including the orbifold projection operator  $\frac{1}{2}(1 + g)$  in the path integral. The first term (proportional to 1) is equivalent, up to the factor of two, to the results given above. On a self-dual circle we may derive the effect of inserting  $g$  through adsorption methods (see Ref. [60] for the construction in the undeformed theory). Because the states are classified by current algebra and we know the orbifold action on the algebra, it is straightforward to compute the  $g$ -inserted trace at self-dual radius. As in the previous sections, to discuss more general radii we must fermionize the theory. When fermionizing we will consider two possible orbifold actions: either  $g$  acts only the  $X$  field (“ $c = 1$  orbifold”) or it acts on both  $X$  and  $Y$  (“ $c = 2$  orbifold”). In either case, we should be able to disentangle the ( $g$ -inserted) partition functions of the  $X$  and  $Y$  systems. The consistency of these three routes is strong evidence that we have correctly orbifolded the deformed boson.

In the orbifold theory, there are a variety of open string annulus calculations that we can do, depending on the details of Chan-Paton factors, as we have discussed briefly above. We will consider these details in Ref. [58] and here simply concentrate on the calculation of the annulus diagram with orbifold insertion. This will be the basic building block needed to construct fractional boundary states.

#### 3.5.1 Self-dual Radius and Adsorption

The orbifold is obtained by defining  $\mathbb{Z}_2$  as  $X \mapsto -X$ , or in terms of the current,

$$J^1 \rightarrow J^1 ; J^2 \rightarrow -J^2 ; J^3 \rightarrow -J^3 . \quad (3.101)$$

At self-dual radius, it is convenient to organize the calculation entirely in terms of the  $\widehat{su(2)}_1$  modules. Since the deformation is in the direction of  $J^1$  rather than  $J^3$ , it is more convenient to work in the  $su(2)$  basis where  $J_0^1$  is diagonal, as we described in Section 3.3. The orbifold action then switches the sign of the ladder operators. The  $g$ -inserted partition function is (see Appendix A for a detailed analysis)

$$\text{Tr } g q^{L_0 - 1/24} = \frac{1}{\eta(q)} \sum_{n \in \mathbb{Z}} (-1)^n q^{(n + \lambda/2)^2} . \quad (3.102)$$

For other radii, we now turn to the fermionic description.

### 3.5.2 Fermionic Description of the Orbifold

Let's discuss the  $\mathbb{Z}_2$  orbifold of the deformed theory. After detailed computations, the two orbifold actions may be determined consistently to be as given in the following table.

$c = 2$ Orb	$c = 1$ Orb
$X \rightarrow -X$	$X \rightarrow -X$
$Y \rightarrow -Y$	$Y \rightarrow Y$
$\psi_1 \rightarrow \psi_1^\dagger$	$\psi_1 \rightarrow i\psi_2 e^{2\pi i\zeta_-}$
$\psi_2 \rightarrow -\psi_2^\dagger$	$\psi_2 \rightarrow i\psi_1 e^{2\pi i\zeta_-}$
$\psi_1^\dagger \rightarrow \psi_1$	$\psi_1^\dagger \rightarrow -i\psi_2^\dagger e^{-2\pi i\zeta_-}$
$\psi_2^\dagger \rightarrow -\psi_2$	$\psi_2^\dagger \rightarrow -i\psi_1^\dagger e^{-2\pi i\zeta_-}$

The phases that appear in the table may look strange; in particular, it might appear that  $g_1$  does not square to one. However, the table refers to the action on single fermions, which do not by themselves create physical states (recall the fermion number projection). The phases in the table are fixed by the requirement that the  $SU(2)_X$  current algebra as well as other fermion bilinears transform in a sensible way under the orbifold actions. In particular,  $g$  does square to one on all physical states, in each case.

In order to proceed we need to rephrase the orbifold as an action in the  $\pm$  basis rather than the  $1 - 2$  basis. This is accomplished by making a similarity transformation on the orbifold generator,  $\hat{U}g\hat{U}^\dagger$ . The action of  $g_1$  on the  $\psi - \psi^\dagger$  and  $\pm$  labels of the field is given by:

$$\hat{U}g_1\hat{U}^{-1} = \begin{pmatrix} iG_1 & 0 \\ 0 & -iG_1^* \end{pmatrix} \quad (3.103)$$

where

$$G_1 = e^{2\pi i\zeta_-} U g U^{-1}, \quad (3.104)$$

with  $g$  from the table,

$$g = \begin{pmatrix} 0 & 1 \\ 1 & 0 \end{pmatrix}, \quad (3.105)$$

and  $U$  was given in a preceding section. The action of  $g_2$  on the  $\psi - \psi^\dagger$  and  $\pm$  labels of the field is given by:

$$\hat{U}g_2\hat{U}^{-1} = \begin{pmatrix} 0 & G_2 \\ G_2^* & 0 \end{pmatrix} \quad (3.106)$$

where

$$G_2 = U g U^{-1} \quad (3.107)$$

and from the table,

$$g = \begin{pmatrix} 1 & 0 \\ 0 & -1 \end{pmatrix}. \quad (3.108)$$

Having determined how the orbifold acts on the fields of the theory, it remains to determine the action on the ground state. Fortunately, this is facilitated by the fact that we knew how the orbifold acted upon the momenta of the bosonic theory. Consistency demands that  $g$  acts on the  $\zeta_-$  and  $\zeta_+$  as it did on the  $X$  and  $Y$  momenta, respectively. The orbifold action on the interacting ground state is:

$$\begin{aligned} g_1 \cdot \left[ |n, +\rangle \otimes \overline{|\bar{n}, +\rangle} \otimes |n', -\rangle \otimes \overline{|\bar{n}', -\rangle} \right]_{(\zeta_+, \zeta_-)} \\ = \left[ |n, +\rangle \otimes \overline{|\bar{n}, +\rangle} \otimes |n', -\rangle \otimes \overline{|\bar{n}', -\rangle} \right]_{(\zeta_+, -\zeta_-)} \\ g_2 \cdot \left[ |n, +\rangle \otimes \overline{|\bar{n}, +\rangle} \otimes |n', -\rangle \otimes \overline{|\bar{n}', -\rangle} \right]_{(\zeta_+, \zeta_-)} \\ = \left[ |n, +\rangle \otimes \overline{|\bar{n}, +\rangle} \otimes |n', -\rangle \otimes \overline{|\bar{n}', -\rangle} \right]_{(-\zeta_+, -\zeta_-)} \end{aligned}$$

We see that  $g_1$  effectively flips the sign of  $\zeta_-$  and  $g_2$  flips the sign of both  $\zeta_+$  and  $\zeta_-$  inside the vacuum states.

### Orbifold-inserted Traces

Because the orbifold action mixes all of the oscillators, at each value of  $n$  there is the possibility for many terms to contribute. The orbifold actions on the vacuum states limit the values of  $\zeta_{\pm}$  which contribute to the  $g$ -inserted partition functions—that is, there will be  $\delta$ -functions which restrict to the fixed points of the orbifold action. As before, we use the same fermion insertion  $(1 + (-1)^{F_T})/2$  and integration measure  $\int_0^1 d\zeta_+ \int_0^1 d\zeta_-$ .

**$c = 1$  Orbifold:** Since  $\zeta_+ \mapsto \zeta_+$  and  $\zeta_- \mapsto -\zeta_-$  under the orbifold action, there is a fixed line at  $\zeta_- = 0$ . Here,  $\alpha = (\lambda - \tilde{\lambda})/2 \pmod{1}$ , and

$$U = \begin{pmatrix} \frac{1}{\sqrt{2}} & -\frac{1}{\sqrt{2}} \\ \frac{1}{\sqrt{2}} & \frac{1}{\sqrt{2}} \end{pmatrix} \quad (3.109)$$

and thus the orbifold action on single fermion states is determined by

$$\hat{U} g_1 \hat{U}^\dagger = \begin{pmatrix} iG & 0 \\ 0 & -iG^{*s} \end{pmatrix} = \begin{pmatrix} -ie^{2\pi i \zeta_-} & 0 & 0 & 0 \\ 0 & ie^{2\pi i \zeta_-} & 0 & 0 \\ 0 & 0 & ie^{-2\pi i \zeta_-} & 0 \\ 0 & 0 & 0 & -ie^{-2\pi i \zeta_-} \end{pmatrix}. \quad (3.110)$$

Note that the factors of  $i$  that appear here are required by consistency (although they did not appear "geometrically"). As we discussed above, it looks as if  $g_1^2 = -1$ ; however, this is acting on single-fermion states—since there are no such physical states, we can allow such an action. It must act as  $g_1^2 = +1$  on all double fermion states however. We can see that we need the factors of  $i$  by examining operators like  $\psi_+\psi_-$ , which consists of  $Y$  only, and thus should be orbifold invariant.

There is also a fixed line at  $\zeta_- = 1/2$ , because  $\zeta$ 's are defined mod 1. Here,  $\alpha = (\lambda + \tilde{\lambda} - 1)/2 \pmod{1}$  and  $U$  is the same as above.

The  $g_1$  trace takes the form  $\int_0^1 d\zeta_+ \int_0^1 d\zeta_- [\delta(\zeta_-) + \delta(\zeta_- - 1/2)]$  times

$$q^{\zeta_+^2 + \alpha^2 - 1/12} \frac{1}{2} \sum_{\pm} \prod_{n=1}^{\infty} (1 \mp ie^{2\pi i \zeta_-} q^{\omega_n^+}) (1 \pm ie^{2\pi i \zeta_-} q^{\omega_n^-}) (1 \pm ie^{-2\pi i \zeta_-} q^{\bar{\omega}_n^+}) (1 \mp ie^{-2\pi i \zeta_-} q^{\bar{\omega}_n^-}).$$

The sum  $\sum_{\pm}$  is the fermion number projection. This result can be written in terms of a product of  $\theta$ -functions; using the sum representation for the  $\theta$ -functions, we then find

$$\frac{q^{\zeta_+^2 + \alpha^2}}{\eta^2(q)} \sum_{n,m \in \mathbb{Z}} q^{n^2/2} q^{m^2/2} (ie^{2\pi i \zeta_-} q^{-\zeta_+ - \alpha})^n (ie^{2\pi i \zeta_-} q^{-\zeta_+ + \alpha})^m \left[ \frac{(-1)^n + (-1)^m}{2} \right]$$

Defining  $m_{\pm} = (n \pm m)/2$ , we find

$$\begin{aligned} Z_{\lambda, \tilde{\lambda}}^{g_1} &= \int d\zeta_+ \sum_{\zeta_- = 0, 1/2} \frac{q^{\zeta_+^2 + \alpha^2}}{\eta^2(q)} \\ &\cdot \sum_{m_+, m_- \in \mathbb{Z}} q^{m_+^2} q^{m_-^2} e^{4\pi i \zeta_- m_+} q^{-2\zeta_+ m_+} q^{-2\alpha m_-} (-1)^{m_-} \\ &\left( \frac{1}{\eta(q)} \int_0^1 d\zeta_+ \sum_{m_+ \in \mathbb{Z}} q^{(m_+ + \zeta_+)^2} \right) \\ &= \left( \sum_{\zeta_- = 0, 1/2} \frac{1}{\eta(q)} \sum_{m_- \in \mathbb{Z}} q^{(m_- + \alpha)^2} (-1)^{m_-} \right). \end{aligned} \quad (3.111)$$

This is to be summed over the two values of  $\zeta_-$ ; for both of those values, the  $\zeta_-$ -dependent term in the  $m_+$  sum equals unity, and we have dropped it. So, we see that the  $g_1$ -inserted partition function decouples nicely into  $X$  and  $Y$ . The integral over  $\zeta_+$  combines with the  $m_+$  sum to give the partition function of the free boson  $Y$  while the  $m_-$  sum is the twisted partition function of  $X$ .

**$c = 2$  Orbifold:** Because both  $\zeta_{\pm}$  are set to zero modulo periodicities in the  $c = 2$  orbifold, we only get contributions from the points  $(0, 0)$  and  $(1/2, 1/2)$ .

The action of the orbifold on the fermion fields is given by:

$$\hat{U}g_2\hat{U}^\dagger = \begin{pmatrix} 0 & 0 & 0 & 1 \\ 0 & 0 & 1 & 0 \\ 0 & 1 & 0 & 0 \\ 1 & 0 & 0 & 0 \end{pmatrix}. \quad (3.112)$$

The diagonal combinations of states are

$$|vac\rangle, \psi_-^\dagger\psi_+|vac\rangle, \psi_+^\dagger\psi_-|vac\rangle, \psi_-^\dagger\psi_+\psi_+^\dagger\psi_-|vac\rangle.$$

For the two points, we find

$$\text{at } \zeta_\mp = 0: \alpha(0) = \frac{\lambda - \tilde{\lambda}}{2}, \quad \text{Casimir energy} = \left(\frac{\lambda - \tilde{\lambda}}{2}\right)^2 - \frac{1}{12}$$

$$\text{at } \zeta_\mp = 1/2: \alpha(1/2) = \frac{\lambda + \tilde{\lambda} - 1}{2}, \quad \text{Casimir energy} = \left(\frac{\lambda + \tilde{\lambda} - 1}{2}\right)^2 - \frac{1}{12}.$$

The trace, with  $g_2$  inserted, becomes:

$$\begin{aligned} Z_{\lambda, \tilde{\lambda}}^{g_2} &= \sum_{(\zeta_-, \zeta_+) = (0,0), (1/2, 1/2)} q^{\alpha^2 - 1/12} \\ &\quad \prod_n \left(1 - (q^2)^{n-1/2+\alpha}\right) \left(1 - (q^2)^{n-1/2-\alpha}\right) \\ &= \left(\frac{q^{-1/24}}{\prod_n (1 + q^n)}\right) \cdot \left(\sum_{\zeta_- = 0, 1/2} \frac{1}{\eta(q)} \sum_{n \in \mathbb{Z}} (-)^n q^{(n+\alpha)^2}\right). \end{aligned} \quad (3.113)$$

We have split the trace into separate contributions from  $(\zeta_-, \zeta_+) = (0, 0)$  and  $(1/2, 1/2)$ . The minus sign in the factors is due to the anti-commutivity of the fermion fields. Note that the powers of  $q$  here are all independent of  $\zeta_+$ , an important feature. The insertion of  $g_2$  restricts the trace to be over states of even fermion number, implying that the total fermion number projection operator acts as the identity in the presence of  $g_2$ . Again, the  $g$ -inserted partition function has factorized into contributions from  $X$  and  $Y$ .

### 3.5.3 Summary of Open String Partition Functions

Before moving on to discuss the space-time effects of these open string theories, it is useful to summarize the results found in this chapter.

At the self-dual radius, one finds

$$Z_{\lambda, \tilde{\lambda}}^g = \frac{1}{\eta(q)} \sum_{n \in \mathbb{Z}} (-)^n q^{(n+(\lambda-\tilde{\lambda})/2)^2} \quad (3.114)$$

using adsorption methods. For infinite radius, we may decouple the  $Y$ -system

from the result of fermionization to obtain

$$Z_1 = \frac{1}{\eta(q)} \int_0^1 d\zeta_- \sum_{m \in \mathbb{Z}} q^{(m+\alpha(\zeta_-))^2} \quad (3.115)$$

and

$$Z_g = \frac{1}{\eta(q)} \sum_{\zeta_- = 0, 1/2} \sum_{m \in \mathbb{Z}} (-1)^m q^{(m+\alpha(\zeta_-))^2} . \quad (3.116)$$

Here,

$$\sin \pi \alpha = \left( \sin^2 \left( \frac{\pi}{2} (\lambda - \tilde{\lambda}) \right) \cos^2 (\pi \zeta_-) + \cos^2 \left( \frac{\pi}{2} (\lambda + \tilde{\lambda}) \right) \sin^2 (\pi \zeta_-) \right)^{1/2} \quad (3.117)$$

Notice that the  $\zeta_- = 0$  term reproduces the self-dual radius result. This is correct, since at self-dual radius half-integer momentum ( $\zeta_- = 1/2$ ) is not present. It is a confirmation of our methods that the contributions at  $\zeta_- = 0$  to  $Z_{\lambda, \tilde{\lambda}}^g$  obtained from fermionization match the result of the self-dual radius adsorption methods.

Also recall that for  $Z_1$ , we can write the result in terms of Virasoro and  $SU(2)$  characters of the closed string channel

$$\begin{aligned} Z_1 &= \frac{1}{\sqrt{2}} \frac{1}{\eta(\tilde{q}^2)} \int_0^1 d\zeta_- \sum_{m \in \mathbb{Z}} (\tilde{q}^2)^{m^2/4} e^{2\pi i \alpha(\zeta_-) m} \\ &= \frac{1}{\sqrt{2}} \sum_{j=0, 1/2, 1, \dots} \chi_{j^2}^{Vir}(\tilde{q}^2) \int_0^1 d\zeta_- \chi_j^{SU(2)}(e^{4\pi i \alpha(\zeta_-) J^3}) . \end{aligned} \quad (3.118)$$

The corresponding result for  $Z_g$  follows from Poisson resummation

$$Z_g = \frac{1}{\sqrt{2}} \frac{1}{\eta(\tilde{q}^2)} \sum_{\zeta_- = 0, 1/2} \sum_{m \in \mathbb{Z}} (\tilde{q}^2)^{(m-1/2)^2/4} e^{2\pi i \alpha(\zeta_-)(m-1/2)} . \quad (3.119)$$

Other radii may be obtained by suitable projection operators, as discussed in Section 3.4.4. A treatment of all possible boundary states of the orbifold theory appears in Ref. [58]. In the next chapter we shall use these results to model initial conditions for spacetimes in the presence of cosmological singularities.

## Chapter 4

# S-branes in the Presence of a Time-Dependent Orbifold

It is interesting to ask how to construct D-branes in Lorentzian orbifolds. Work in this direction includes studies of D-branes in Misner space.<sup>1</sup> Here we would like to address a different issue. The D-branes of bosonic string theory are unstable, and such branes (or configurations of stable branes that destabilize at a subcritical separation) exist also in supersymmetric theories. Hence one must be able to describe their decay in Lorentzian orbifolds. Understanding of the brane decay by itself is an important topic for completeness of string theory. Further such processes play an important role in many cosmological scenarios, adding to the interest in this problem with applications in mind.

There are many ways to investigate brane decay. The most straightforward and hence in a sense a most illuminating one is to work on the level of worldsheet string theory and attempt to deform the action by an operator that describes the decay in the form of a rolling tachyon background [56, 77]. Such deformations must be exactly marginal, i.e. preserve the conformal invariance even at large deformations in order not to spoil the unitarity of the theory. The construction of such exactly marginal deformations is difficult in general, and a hurdle for studies of brane decay in Lorentzian orbifolds.

In this chapter we take the first steps to investigating brane decay (S-branes [55]) in time-dependent string backgrounds, in particular on the  $\mathbb{R}^{1,d}/\mathbb{Z}_2$  space-time orbifolds. On orbifold backgrounds, it turns out that there exists a new class of S-branes that we call *fractional* S-branes, in analogy to the fractional D-branes on Euclidean orbifolds, which model initial conditions near a singularity.

### 4.1 The Boundary State Interpretation

Having described open string partition functions in the previous chapter, the next task is to pull out interesting space-time physics in the closed string channel. We consider the calculation of the overlap between the deformed boundary state and various closed string states; these correspond to one-point functions on the disk. Here we will be interested in extracting the overlap with lowest lying closed string states, as they contain information about the center of mass

---

<sup>1</sup>D-branes in other time-dependent backgrounds have been investigated in [31, 25, 71, 72, 73, 74, 75, 76].

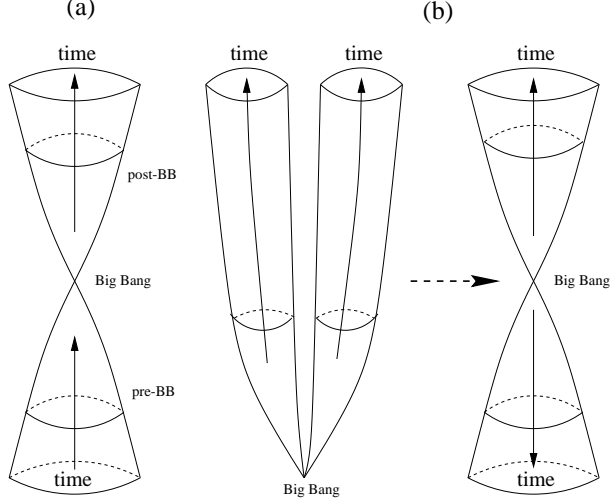


Figure 4.1: The pre-Big Bang scenario (a), and the creation of two-branched Universe from the Big Bang, which is interpreted as a spacetime  $\mathbb{Z}_2$  orbifold (b).

position. In the untwisted sector, this is the tachyon, and this problem has been studied extensively ([78] is a review). The overlap with the tachyonic vacuum in the infinite radius theory is the function

$$f_\lambda(x) = \frac{1}{1 + e^{ix} \sin(\pi\lambda)} + \frac{1}{1 + e^{-ix} \sin(\pi\lambda)} - 1, \quad (4.1)$$

also corresponding to the open string disk partition function in the S-brane background.

One could attempt to get at these results by factorization of the annulus amplitudes in the closed string channel. The idea would be that we can try to isolate the disk amplitudes via

$$\langle B; \tilde{\lambda} | \Delta | B; \lambda \rangle \rightarrow \sum_{\psi} \langle \psi | B; \tilde{\lambda} \rangle^* \Delta_{\psi} \langle \psi | B; \lambda \rangle \quad (4.2)$$

and we want to isolate  $\langle \psi | B; \lambda \rangle$  for suitable  $\psi$ . In the untwisted sector, we would like  $|\psi\rangle$  to be a momentum  $p$  tachyon. We have

$$Z_1 = \frac{1}{\sqrt{2}} \frac{1}{\eta(\tilde{q}^2)} \int_0^1 d\zeta_- \sum_{n \in \mathbb{Z}} (\tilde{q}^2)^{n^2/4} e^{2\pi i \alpha(\zeta_-) n} \quad (4.3)$$

Because we are interested in information describing the center of mass positions, we need to isolate the contributions of Virasoro primaries that do not correspond to oscillator excitations. This subset of states will build up  $f_\lambda(x)$ .

### Untwisted Sector: Self-Dual Radius

At self-dual radius, we have  $\zeta_- = 0$ , and  $\alpha = (\lambda - \tilde{\lambda})/2$ , so the amplitude becomes

$$Z_{1;sd} = \frac{1}{\sqrt{2}} \frac{1}{\eta(\tilde{q}^2)} \sum_{n \in \mathbb{Z}} (\tilde{q}^2)^{n^2/4} e^{i\pi(\lambda - \tilde{\lambda})n} \quad (4.4)$$

It is tempting to simply take the above amplitude and discard the eta function  $\eta(\tilde{q}^2)$ , as this is usually associated with oscillator contributions. We would obtain a phase  $e^{i\pi\lambda n}$  for each  $n$ . However, this would not give the proper  $f_\lambda(x)$ . The issue here is that the discrete primaries are also built out of the oscillators. We should subtract the contributions from both conformal descendants and the discrete primaries to identify the quantity  $f_\lambda(x)$ . This is in fact what the  $SU(2)$  formalism does for us – it converts the annulus to the true Virasoro character, and gives a coefficient which is related to an  $SU(2)$  character,

$$Z_1 = \frac{1}{\sqrt{2}} \sum_{j=0,1/2,1,\dots} \chi_{j^2}^{Vir}(\tilde{q}^2) \sum_{m=-j}^j \mathcal{D}_{m,m}^{(j)} \left( e^{2\pi i(\lambda - \tilde{\lambda})J^1} \right) .$$

This factorizes into the Ishibashi states  $\mathcal{D}_{-m,n}(e^{2\pi i\lambda J^1})|j, m, n\rangle$ . The non-oscillator parts of this correspond to  $m, n = \pm j$  and we arrive at

$$\begin{aligned} \sum_p e^{ipx} \langle p, p|B; \lambda \rangle_{sd} &= \mathcal{D}_{-j,j}(\cdot) \sum_p e^{ipx} \langle p, p|j, j, j\rangle \\ &\quad + \mathcal{D}_{j,-j}(\cdot) \sum_p e^{ipx} \langle p, p|j, -j, -j\rangle \\ &\quad + \mathcal{D}_{-j,-j}(\cdot) \sum_p e^{ipx} \langle p, p|j, j, -j\rangle \\ &\quad + \mathcal{D}_{j,j}(\cdot) \sum_p e^{ipx} \langle p, p|j, -j, j\rangle \\ &= \sum_m e^{imx} (-\sin \pi\lambda)^{|m|} \\ &\quad + \sum_m e^{im\tilde{x}} (i \cos \pi\lambda)^{|m|} \equiv f_\lambda(x) + \tilde{f}_\lambda(\tilde{x}) , \end{aligned} \quad (4.5)$$

where we reintroduced the variable  $\tilde{x}$ , T-dual of  $x$ . It is also possible to study the overlaps of boundary states with low lying states within the dual theory on the circle of twice the self-dual radius. In this case however, there are some subtleties involving the identification of zero modes in the two representations.

### Untwisted Sector: Infinite Radius

At infinite radius, this computation simplifies: the  $\bar{f}$  contribution decouples. We can see this directly given our infinite radius expression

$$Z_1 = \frac{1}{\sqrt{2}} \frac{1}{\eta(\tilde{q}^2)} \int_0^1 d\zeta_- \sum_{m \in \mathbb{Z}} (\tilde{q}^2)^{m^2/4} e^{2\pi i \alpha(\zeta_-)m}, \quad (4.7)$$

in the closed channel. Fortunately, once this is rewritten in terms of the Virasoro character, analogous to the above discussion, the  $\zeta_-$  integral is easily performed. The net effect is to reduce the result to

$$\begin{aligned} \sum_p e^{ipx} \langle p, p | B; \lambda \rangle_\infty &= \mathcal{D}_{-j,j}(\cdot) \sum_p e^{ipx} \langle p, p | j, j, j \rangle \\ &\quad + \mathcal{D}_{j,-j}(\cdot) \sum_p e^{ipx} \langle p, p | j, -j, -j \rangle \\ &= \sum_m e^{imx} (-\sin \pi \lambda)^{|m|} \\ &= \frac{1}{1 + e^{ix} \sin(\pi \lambda)} + \frac{1}{1 + e^{-ix} \sin(\pi \lambda)} - 1 = f_\lambda(x) \end{aligned} \quad (4.8)$$

so we have rederived (4.1).

### Twisted Factorization: Self-Dual Radius

Now in the twisted sector, we can follow the same path. Here, it is in fact easier, because there is no subtlety concerning the Virasoro character – it is just what appears in the amplitude

$$Z_g = \frac{1}{\sqrt{2}} \frac{1}{\eta(\tilde{q}^2)} \sum_{\zeta_-} \sum_{m \in \mathbb{Z}} (\tilde{q}^2)^{(m-1/2)^2/4} e^{2\pi i \alpha(\zeta_-)(m-1/2)}. \quad (4.10)$$

The non-oscillator part of this corresponds to the  $m = 0, 1$  contributions. Recall that there are no zero modes in the twisted sectors, so we just need to carefully enumerate the states that are contributing to the partition function. We note that since we have considered the most general deformation (with separate deformations  $\lambda, \tilde{\lambda}$  on each boundary), we have enough information to do so.

At self-dual radius, we have only  $\zeta_- = 0$ , and the amplitude reduces to

$$Z_g = \frac{1}{\sqrt{2}} \frac{1}{\eta(\tilde{q}^2)} \sum_{m \in \mathbb{Z}} (\tilde{q}^2)^{(m-1/2)^2/4} e^{i\pi(\lambda-\tilde{\lambda})(m-1/2)}. \quad (4.11)$$

Keeping only  $m = 0, 1$ , we find

$$Z_{g,vac} = \frac{1}{\sqrt{2}} (\tilde{q}^2)^{1/16} \left[ e^{i\pi(\lambda-\tilde{\lambda})/2} + e^{-i\pi(\lambda-\tilde{\lambda})/2} \right]. \quad (4.12)$$

The ability to separate this amplitude into two factors depending on either  $\lambda$  or  $\tilde{\lambda}$  only, implies that there are two orthogonal states contributing here, which

we will denote by  $|I\rangle_T$  and  $|II\rangle_T$ . We are finding that

$$|B, \lambda; 0\rangle_{T;sd} = 2^{-1/4} e^{i\pi\lambda/2} |I\rangle_T + 2^{-1/4} e^{-i\pi\lambda/2} |II\rangle_T . \quad (4.13)$$

We re-emphasize here that we are not considering the full boundary state, but really only its overlap with the twisted vacua. The full boundary state contains oscillator excitations as well. However, the dependence on the twisted vacua already contains the information about the space-time positions.

At  $\lambda = 0$ , this reduces to

$$|B, 0; 0\rangle_{T;sd} = 2^{-1/4} (|I\rangle_T + |II\rangle_T) \equiv |N, 0; 0\rangle_{T;sd} , \quad (4.14)$$

which must coincide with one of the usual Neumann states [79]. We will verify this below. Further, at  $\lambda = 1$ , it reduces to

$$|B, 1; 0\rangle_{T;sd} = i 2^{-1/4} (|I\rangle_T - |II\rangle_T) \equiv |N, 1; 0\rangle_{T;sd} , \quad (4.15)$$

which must be the other Neumann state. Note that these two states are orthogonal. Next consider the Dirichlet states. We should get these by deforming to  $\lambda = 1/2$  and  $\lambda = -1/2$ . The former corresponds to a D0-brane at the fixed point  $X = 0$ , the latter to a D0-brane at  $X = \pi\sqrt{\alpha'}$ . So we identify<sup>2</sup>

$$|B, 1/2; 0\rangle_{T;sd} = 2^{-1/4} (e^{+i\pi/4} |I\rangle_T + e^{-i\pi/4} |II\rangle_T) \equiv |0\rangle_T \quad (4.16)$$

and

$$|B, -1/2; 0\rangle_{T;sd} = 2^{-1/4} (e^{-i\pi/4} |I\rangle_T + e^{+i\pi/4} |II\rangle_T) \equiv |\pi\sqrt{\alpha'}\rangle_T . \quad (4.17)$$

These states were called  $|D(\phi_0)_T\rangle$  with  $\phi_0 = 0, \pi r$  respectively in [79] ( $r = \sqrt{\alpha'}$  for selfdual radius). Note that they are orthogonal. Now we can represent the states that we called  $|I\rangle_T, |II\rangle_T$  in terms of the Dirichlet states:

$$\begin{aligned} |I\rangle_T &= 2^{-3/4} (e^{-i\pi/4} |0\rangle_T + e^{i\pi/4} |\pi\sqrt{\alpha'}\rangle_T) \\ |II\rangle_T &= 2^{-3/4} (e^{i\pi/4} |0\rangle_T + e^{-i\pi/4} |\pi\sqrt{\alpha'}\rangle_T) \end{aligned}$$

and plug these back into the general expression for the deformed twisted boundary state (4.13). We obtain

$$|B, \lambda; 0\rangle_T = \cos \left[ \frac{\pi}{2} \left( \lambda - \frac{1}{2} \right) \right] |0\rangle_T + \cos \left[ \frac{\pi}{2} \left( \lambda + \frac{1}{2} \right) \right] |\pi\sqrt{\alpha'}\rangle_T . \quad (4.18)$$

---

<sup>2</sup>There is an unfortunate inconsistency in the literature which would seem to imply that  $\lambda = 1/2$  should correspond to  $X = \pi\sqrt{\alpha'}$ . However, those statements correspond to a situation with translational invariance (so a choice was made), whereas in the case of the orbifold, the position is fixed uniquely. This will be demonstrated carefully in the next subsection.

At  $\lambda = 0, 1$  we then obtain the two Neumann boundary states

$$\begin{aligned} |N, 0; 0\rangle &= 2^{-1/2}(|0\rangle_T + |\pi\sqrt{\alpha'}\rangle_T) \\ |N, 1; 0\rangle &= 2^{-1/2}(|0\rangle_T - |\pi\sqrt{\alpha'}\rangle_T) . \end{aligned} \quad (4.19)$$

These agree with the expressions in [79]. In fact, [79] *assumed* the form of the two twisted Neumann boundary states. Here we have *derived* them by deforming from known (Dirichlet) states.

### Twisted Factorization: Infinite Radius

It is instructive to also look at this factorization in the infinite radius theory. In this case, both  $\zeta_- = 0$  and  $\zeta_- = 1/2$  contribute and we arrive at

$$Z_g = \frac{1}{\sqrt{2}} \frac{1}{\eta(\tilde{q}^2)} \sum_{m \in \mathbb{Z}} (\tilde{q}^2)^{(m-1/2)^2/4} \left[ e^{i\pi(\lambda-\tilde{\lambda})(m-1/2)} + e^{i\pi(\lambda+\tilde{\lambda}-1)(m-1/2)} \right] . \quad (4.20)$$

The contribution of the twisted vacua is

$$Z_{g,vac} = \frac{1}{\sqrt{2}} (\tilde{q}^2)^{1/16} \left[ e^{i\pi(\lambda-\tilde{\lambda})/2} + e^{-i\pi(\lambda-\tilde{\lambda})/2} + e^{i\pi(\lambda+\tilde{\lambda}-1)/2} + e^{-i\pi(\lambda+\tilde{\lambda}-1)/2} \right] . \quad (4.21)$$

We note that this expression factorizes

$$Z_{g,vac} = \frac{1}{\sqrt{2}} (\tilde{q}^2)^{1/16} \left[ e^{-i\pi\tilde{\lambda}/2} - ie^{i\pi\tilde{\lambda}/2} \right] \left[ e^{i\pi\lambda/2} + ie^{-i\pi\lambda/2} \right] \quad (4.22)$$

and thus we interpret this as only one state contributing,

$$|B, \lambda\rangle_{T;\infty} = 2^{-1/4} \left[ e^{i\pi\lambda/2} + ie^{-i\pi\lambda/2} \right] |0\rangle_T . \quad (4.23)$$

Note that the state  $|B, -1/2\rangle_{T;\infty}$  is orthogonal to  $|B, 1/2\rangle_{T;\infty}$  as well as itself: that is, it decouples. This corresponds to the fact that the second fixed point, present at finite radius, has moved off to infinity, and the corresponding twisted boundary states decouple. Similarly, by looking at integer  $\lambda$ , it is possible to see that  $|\pi\sqrt{\alpha'}\rangle_T$  decouples. Thus, at infinite radius we only obtain the contribution from the twisted sector at the remaining fixed point  $X = 0$ .

## 4.2 Back to the Lorentzian Signature

After the Euclidean computations, we will now move back to Lorentzian signature. As discussed in Section 2.2, in the case of the orbifold there are some subtleties. We will also be interested in analyzing how the brane decays into closed strings in the orbifold. We will compute the average total energy and number densities of the emitted untwisted closed strings and compare the calculation and the results with those of [65]. The computations involve a prescription

for a time integration contour, which in turn is related to how the initial state of the brane is prepared. A natural contour to use on the orbifold turns out to be the Hartle-Hawking (HH) contour which was introduced in [65]. With this choice, on the fundamental domain we can interpret the unstable brane to nucleate at the origin of time and then decay into closed strings.

Let us first review the standard case without the orbifold. Upon Wick rotation back to the Lorentzian signature the overlap of the deformed boundary state with the vacuum becomes

$$f(x^0) \equiv {}_\infty\langle 0|D(\pi\lambda)\rangle_\infty = \frac{1}{1 + e^{x^0} \sin(\pi\lambda)} + \frac{1}{1 + e^{-x^0} \sin(\pi\lambda)} - 1. \quad (4.24)$$

The full boundary state has the structure

$$|B\rangle = \mathcal{N}_p |B\rangle_{X^0} |B\rangle_X |B\rangle_{bc} \quad (4.25)$$

where

$$|B\rangle_{X^0} = f(x^0)|0\rangle + \sigma(x^0)\alpha_{-1}^0\tilde{\alpha}_{-1}^0|0\rangle + \dots \quad (4.26)$$

with

$$\sigma(x^0) = \cos(2\pi\lambda) + 1 - f(x^0). \quad (4.27)$$

To compute the overlap with any on-shell closed string state, it is convenient to express the vertex operators in the gauge

$$V = e^{iEX^0} V_{sp} \quad (4.28)$$

where  $V_{sp}$  contains only the space part. The overlap then takes a simple form

$$\langle V|B\rangle = \langle 0|e^{iEX^0}|B\rangle_{X^0} \times (\text{phase}) \quad (4.29)$$

yielding the amplitude

$$I(E) = i \int_{\mathcal{C}} dx^0 e^{iEx^0} f(x^0) \quad (4.30)$$

with a suitable choice of the integration contour  $\mathcal{C}$ .

In the case of the orbifold, the computations are simplest to perform in the covering space. As discussed in Section [48], a new feature is the need to double the Hilbert space by hand upon Wick rotating back to the Lorentzian signature. This is because on the covering space a single quantum corresponds to two copies propagating into the opposite time directions  $X^0$  and  $X'^0 = -X^0$ .

The on-shell closed string states then take the form

$$|V\rangle = \frac{1}{\sqrt{2}} \begin{pmatrix} e^{iEX^0} V_{sp}|0\rangle \\ e^{iEX'^0} V'_{sp}|0\rangle \end{pmatrix}. \quad (4.31)$$

Similarly, the time direction part of the boundary state becomes

$$|B\rangle_{X^0} = \frac{1}{\sqrt{2}} \begin{pmatrix} f(x_0)|0\rangle \\ f(x'_0)|0\rangle \end{pmatrix} + \dots. \quad (4.32)$$

Note however that

$$f(x'^0) = f(x^0) = \frac{1}{1 + e^{x^0} \sin(\pi\lambda)} + \frac{1}{1 + e^{-x^0} \sin(\pi\lambda)} - 1 \quad (4.33)$$

because of time reflection symmetry. The overlap with the closed string state becomes

$$\langle V|B\rangle = \frac{1}{2}(e^{iEx^0} f(x^0) + e^{iEx'^0} f(x'^0)). \quad (4.34)$$

Let us pause to compare the physical interpretation of the above with the standard full S-brane. The full S-brane corresponds to formation and decay of an unstable brane, centered at the origin of the time axis. On the orbifold, the full Minkowski space is replaced by the covering space, with a two-branched time direction. The unstable brane is centered at the origin of the time coordinates, but decays into closed strings propagating into the opposite time directions, as illustrated in Figure 5.

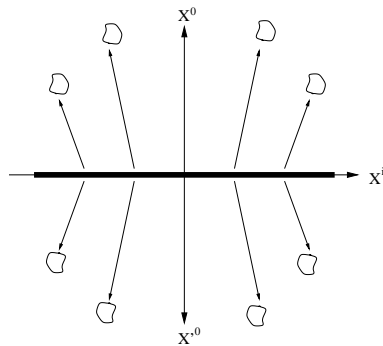


Figure 4.2: Untwisted closed string emission in the covering space.

For the decay amplitude calculation, we then need a contour integration prescription. The fundamental domain has a semi-infinite time axis,  $X^0 \geq 0$ . We have set the decay of the brane to start at  $X^0 = 0$ . Since there is no past to  $X^0 = 0$ , we cannot build up the brane from some closed string initial state. Instead, it is most natural to adopt the prescription in [65] for “nucleating” the brane via smeared D-instantons (see also [66]) in imaginary time. This

corresponds to using a Hartle-Hawking time contour, coming in from  $X^0 = i\infty$  along the imaginary time axis to the origin and then proceeding along the real time axis to  $X^0 = \infty$ . For the actual calculation, we move back to the covering space where time runs from  $X^0 = 0$  to opposite time directions  $X^0 \rightarrow \infty$  and  $X'^0 = -X^0 \rightarrow \infty$ . The HH contour then maps to the double contour with branches (see Fig. 6.)

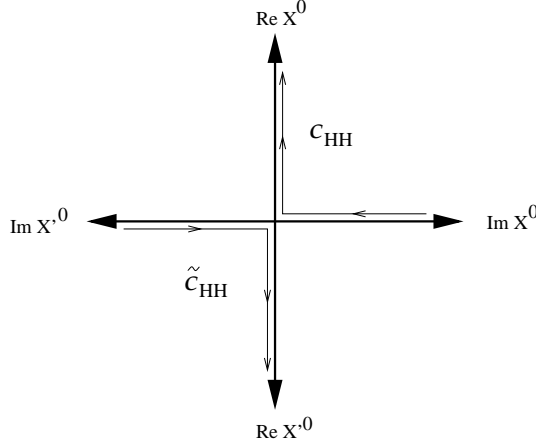


Figure 4.3: The double HH contour in the covering space.

$$C_{HH}, \tilde{C}_{HH} : X^0, X'^0 = i\infty \rightarrow 0 \rightarrow \infty . \quad (4.35)$$

Applying the contour to the overlap (4.34), we get

$$\begin{aligned} \langle V|B \rangle &= \frac{1}{2} \int_{C_{HH}} e^{iEx^0} f(x^0) dx^0 + \frac{1}{2} \int_{\tilde{C}_{HH}} e^{iEx'^0} f(x'^0) dx'^0 \\ &= e^{-iE \ln \lambda} \frac{\pi}{\sinh(\pi E)} , \end{aligned} \quad (4.36)$$

as in [65] for the full brane with the HH contour. The same is true for the total average energy and average number densities for the produced untwisted closed strings on the fundamental domain. The results are the same as in the standard case,

$$\frac{\bar{N}}{V_p} \sim \sum_n n^{-1-p/4} ; \frac{\bar{E}}{V_p} \sim \sum_n n^{-1/2-p/4} , \quad (4.37)$$

where the sums are over the level numbers. To conclude, in the orbifold the decay in the untwisted sector is quantitatively the same as in the usual case.

The twisted sector is more problematic conceptually. Since the twisted strings are localized in time, the concept of “producing” them in the decay is ill defined. Moreover, there are very few physical states in the twisted sector. At present we do not have much more to say about this matter.

### 4.3 Conclusions and Outlook

The decay of unstable D-branes or D-brane configurations is an important open question in string theory. They may play a crucial role in cosmology, and there already exist several scenarios making use of them. While spacetime orbifolds may be considered just toy models, capturing some features of string theory in more general time-dependent backgrounds, they are nevertheless useful for gaining insights into problems associated with quantum string theory. We have argued that the twisted sector which exists in orbifolds may contribute to the decay of unstable branes. In particular, we have presented a detailed analysis of how to implement the orbifold identifications into the decay, in a simple example, both in the open string and closed string formalism, and argued that this leads to a new class of S-branes, which we have called fractional S-branes, in analogy to the fractional branes of Euclidean orbifolds. We expect that the existence of fractional S-branes is a generic feature of spacetime orbifolds, and may reflect some physics of D-brane decay in more general time-dependent backgrounds. They may also be relevant for the question of resolution of spacelike singularities.

In particular, we have constructed a model where the D-brane decay has a semi-infinite duration, without a prior build-up phase. This is in contrast to the full S-brane and half S-brane constructions, where either the brane must first be formed from a fine-tuned closed string initial state, or the decay starts from infinite past without any parameter to control its pace. For potential applications of our construction, we can make at least the following speculative remarks.

(i) We have presented a model where an unstable brane, prepared at the “Big Bang” origin of the spacetime, stores a large amount of energy which then gets released in the decay into heavy closed string modes and the subsequent cascade into lighter excitations. Presumably the large energy backreacts into the spacetime and converts it into an expanding cosmological model. The initial condition, while defined at an initial spacelike singularity, is still under control because it has a well defined dual formulation in terms of open string worldsheet theory. If the unstable brane is taken to be volume filling, it also provides a homogeneous<sup>3</sup> initial condition. This may be compared with brane cosmological models where a collision of almost parallel branes provides a homogeneous initial condition – in our case the homogeneity only involves a single brane.

(ii) The idea of an initial unstable brane at the Big Bang may be coupled with string/brane gas cosmology [80, 81]. Take the spacelike directions to be compactified to Planck Scale, and the initial unstable brane to be wrapped in all directions. The brane then decays into closed strings, which interact and presumably thermalize; thus brane decay could be viewed as the origin of the hot string gas.

(iii) In our orbifold construction, the covering space of the orbifold can be

---

<sup>3</sup>Except for possible effects at the conical singularity.

viewed as a model where two branches of spacetime originate from the same Big Bang event. One may view the other branch and the images of closed strings in it simply as a calculational trick, in analogy to the thermal ghosts in the real time formulation of finite temperature quantum field theory or thermofield dynamics. But one could also view it as a real branch of the spacetime, so that the total spacetime contains a multi-branched arrow of time.

(iv) If the other branch of the spacetime from the origin of time is viewed simply as a calculational trick, one may ask if this trick could be applied in other cases. Consider for example the setup of  $D\bar{D}$ -inflationary models, where a D-brane and an anti D-brane first approach each other, with the scalar excitation from interpolating open string providing the rolling inflaton, and then form an unstable system where the rolling tachyon provides an exit mechanism from inflation and may be responsible for the subsequent reheating. It is not well understood how to actually model this in the language of the open string sigma model. If the rolling tachyon has a hyperbolic cosine profile, then it contains an unwanted stage where the tachyon rolls "up". If it only has an exponential profile, then the decay starts at infinite past leaving no room for the inflationary stage. It may be possible to develop a model, where the decay is modeled by our construction, viewing the other branch or time direction from the origin simply as a calculational trick.

All the above comments are very tentative, but we believe they illustrate that there are exciting possibilities ahead to unravel and study.

# Chapter 5

## Entanglement Entropies in Quantum Field Theories

Entanglement entropy represents a complicated, non-local, observable. Interest in quantum mechanical entropy as a measure of information has a long history, going back at least as far as von Neumann. In a field theory context interest in entanglement entropy began as a possible explanation of the *Bekenstein – Hawking* area law for the entropy of black holes,

$$S_{BH} \sim \frac{\text{Area}}{4\pi G_N}. \quad (5.1)$$

The hope was to identify this entropy with the measure of how much physics behind a blackhole’s horizon is entangled with physics outside the horizon.

Indeed, simple calculations indicated the leading contribution to entanglement entropy [82],  $S_{ent} \propto \text{Area}$ . Unfortunately, the coefficients are generally regulator dependent, spoiling the hope that this provides the microscopic origin for black hole entropy (in most dimensions).

However, it has been discovered that in low dimensional field theories, the entanglement entropy can be a universal number. Specifically, in  $1 + 1$  dimensional conformal field theories the entropy scales logarithmically with a region’s size and in topological field theories the entropy is expected to be a universal constant.

Motivated by completely distinct physics, entanglement entropy is of interest in condensed matter systems [83, 84, 85, 86, 87, 88]. In some systems, one has the possibility of quantum phase transitions (phase transitions which may occur at absolute zero temperature). These are phase transitions in the behavior of quantum fluctuations as physical parameters are varied. During finite temperature phase transitions, the energy and themodynamical entropy determine which phase is physically the realized. At zero temperature, in a topological phase, the entanglement entropy serve as a useful order parameter labeling different quantum phases of matter.

### 5.1 Entanglement

Few quantities highlight the difference between classical and quantum mechanics as strongly as entanglement. The origin of entanglement lies in the fact that, while phase space of independent classical multiparticle systems is the Cartesian

product of the single particle spaces, the quantum mechanical Hilbert space is a tensor product of the individual Hilbert spaces. As a consequence, subsystems may become entangled and a generic quantum mechanical state may not be written as the simple product of states associated with individual subsystems,  $|\psi_{\text{gen}}\rangle \neq |\psi_1\rangle \otimes |\psi_2\rangle \dots \otimes |\psi_n\rangle$ . The presence of entanglement underscores the fact that, for quantum systems, complete knowledge of a pure multiparticle state does not guarantee any knowledge about the state of subsystems.

Generally, quantum mechanical systems should be described by density matrices. Subsystems are said to be entangled if the density matrix for the whole system is not the tensor product of the subspace density matrices.

Another way to think about entanglement is through information. To specify the state of a classical system composed of  $m$  identical subsystems, one needs  $m$  numbers. For a quantum state, we generally need to specify  $(\dim V)^m$  numbers, where  $\dim V$  is the number of states in each subsystem's Hilbert space. Entangled states encode more information than classical systems.

### 5.1.1 Entanglement Entropy

Practically speaking, to be a useful concept, we need a measure of entanglement. We begin by splitting the whole system into two subsystems,  $A$  and  $B$ . We may define a reduced density matrix,  $\rho_A$ , by tracing the density matrix over the  $B$  subsystem. When discussing such bipartite systems a common measure of entanglement is the von Neumann entropy,

$$S_A = -\text{Tr}(\rho_A \ln \rho_A). \quad (5.2)$$

This quantity vanishes for unentangled states and therefore acts as a measure of how much more information is encoded in a quantum state than its closest classical counterpart. Ideally, we would like to simply compute this quantity from the eigenvalues of the reduced density matrix, however in practice we shall define this through the replica trick.

$$S_A = -\left. \frac{\partial}{\partial n} \rho_A^n \right|_{n=1} \quad (5.3)$$

Using the replica trick we may prove the symmetry property of pure state entanglement entropies,

$$S_A = S_B. \quad (5.4)$$

If we write the general pure state  $|\psi\rangle = \sum_{i_A, i_B} C_{i_A i_B} |i_A\rangle |i_B\rangle$ , the reduced density matrices become

$$[\rho_A]_{ij} = \sum_k C_{ik} C_{jk}^* \quad (5.5)$$

$$[\rho_B]_{ij} = \sum_k C_{ki} C_{kj}^* \quad (5.6)$$

We find

$$\begin{aligned}
Tr_A \rho_A^2 &= \sum_{a_1, a_2, b_1, b_2} C_{a_1 b_1} C_{a_2 b_1}^* C_{a_2 b_2} C_{a_1 b_2}^* \\
&= \sum_{a_1, a_2, b_1, b_2} C_{a_1 b_1} C_{a_1 b_2}^* C_{a_2 b_2} C_{a_2 b_1}^* \\
&= Tr_B \rho_B^2.
\end{aligned} \tag{5.7}$$

Similarly, we find

$$Tr_A \rho_A^n = Tr_B \rho_B^n \tag{5.8}$$

and the equivalence of the two entropies follows directly.

### Two State Systems

As a simple warm up lets consider a simple example built from two state systems. We may define two states

$$|\psi_{cl}\rangle = |+\rangle_A \otimes |+\rangle_B \tag{5.9}$$

$$|\psi_{qu}\rangle = \frac{1}{\sqrt{2}} (|+\rangle_A \otimes |+\rangle_B + |-\rangle_A \otimes |-\rangle_B), \tag{5.10}$$

by inspection, the first is unentangled while the second is entangled. Defining the pure state density matrices  $\rho \sim |\psi\rangle\langle\psi|$ , we compute the reduced density matrices,

$$\rho_{A,cl} = |+\rangle_A \langle +|_A \tag{5.11}$$

$$\rho_{A,qu} = \frac{1}{2} (|+\rangle_A \langle +|_A + |-\rangle_A \langle -|_A). \tag{5.12}$$

The respective entanglement entropies are

$$S_{cl} = 0 \tag{5.13}$$

$$S_{qu} = \ln(2). \tag{5.14}$$

In fact, it is not too hard to show that  $|\psi_{qu}\rangle$  has the maximal entropy in this two state example.

### 5.1.2 Field Theory Systems

In general, one would not expect the entanglement entropy to be a universal quantity in a field theory. One should worry about strong dependence upon the way two regions are split and the precise microstructure of the theory. On dimensional grounds, in  $D+1$  dimensions, the entropy should be given in powers of an ultraviolet cutoff,  $\Lambda$ ,

$$S_{gen} \sim \sigma_D (L \Lambda)^D + \sigma_{D-1} (L \Lambda)^{D-1} + \dots + \sigma_0 (L \Lambda)^0 + a_0 \ln(L \Lambda). \tag{5.15}$$

However, because the entanglement entropy is independent of how we partition the region, it may only depend upon information shared by both regions. This forces the volume term,  $\sigma_D$ , to vanish. The leading term becomes  $\sigma_{D-1}(L\Lambda)^{D-1}$  which scales as the area between the regions. This area law dependence was the initial motivation to identify black hole entropy with entanglement entropy. Unfortunately, the coefficient in the leading term is not a universal quantity, its value depends upon the choice of regularization.

In the most general case one does not expect any of the coefficients to be universal. However, in low dimensional critical systems, the coefficient of the  $\ln(L\Lambda)$  or constant terms may be universal (but not both). If one has the  $\ln L\Lambda$  term, a constant term is regulator dependent. However, if all length scale dependence cancels (as in a topological field theory) the constant term also becomes universal. There are at least two known examples where the entanglement entropy becomes universal, 1 + 1 dimensional conformal field theories and 2 + 1 dimensional Chern-Simons theories. In 1 + 1 dimensional conformal field theory of central charge  $c$ , a computation we shall review, the entanglement entropy depends logarithmically upon the partitioned region's size. The resulting universal quantity is

$$S_{1+1} \sim \frac{c}{3} \ln(L). \quad (5.16)$$

It is important to note that, while universal, these 1 + 1 dimensional entropies may be very challenging to realize experimentally due to their nonlocal character. In the next chapter we shall compute entanglement entropies for 2 + 1 dimensional Chern-Simons theories. As a topological field theory, there is no dependence upon length scales, leaving only a non-zero constant term. These numbers are of interest for the hypothetical construction of topological quantum computers. Experimentally, these Chern-Simons theories may be realized as effective field theory for the topological phase of fractional quantum Hall materials.

### Replica Trick

A pure state entanglement entropy is not a simple object to compute in a field theory. The direct route used for quantum mechanical systems only works when one knows a pure state wavefunctional or density matrix. Unfortunately, the list of field theories where one has any knowledge of energy eigenfunctionals is very small. Instead, if the ground state is unique, there is an alternate construction where we replace the ground state density matrix with the zero temperature limit of a thermal density matrix.

In a thermal approach, the density matrix may be represented as a Euclidian time evolution operator. In this picture the "legs" of the density matrix correspond to states separated in Euclidean time by  $\beta \equiv \frac{1}{T}$ . In practice, it is simpler to think in terms of a path integral representation, where the field

configurations are fixed at initial and final Euclidean times.

$$\rho(\phi(x)|\chi(y)) = \frac{1}{Z_1} \int [d\varphi] \Big|_{\varphi(0,x)=\chi(x)}^{\varphi(\beta,x)=\phi(x)} e^{-S_\beta[\varphi]} \quad (5.17)$$

Matrix multiplication is accomplished by summing over intermediate configurations, defined on a region of size  $2\beta$ .

$$\begin{aligned} [\rho^2](\phi(x)|\chi(y)) &= \int [d\phi'] \rho(\phi(x)|\phi'(x)) \rho(\phi'(x)|\chi(x)) \\ &= \frac{1}{Z_1^2} \int [d\varphi] \Big|_{\varphi(0,x)=\chi(x)}^{\varphi(2\beta,x)=\phi(x)} e^{-S_{2\beta}[\varphi]} \end{aligned} \quad (5.18)$$

To construct the reduced density matrix in region  $A$ , we are to trace the full density matrix over the states localized in region  $B$ . If we write

$$\phi(x) = \left\{ \begin{array}{ll} \phi_A(x) & x \in A \\ \phi_B(x) & x \in B \end{array} \right\}, \quad (5.19)$$

the reduced density matrix becomes

$$\begin{aligned} \rho_A(\phi_A(x)|\chi_A(y)) &= \frac{1}{Z_1} \int [d\phi_B] \rho(\phi_A, \phi_B | \chi_A, \phi_B) \\ &= \frac{1}{Z_1} \int [d\varphi_A] \Big|_{\varphi_A(0,x)=\chi_A(x)}^{\varphi_A(\beta,x)=\phi_A(x)} [d\varphi_B] e^{-S_\beta[\varphi_A, \varphi_B]}. \end{aligned} \quad (5.20)$$

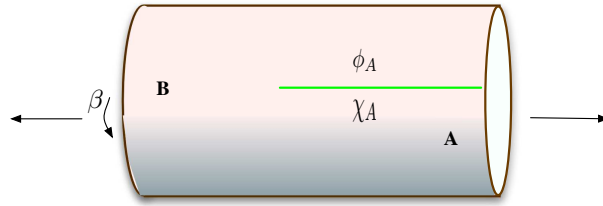


Figure 5.1: The field takes different values on either side of the cut in the  $A$  region.

It is helpful to see how this works in  $1 + 1$  dimensions when  $A$  and  $B$  are two half infinite regions. The full density matrix is represented by an infinite cylinder with an infinite cut in the non-periodic direction. Along the two sides of the cut the field takes fixed values corresponding to the "legs" of the matrix element.

The reduced density matrix may also be given a simple geometric picture as a cylinder with a semi-infinite cut in the  $A$  region (see figure 5.1). Along the cut in the  $A$  region the field takes fixed values, as is appropriate for a matrix defined in region  $A$ .

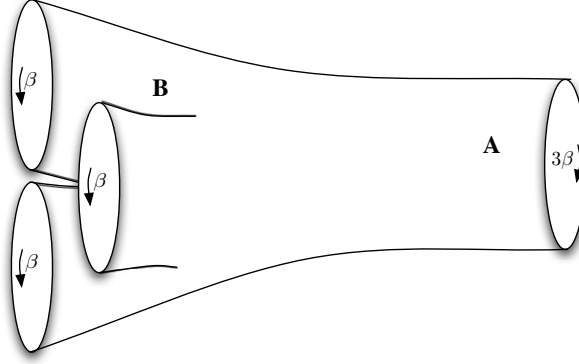


Figure 5.2: After gluing  $\rho_A^n$  together the  $A$  system lives on a circle of size  $n\beta$  whereas the  $n$   $B$  regions each live on circles of size  $\beta$

To construct  $Tr \rho_A^n$  we simply repeat this process  $n$  times and then perform a trace over the final two labels. The resulting expression is

$$Tr \rho_A^n = \frac{Z_n}{Z_1^n} \tag{5.21}$$

where  $Z_i$  is path integral over a spatial domain shown in fig 5.2, subject to the appropriate identifications.

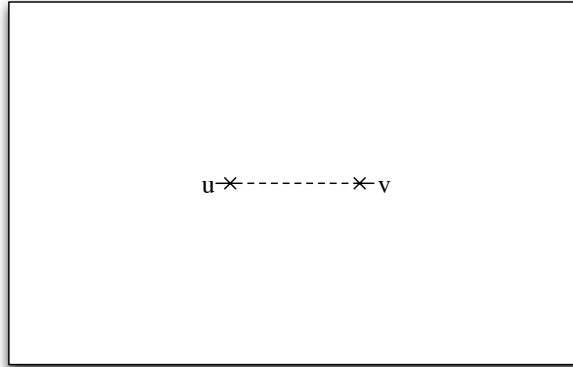


Figure 5.3: The result of mapping the  $n$ -sheeted geometry to a single sheet

**Conformal Mapping Trick** In general, the above thermal construction is the simplest known construction. Unfortunately, in even the simplest situations, things become unwieldy. However, if one is only interested in  $1+1$  dimensional conformal field theories, one can go farther<sup>1</sup>. The key insight is to realize that the above  $n$ -sheeted geometry may be mapped onto a single copy of the complex

<sup>1</sup>For a brief review of conformal field theories see A.1. A longer discussion may be found in [62]

plane, with branch cuts (see figure 5.3). The fields are only required to be periodic around the branch cut up to an  $n$ th root of unity. [83, 89]

This description of the entropy may be described in terms of a orbifold, with twisted states corresponding to aperiodic configurations. (see appendix A.1) The idea is to study stress tensor expectation values on the  $n$  sheeted geometry. The expectation value on a single sheet vanishes, leaving only the anomalous term. If the  $A$  region lies between point  $u$  and  $v$  and  $B$  is infinite in extent, [83, 89]

$$\langle T(z) \rangle_{n\text{-sheet}} = \left(1 - \frac{1}{n^2}\right) \frac{c}{24} \frac{(u-v)^2}{(z-u)^2(z-v)^2}. \quad (5.22)$$

From the poles, we can read off the conformal weight of the twist fields,

$$h_n = \frac{c}{24} \left(1 - \frac{1}{n^2}\right). \quad (5.23)$$

From the conformal weights, we may deduce the partition function on the  $n$ -sheeted geometry (a product of contributions from  $n$  distinct twist fields),

$$\text{Tr } \rho_A^n \sim (u-z)^{-c/6(n-1/n)}. \quad (5.24)$$

The resulting entanglement entropy is

$$S \sim \frac{c}{3} \ln(L_A), \quad (5.25)$$

where  $L_A$  is the length of the  $A$  region. Because orbifold partition functions are written as correlation functions of twist fields, we may extend the above result to any geometry obtainable via a conformal mapping through Ward identities. Importantly, if the entire region has a finite size  $L = \ell_A + \ell_B$ , the entropy becomes:

$$S = \frac{c}{3} \ln(L \sin(\pi \ell_A / L)). \quad (5.26)$$

Note that this entropy is invariant under  $\ell_A \rightarrow \ell_B = L - \ell_A$  reflecting the symmetry property.

In appendix D we review an extension of the conformal computation to include mass terms for free bosons and fermions. The result, when both regions are half infinite is

$$\begin{aligned} \text{Tr } \frac{\partial}{\partial m^2} \ln(\rho_A^n) &= -\frac{c}{24} \frac{1}{m^2} \left(n - \frac{1}{n}\right) \\ \text{Tr } \rho_A^n &= \gamma_n e^{-\frac{c}{24} \ln(m^2) \left(n - \frac{1}{n}\right)}, \quad (\gamma_1 = 1) \\ S_A &= \frac{c}{6} \ln \frac{1}{m}, \end{aligned} \quad (5.27)$$

where  $c_{bos} = 1$  and  $c_{ferm} = \frac{1}{2}$ . Note the relative factor of  $\frac{1}{2}$  between the massless and massive computations reflects the fact that the massive computation only had a single interface between regions  $A$  and  $B$ .

As we shall see in the next chapter, this scaling with the number of discon-

nected interfaces is more general than the present examples might imply. In fact, in Chern-Simons theories, we shall see that only physics localized along the interfaces contributes to the entanglement. The present example represents a theoretical oddity in that it is a nonlocal universal quantity, but it is difficult to imagine one will find experimental verification. One would need to be able to measure a macroscopic subspace of a sample without disrupting the complementing regions. The best one can probably hope for is numerical confirmation through simulations. In Chern-Simons examples to be considered, things are possibly more promising because the theories have no length scales in the topological phase. This may possibly reduce the region over which one must measure the system.

## 5.2 *AdS/CFT* Description of Entanglement Entropy

Because it relies solely upon properties of conformal field theories, the construction outlined by Cardy and Calabrese [83, 89] is quite general. Unless the conformal field theory possesses a free field description, it is difficult to find an independent, explicit calculation. However, in the last decade new perspectives on CFT's have been obtained by using holographic dualities. Specifically, there are known examples of  $d$  dimensional CFT's dual to  $d + 1$  dimensional gravitational theories. It is interesting to ask, at least for conformal field theories, can we obtain entanglement entropies from a holographic perspective. At least for  $1 + 1$  dimensional conformal field theories, the we may answer in the affirmative as discussed in [90, 91, 92, 93].

### 5.2.1 *AdS/CFT*

$AdS_{d+1}$  space is the maximally symmetric space of constant negative spatial curvature. As a space of constant curvature, it may be obtained as a hypersurface in a flat space of signature  $2 + d$ :

$$AdS_{d+1} : -(x^0)^2 - (x^{d+1})^2 + \sum_{i=1}^d (x^i)^2 = R^2. \quad (5.28)$$

If we define global coordinates,

$$x^0 = R \cosh \rho \cos \tau \quad (5.29)$$

$$x^{d+1} = R \cosh \rho \sin \tau \quad (5.30)$$

$$x^i = R \sinh \rho \Sigma^i \quad (\Sigma^i \text{ are coordinates on } S^{d-1}), \quad (5.31)$$

the metric may be written

$$ds^2 = R^2 (-\cosh^2 \rho d^2 t + d^2 \rho + \sinh^2 \rho d\Omega_d^2). \quad (5.32)$$

As a space of maximal symmetry, this metric possesses a large isometry group. In  $d+1$  spacetime dimensions the description as an embedding in a larger space makes the  $SO(2, d+1)$  symmetry group manifest. As mentioned in appendix A.1, this is also the symmetry group of a conformal field theory in  $d+1$  dimensions.

Frequently, it is more useful to work in Poincare coordinates

$$ds^2 = R^2 \frac{d^2 z - d^2 t + \sum_i^{d-1} d^2 x_i}{z^2}. \quad (5.33)$$

The "boundary" of  $AdS$  space occurs at  $z \rightarrow 0$ . The boundary space for  $AdS_{d+1}$  is  $R \times S^{d-1}$  (Minkowski space with a point at spatial infinity).

The general structure of  $AdS/CFT$  dualities was proposed in [94, 95, 96]. The basic proposal is to relate quantum gravitational physics to a conformal field theory living at the boundary of  $AdS$  space. Schematically, we are to identify the boundary values of  $AdS$  fields with sources for  $CFT$  operators, and then equate partition functions.

$$\langle e^{i \int d^d x \phi_0 \mathcal{O}} \rangle_{CFT} = Z_{AdS_{d+1}} \Big|_{\phi \rightarrow \phi_0}. \quad (5.34)$$

While this is a fascinating proposal, one must still identify both the field content to be excited in  $AdS$  space and which  $CFT$  lives at the boundary. In the string theory literature the geometry most thoroughly examined is  $AdS_5 \times S^5$ , which is dual to  $N = 4$  supersymmetric Yang-Mills theory. In this case the relationship has undergone numerous tests on both sides, with no known problems. In other dimensions, the duality is much less tested. One would like to study non-conformal field theories. On the gravitational side this would correspond to studying spacetimes which are merely asymptotically  $AdS$  spaces, an example of which are black hole geometries. See [92, 93] for progress in these directions.

### 5.2.2 Entanglement in $AdS_3$ Space

Following [90, 91, 92, 93], we may rephrase entanglement entropy calculations in terms of gravitational quantities. The  $CFT_2$  shall live on the asymptotic boundary of  $AdS_3$ , which is a compact circle of size  $L = \ell_A + \ell_B$ . From the  $AdS_3/CFT_2$  correspondence, we may write the  $CFT$  central charge in terms of gravitational quantities,

$$c = \frac{3R}{2G_N^{(3)}}. \quad (5.35)$$

In addition, to render  $CFT$  quantities finite we need an  $UV$  cutoff,  $\frac{1}{a}$ . In line

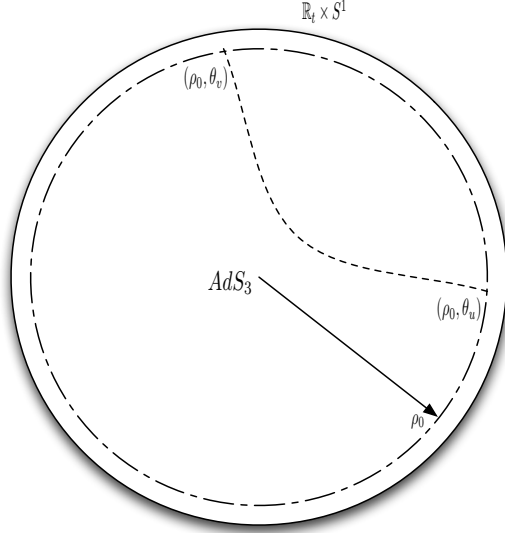


Figure 5.4: Boundary operators in  $AdS_3/CFT_2$

with the duality, an  $UV$  cutoff in the  $CFT$  is dual to an  $IR$  cutoff in the  $AdS$  geometry,

$$e^{\rho_0} = \frac{L}{a}. \quad (5.36)$$

The basic result of  $AdS/CFT$  we need here is that the correlation function of two boundary operators (with scaling dimension  $\Delta$ , depends on the geodesic distance between them, in  $AdS$  space.

$$\langle \phi(z)\phi(w) \rangle_{CFT} \sim e^{2\Delta L_{zw}/R}. \quad (5.37)$$

To compute the partition function on the  $n$ -sheeted geometry, we must compute the correlation function of two twist fields at points  $u$  and  $v$ . In the previous section, we computed their conformal weights,  $\frac{c}{24}(1 - 1/n^2)$ . If we parametrize the boundary geometry with the coordinate  $\theta \in [0, 2\pi L)$ , the  $AdS$  geodesic connecting the points  $(\rho_0, \theta_u)$  and  $(\rho_0, \theta_v)$  may be computed [92]. The geodesic length is

$$\text{Length} = \cosh^{-1} \left( 1 + 2 \sinh^2 \rho_0 \sin^2 \frac{\pi \ell_A}{L} \right). \quad (5.38)$$

If the parameter  $a$  is small, as before, we may determine the entanglement entropy from the twist field correlators:

$$S_A = \frac{c}{3} \ln \left( e^{\rho_0} \sin \frac{\pi \ell_A}{L} \right) \sim \frac{c}{3} \ln \left( L \sin \frac{\pi \ell_A}{L} \right). \quad (5.39)$$

Note that this is precisely what we found for the entanglement entropy on a finite geometry.

While this  $AdS_3$  description does not allow one to perform an explicit com-

putation of the entanglement entropy, it does provide a different perspective on the  $CFT_2$  results. In addition, the  $AdS_3$  perspective appears to be valid higher dimensions, possibly providing a route to discuss entanglement entropies, when one does not have the tools of two dimensional conformal field theories at one's disposal.

# Chapter 6

## Entanglement Entropy in Chern-Simons Theories

### 6.1 Introduction

In the previous chapter we discussed the behavior of entanglement entropies in  $1 + 1$  dimensional CFT's. However, it turns out that the systems for which the concept of entanglement entropy is particularly powerful are the *topological phases* of condensed matter systems and in topological quantum field theories<sup>1</sup>. Although some of the following concepts can in principle have wider applicability, in this chapter we will only concern ourselves with topological phases in two space dimensions. It has been shown recently [98, 99] that, for a physical system in a topological phase (which will be defined below) in two space dimensions, the entanglement entropy for a large simply connected region  $A$  of linear size  $L$  with a smooth boundary, and a subset of a simply connected region, has the form

$$S_A = \alpha L - \gamma \tag{6.1}$$

where  $\alpha$  is a non-universal coefficient. The universal constant term  $\gamma$ , the *topological entropy*, characterizes the topological state and it is a property of a topological field theory. For a general topological field theory it is given by [98, 99]

$$\gamma = \log \mathcal{D} = \log \sqrt{\sum_i \mathcal{D}_i^2} \tag{6.2}$$

where  $\mathcal{D}_i$  are the quantum dimensions of the quasiparticles (labelled by  $i$ ) of the excitation spectrum associated with this phase, and  $\mathcal{D}$  is the effective quantum dimension.[100]

Topological phases in two space dimensions satisfy the following properties. They are “liquid” phases, a translationally invariant ground states that do not break spontaneously any symmetries of the system. On manifolds with a non-trivial topology (*e.g.* a torus) the ground states exhibit a non-trivial degeneracy which is robust since it cannot be lifted by the action of any local perturbation. In these phases the excitation spectrum is gapped. In the limit of low energies and long distances the wave functions of a set of excitations, vortices of these fluids, exhibit non-local properties that do not depend on the positions of the

---

<sup>1</sup>The content of this chapter is largely taken from a paper to appear [97]

excitations. The states of the excitations of a topological state span a topologically protected Hilbert space, and the rate of growth of the dimension of this Hilbert space (as a function with the number of excitations of type  $i$ ) is the quantum dimension  $\mathcal{D}_i$  of the excitation. In the limit of a vanishing correlation length  $\xi \rightarrow 0$ , the effective field theory of a topological phase is a topological field theory. The path integral (partition function) of a topological field theory is a topological quantity in the sense that it is independent of the metric of the space. The prototype of a topological field theory is Witten's Chern-Simons gauge theory of the Jones polynomial[101, 102].

The non-local behavior of the excitations of a topological phase in two space dimensions is closely related to the braiding properties of their world lines which, in turn, determine the analytic properties of their wave functions. These excitations are generally known as anyons and carry fractional statistics.[103, 104] Excitations with Abelian fractional statistics are labeled by one-dimensional representations of the braid group and their quantum dimensions  $\mathcal{D}_i = 1$ , and their associated Hilbert spaces are one dimensional. Excitations with non-Abelian statistics are labeled by multi-dimensional representations of the braid group, have quantum dimensions  $\mathcal{D}_i > 1$ , and their associated Hilbert spaces are multi-dimensional. Such non-Abelian excitations, and of their topologically protected Hilbert spaces are the basis of the concept of topological quantum computation.[105, 106, 107]

FQH systems are experimentally interesting examples of systems for which one would like to be able to compute the topological entanglement entropy. The entanglement entropy for the (Abelian) Laughlin FQH wave functions [108], as well as for the non-Abelian FQH pfaffian wave functions [109, 110], was calculated numerically recently in several papers[111, 112] (and in the topological phase of the quantum dimer model on the triangular lattice [113]) which attempted to extract the topological entropy  $\gamma$  for these states. This is, in practice, difficult to do numerically due to the large non-topological area term which needs to be subtracted. Similarly, the computation of the topological entropy in the conceptually much simpler  $\mathbb{Z}_2$  topological phase of the quantum dimer model on a triangular lattice, which has a small but finite correlation length, presents similar difficulties[113].

In their topological phases, FQH systems actually possess a Chern-Simons effective field theory description. It shall be the goal of the rest of this chapter to describe how one may directly compute topological entanglement entropies from knowledge of Chern-Simons path integrals. The main advantage to this description is its manifest topological nature. There is no need to subtract large uninteresting non-topological effects.

Most of the necessary technical details may be found in the work of Witten[101, 102] for the partition functions of Chern-Simons gauge theories to the computation of the topological entanglement entropy. We use the standard “replica” approach to compute the entropy[114, 83]. This requires to understand what is

the 3-manifold resulting from gluing  $n$  copies of the system in a suitable fashion [83], needed to compute the entropy for a number of cases of interest. The key aspect of our approach is the identification of a suitable configuration of Wilson loops for each case of interest and to compute it by reducing it to already known cases by using surgeries. Alternatively, it is also possible in principal to use a more conventional approach using the wave function of the Chern-Simons gauge theory[102]. This approach is fraught with regulator subtleties as commented on in A.8. We shall only touch upon this approach, leaving it to further work.

This chapter is organized as follows. In Section 6.2 we set up the calculation of the topological entanglement entropy  $\gamma$  in Chern-Simons gauge theories. In Section 6.3.1 we show how the computation of the entropy can be carried out using the methods developed by Witten [101] and use them to compute the entropy for the simplest cases, a simply connected region on a sphere and a torus, and multiply-connected regions on a sphere and on a torus. In Section 6.4 we discuss the general case of a manifold of genus  $g$ . The different states are labeled by a Wilson loop on each cycle. Depending on the choice of the regions being observed, the entropy now depends on the quantum dimensions for each Wilson loop piercing these regions. Section 6.5 we shall apply our results to  $U(1)_m$  and  $SU(2)_k$  theories and discuss various possible extensions and applications.

## 6.2 Entanglement Entropy and Chern-Simons Gauge Theory

We consider Chern-Simons theory in three dimensions with group  $G$  and level  $k$ . To begin, we can think in terms of a 3-geometry of the form  $\mathbb{R} \times \Sigma$ , with  $\Sigma$  a closed genus  $g$  surface. This is of particular relevance for constructing wavefunctions for this theory. This geometry may be mapped to  $\tilde{\Sigma}$ , consisting of  $\Sigma$  and its interior. As discussed in A.8, the Hilbert space  $\mathcal{H}_\Sigma$  of this theory is accounted for by the appropriate conformal blocks of the corresponding WZW conformal field theory. For example, for the sphere  $S^2$  there is a unique state, while for the torus  $T^2$ , the various degenerate states may be obtained by placing Wilson lines in representation  $R$  along the center of the solid torus. For higher genus, we may account for all of the states by choosing a basis of one-cycles for the solid geometry, and placing Wilson loops along each.

To define an entanglement entropy, we cut  $\Sigma$  into two pieces, which we refer to as A and B. Depending on the genus and the manner of this cutting, A and B will in general consist of a number of connected components, as will the interface between them. Formally, if we may write  $\mathcal{H}_\Sigma \sim \mathcal{H}_A \otimes \mathcal{H}_B$ , then the entanglement entropy would be defined via

$$S_A = -Tr \rho_A \log \rho_A = -\left. \frac{d}{dn} Tr \rho_A^n \right|_{n=1} \quad (6.3)$$

with  $\rho_A$  the density matrix obtained by tracing a pure state  $\psi$  over  $\mathcal{H}_B$ . Given a path integral representation for the pure state wavefunctional (as in Ref. [102] and A.8), this may be written as a gauged WZW path integral),  $Tr\rho_A^n$  may be constructed by taking  $n$  copies of A and B and gluing them together in a fashion analogous to the two dimensional examples in 5.1.2. The resulting 3-geometry shall be referred to as  $\tilde{\Sigma}_n$ . We interpret  $Tr\rho_A^n$  then as the Chern-Simons path integral on  $\tilde{\Sigma}_n$ .

In the rest of this section we shall sketch wavefunctional computations analogous to those in 5.1.2 for completeness, although we emphasize this shall not be the approach taken to actually perform computations. The (anti-holomorphic) Chern-Simons wavefunctional introduced in A.8 split into data living on region A and data on B <sup>2</sup>

$$\langle \bar{B}_i | \langle \bar{A}_i | \Psi \rangle \sim \int [dg_{A,i} dg_{B,i}] e^{-kI_A(g_{A,i}) - kI_B(g_{B,i})} e^{-\frac{k}{2\pi} \int_{\Sigma_A} Tr \bar{A}_i g_{A,i}^{-1} \partial g_{A,i} - \frac{k}{2\pi} \int_{\Sigma_B} Tr \bar{B}_i g_{B,i}^{-1} \partial g_{B,i}} \quad (6.4)$$

This should be interpreted as a sum over histories with a spatial section of fixed topology. Here, we have split the integral into contributions of fields in regions A and B. Formally,  $Tr\rho_A^n$  may then be constructed by gluing together suitable such factors

$$\int \prod_{k=1}^n [d\mu(A_k) d\mu(B_k)] \langle \bar{B}_1 | \langle \bar{A}_1 | \Psi \rangle \langle \Psi | B_1 \rangle | A_2 \rangle \langle \bar{B}_2 | \langle \bar{A}_2 | \Psi \rangle \langle \Psi | B_2 \rangle | A_3 \rangle \dots \langle \bar{B}_n | \langle \bar{A}_n | \Psi \rangle \langle \Psi | B_n \rangle | A_1 \rangle \quad (6.5)$$

As a result, we obtain a functional integral with explicit gluing conditions on the gauge and WZW fields at the interfaces between the A and B regions. Equivalently, this can be interpreted (after integrating over the WZW fields) as a Chern-Simons path-integral on the glued geometry  $\tilde{\Sigma}_n$ . This 3-geometry consists of  $n$  copies of the 3-manifolds for  $|\psi\rangle$  and  $\langle\psi|$ : we draw the A and B regions on the boundary surfaces and glue  $|\psi\rangle_1$  with  $\langle\psi|_1$  through B,  $\langle\psi|_1$  and  $|\psi\rangle_2$  through A,  $|\psi\rangle_2$  with  $\langle\psi|_2$  through B... and finally glue  $\langle\psi|_n$  and  $|\psi\rangle_1$  through A. It is clear from this construction that the result will be symmetric between A and B.

Different states correspond to different configurations of Wilson loops inside the 3-manifold. In fact, if we arrange the handles of  $\Sigma$  as in Fig. 6.1, a set of complete state in the Chern-Simons Hilbert space can be generated by doing the path integrals on the solid multi-torus with unlinked Wilson loops embedded as in the Fig. 6.1.

Each Wilson loop can carry any of the representations which correspond to the integrable representations in the level  $k$  Kac-Moody algebra. That means the dimension of the Hilbert space on a surface with  $m$  handles is  $\dim(S)^m$ ,

<sup>2</sup>Written in this form, the gauge field measure includes a factor  $e^{\frac{k}{2\pi} \int Tr \bar{A} A}$ .

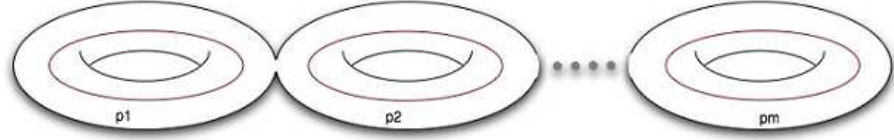


Figure 6.1: A general  $m$ -handled surface. Red lines are the Wilson loops. Different states are generated by the choice of Wilson line's representation.

where  $S$  is the modular  $S$  matrix. The two pieces corresponding to  $|\psi\rangle$  and  $\langle\psi|$  are identical with different orientations, and the Wilson loops carry conjugate representations.

As is apparent from their functional form, directly using the explicit wavefunctionals is filled with regulator ambiguities. One has the obvious problems that the wavefunctional itself is defined through a path integral, but there are also subtleties in cutting and gluing the path integral. There are also conceptual issues as to what is the gauge symmetry on an  $n$ -sheeted Riemann surface. In light of these issues, we will proceed more formally, and evaluate  $Tr\rho_A^n$  by surgery. This has the advantage of sidestepping the technical path integral issues. We will present the construction graphically; implicitly making use of the fact that  $2 + 1$  Chern-Simons field theories are topological field theories.

## 6.3 Explicit Entropy Computations

### 6.3.1 Surgery Properties

In section A.6 we described an explicit correspondence between WZW conformal blocks and the Hilbert space of Chern-Simons theory in particular gauges. Here we shall not use such explicit wavefunctionals, which we shall see contain more information than we need. Instead, given a framed, closed 2 dimensional surface,  $\Sigma$ , we may think of the Chern-Simons path integral over the surface's interior as generating a wavefunctional along the surface. For our purposes, the functional form of these wavefunctionals will not be important. As we are only interested in computing traces, it is sufficient to be able to write entanglement entropy calculations in terms of path integrals over complicated geometries.

Chern-Simons path integrals possess unusual properties which often allow one to relate the values of path integrals on different manifolds. We shall generally refer to this procedure as "surgery". All of the ideas described in this section may be found in [101]. The strategy shall be to use the values of simple path integrals and the rules for surgery to reconstruct complicated geometries occurring in entropy calculations. To this end we need to develop several basic tools in order to perform path integral surgeries.

## Connected Sums

Surgery manipulations begin with a simple observation about one dimensional vector spaces. If we have any three vectors in a one dimensional Hilbert space,  $\chi_1, \chi_2$ , and  $\chi_3$ :

$$\langle \chi_1 | \chi_2 \rangle = \frac{\langle \chi_1 | \chi_3 \rangle \langle \chi_3 | \chi_2 \rangle}{\langle \chi_3 | \chi_3 \rangle}. \quad (6.6)$$

We emphasize that this works for any one dimensional space. If we tensor  $m$  one dimensional vector spaces together, the resulting space is again one dimensional. Specifically, if we had

$$|\Psi_i\{\chi_{i_r}\}\rangle \equiv |\chi_{i_1}\rangle \otimes \dots \otimes |\chi_{i_m}\rangle, \quad (6.7)$$

the same logic dictates

$$\langle \Psi_1\{\chi_{1_r}\} | \Psi_2\{\chi_{2_r}\} \rangle = \frac{\langle \Psi_1\{\chi_{1_r}\} | \Psi_3\{\chi_{3_r}\} \rangle \langle \Psi_3\{\chi_{3_r}\} | \Psi_2\{\chi_{2_r}\} \rangle}{\langle \Psi_3\{\chi_{3_r}\} | \Psi_3\{\chi_{3_r}\} \rangle} \quad (6.8)$$

$$= \prod_{s=1}^m \left( \frac{\langle \chi_{1_s} | \chi_{3_s} \rangle \langle \chi_{3_s} | \chi_{2_s} \rangle}{\langle \chi_{3_s} | \chi_{3_s} \rangle} \right). \quad (6.9)$$

The next step is identify one dimensional Hilbert spaces in Chern-Simons theories, namely we are interested in geometries glued along  $S^2$ 's with few Wilson loops puncturing the  $S^2$ . The geometry obtained from two 3-geometries glued along an  $S^2$  is called the connected sum. The path integral on the connected sum of  $M_1$  and  $M_2$  may be thought of as the overlap of two states  $|\chi_1\rangle$  and  $|\chi_2\rangle$  defined on  $S^2$ .

$$Z(M_1 + M_2) = \langle \chi_1 | \chi_2 \rangle \quad (6.10)$$

Because these Hilbert spaces are one dimensional, we may introduce a third state on  $S^2$  from the path integral on a 3-ball,  $|\chi_3\rangle$ . Using our deep insight into one dimensional vector spaces, and the fact that two 3-balls of opposite orientations glued along their boundary is equivalent to  $S^3$  [101]<sup>3</sup>,

$$Z(M_1 + M_2) = \frac{Z(M_1)Z(M_2)}{Z(S^3)}. \quad (6.11)$$

If we define CFT's on two disconnected 2-geometries, they are completely independent. Hence, the combined space of conformal blocks shall be the tensor product of individual spaces. Thus, a Chern-Simons path integral over two spaces glued along  $m$   $S^2$ 's becomes

$$Z(M_1(+)^m M_2) = \frac{Z(M_1)Z(M_2)}{Z(S^3)^m}. \quad (6.12)$$

---

<sup>3</sup>Gluing two 3-balls produces  $S^3$  much as gluing two disks along their boundary forms  $S^2$ . Consequently, if one "slices"  $S^3$  one obtains an  $S^2$ . The two dimensional analogue is how a plane intersects  $S^2$  along  $S^1$ .

There are other one dimensional Hilbert spaces. Of particular use will be the Hilbert space on  $S^2$  with one or two punctures. The space with a single marked point is trivially the same as no marked points. More interesting is when  $S^2$  has two marked points in representations  $\rho$  and  $\rho^*$ . A simple example is the "3-necklace"<sup>4</sup> when we have  $m$   $S^3$ 's glued end to end along  $S^2$ 's each of which are punctured by Wilson loops in representations  $\rho$  and  $\rho^*$ . Because each of these Hilbert spaces is one dimensional, we may again glue in states from a third one dimensional space. In this case we want states defined on the surface of a 3-ball with punctures in representations  $\rho$  and  $\rho^*$ . These state may be viewed as a Wilson line in the 3-ball's volume connecting the two boundary points. This time, the product of two auxiliary states is a Chern-Simons path integral on  $S^3$  with one Wilson loop in representation  $\rho$ .

$$Z_m(3 - \text{necklace}, \rho, \rho^*) = \frac{Z(S^3, \rho)^m}{Z(S^3, \rho)^m} = 1. \quad (6.13)$$

Intuitively we may understand this as saying the Wilson loops annihilate leaving an empty 3-geometry with one cycle ( $S^2 \times S^1$ ). If instead the "necklace" is open, implying only  $m - 1$   $S^2$ 's, the path integral would be

$$\frac{Z(S^3, \rho)^m}{Z(S^3, \rho)^{m-1}} = S_\rho^0. \quad (6.14)$$

### Handle Gluing

The next surgery operation we shall need is the ability to manipulate handles. There are two important things to remember, the conformal blocks on a  $T^2$  are labeled by the WZW primary fields and the way these conformal blocks behave under modular transformations. In the Chern-Simons language, the different states along  $T^2$  may be obtained by the Chern-Simons path integral with a Wilson loop in the torus' interior. In a WZW theory, if we perform a modular transformation upon the torus, the conformal blocks map into themselves (see A.2 and A.4). The effect of a modular transformation on the Chern-Simons Hilbert space is to map one state into another. However, the modular transformation  $S$  exchanges the torus' two cycles,  $a \rightarrow b$  and  $b \rightarrow -a$ . Thus, a loop which is not contractable, becomes contractable after an  $S$  transformation. In this way we may relate 3-geometries with different numbers of handles.

As an example, consider the  $S$  transformation relating  $S^3$  and  $S^2 \times S^1$ . It is first necessary to understand how to glue together solid tori. We begin by viewing a solid torus as  $D^2 \times S^1$ . The choice of trivial gluing or first acting with  $S$ , alters the gluing of the two initial solid torii's cycles. Specifically, labeling solid torus 1's cycles  $a_1$  and  $b_1$  (similarly for torus 2), if we glue  $a_1 \rightarrow a_2$  and

---

<sup>4</sup>For a two dimensional analogue, imagine the surface of a pearl necklace. Then imagine that each pearl ( $S^2$ ) has two caps cut off and is glued to the adjacent pearl along an  $S^1$ . The analogue of a the loop we are describing would be to draw a line around the necklace (on the pearls' surface). This loop will pierce each  $S^1$  once.

$b_1 \rightarrow b_2$ , a non-contractable loop in one solid torus cannot be contracted by passing into the second solid torus. The two  $D^2$  are simply glued together to form  $S^2$  and the three geometry is  $S^2 \times S^1$ . However, if we act with  $S$  before gluing, we find that any non-contractable loop in either torus may be contracted by pulling it across the interface. This new space is topologically  $S^3$ .

Suppose we have a single Wilson loop in a representation  $\rho_i$  in  $S^3$ . If we draw a tubular surface encasing this loop, we may write the path integral as an overlap of two states defined on the  $T^2$ ,

$$Z(S^3, \rho_i) = \langle \psi | \rho_i \rangle. \quad (6.15)$$

On the other hand, we could view the state  $|\rho_i\rangle$  as the image under a modular transformation of other states,

$$|\rho_i\rangle = S_i^j |\rho_j\rangle. \quad (6.16)$$

Because the  $S$  transformation exchanges the cycles, we have

$$Z(S^3, \rho_i) = \sum_j S_i^j Z(S^2 \times S^1, \rho_j). \quad (6.17)$$

We may push this example further because we know a lot about conformal blocks on  $S^2$ , the only non-vanishing one point function lives in the trivial representation (which is equivalent to no insertion at all). [101]

$$Z(S^2 \times S^1, \rho_j) = \delta_j^0 \quad (6.18)$$

$$\rightarrow Z(S^3, \rho_i) = \sum_j S_i^j \delta_j^0 \quad (6.19)$$

$$= S_i^0. \quad (6.20)$$

### Path Integral on a $m$ -Handlebody

Assume we have a 3-geometry with  $m$  non-contractible cycles,  $X_m$ . If we perform  $S$  transformations along the  $m$  cycles, we will obtain an  $S^3$  with  $m$  unlinked loops labeled by representations  $\{\rho_r\}$ :

$$Z(X_m) = \sum_{\{r_i\}} S_0^{r_1} \dots S_0^{r_m} Z(S^3, \rho_{r_1}, \dots, \rho_{r_m}). \quad (6.21)$$

If we split the  $S^3$  into two balls, one with  $m-1$  loops and a second with a single loop, we may view this as the connected sum of two  $S^3$ 's. Continuing in this way we may view the  $m$ -handlebody as  $m$   $S^3$ 's (each with a single loop), glued

along  $m - 1$   $S^2$ 's. Using properties of the  $S$  matrix described in A.4,

$$\begin{aligned}
Z(X_m) &= \sum_{\{\rho_i\}} S_0^{r_1} \dots S_0^{r_m} \frac{Z(S^3, \rho_{r_1}) \dots Z(S^3, \rho_{r_m})}{Z(S^3)^{m-1}} \\
&= \left( \sum_{\rho_{r_1}} S_0^{r_1} S_{r_1}^0 \right) \dots \left( \sum_{\rho_{r_m}} S_0^{r_m} S_{r_m}^0 \right) (S_0^0)^{1-m} \\
&= (S_0^0)^{1-m}.
\end{aligned} \tag{6.22}$$

This may be generalized to allow for distinct Wilson loops along each of the  $m$  cycles:

$$\begin{aligned}
Z(X_m, \{\rho_{\ell_m}\}) &= \left( \sum_{\{\rho_1\}} S_{\ell_1}^{r_1} S_{r_1}^0 \right) \dots \left( \sum_{r_m} S_{\ell_m}^{r_m} S_{r_m}^0 \right) (S_0^0)^{1-m} \\
&= (S_0^0)^{1-m}
\end{aligned} \tag{6.23}$$

### 6.3.2 Entanglement Entropy on $S^2$ with One A-B Interface

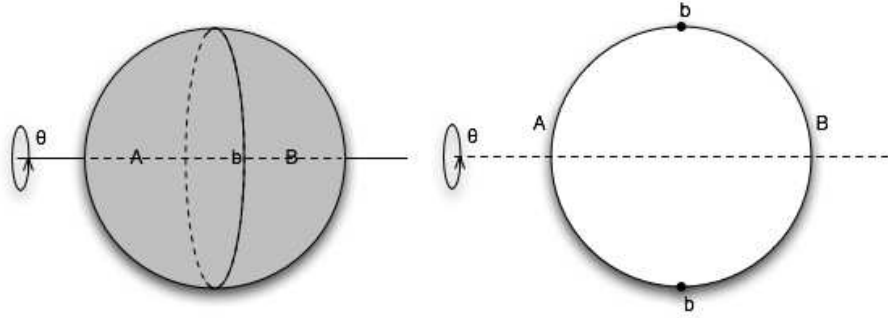


Figure 6.2: Shading implies a 3-d solid ball. This can be made by rotating a disk about an axis passing the origin, as shown at right.

Having developed the machinery necessary to perform surgery, let us proceed to the simplest entanglement entropy, in which the spatial topology is a 2-sphere. The Hilbert space on  $S^2$  is one dimensional, and so there is only one choice of state. The 3-geometry is the 3-ball shown in Fig. 6.2. If we take the A and B regions to be connected, then they are disks, as shown in the figure. To construct  $tr\rho_A^n$ , we glue  $2n$  such pieces together. In Fig. 6.3, we show how to systematically perform this gluing. We have drawn the  $n = 2$  case explicitly, but it is not hard to generalize to higher  $n$ . In the figure, we have used 1 and 2 to label  $|\psi\rangle_1$  and  $\langle\psi|_1$ , 3 and 4 for  $|\psi\rangle_2$  with  $\langle\psi|_2$ . The four slices form four 3-balls (or as shown, rotated disks); when glued together to form  $tr\rho_A^n$ , we find an  $S^2$ , rotated about the axis, which has the topology  $S^3$ . One can easily check that for higher  $n$ , we obtain the same result, the  $S^2$  being obtained by

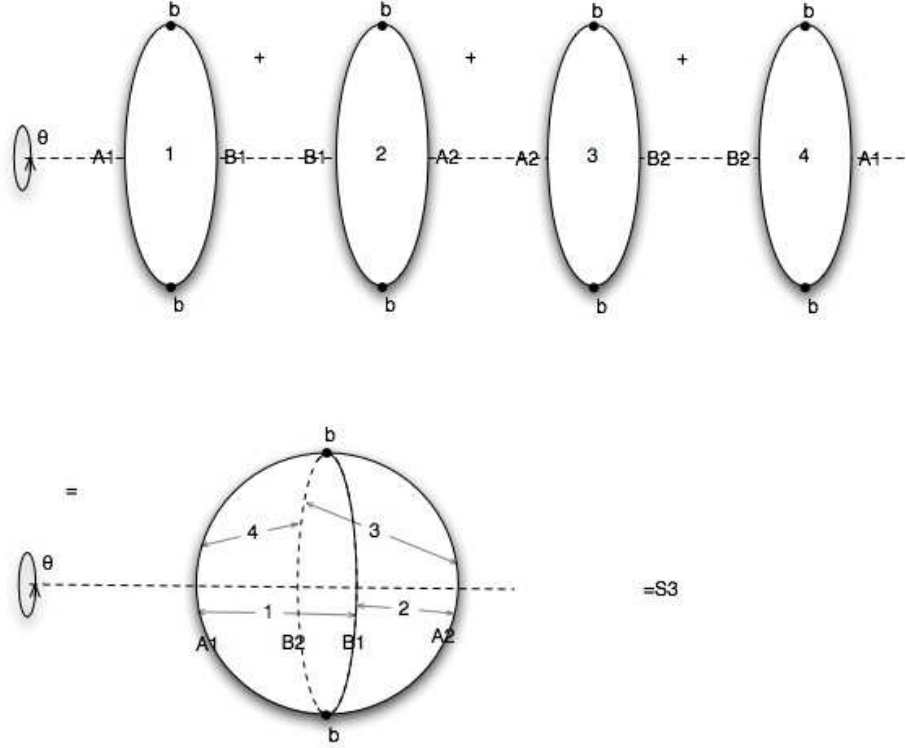


Figure 6.3: The overall manifold is generated by four pieces of disks glued together one after another and rotated along the same axis as in Fig. 6.2.

sequentially gluing  $2n$  disks. Thus we have

$$\frac{\text{Tr} \rho_A^n(S^{2,1})}{(\text{Tr} \rho_A(S^{2,1}))^n} = \frac{Z(S^3)}{(Z(S^3))^n} = (Z(S^3))^{1-n} = S_{00}^{1-n}. \quad (6.24)$$

where we have used formulae noted above. Finally, using eq. (6.3), we obtain

$$S_A^{(S^2,1)} = \ln S_{00} \quad (6.25)$$

### 6.3.3 Entanglement Entropy on $T^2$ with One Component A-B Interface

The Hilbert space on  $T^2$  is isomorphic to the space of integrable representations  $\rho_j$  of the Kac-Moody algebra. These states are generated by doing the path integrable on a solid torus with Wilson loop in representation  $\rho_j$  lying along the non-contractible loop. We will consider a slicing of the torus into A and B regions such that there is a single connected interface component, as shown in Fig. 6.4.

To define the entanglement entropy, we must choose a pure state, and here we have a choice. To begin, let us first choose the trivial representation (equivalent to no Wilson loop). In Fig. 6.4, we have redrawn the solid torus as a ball with



Figure 6.4: The solid torus with A B regions indicated as on the LHS is topologically the same as a solid 3-ball with a solid torus “planted” in the A region.

a solid torus attached in the A region. This is useful, since we have already studied the solid ball in the previous subsection, and to compute  $\text{tr}\rho_A^n$  here, we need to follow that analysis and also keep track of the gluing of the extra toroidal fixtures. The gluing for  $n = 2$  is shown in Fig. 6.5. Note that a solid torus can be thought of as  $D_2 \times S^1$ , and two copies glued together (with opposite orientations) gives an  $S^2 \times S^1$ . Thus the resulting manifold will be

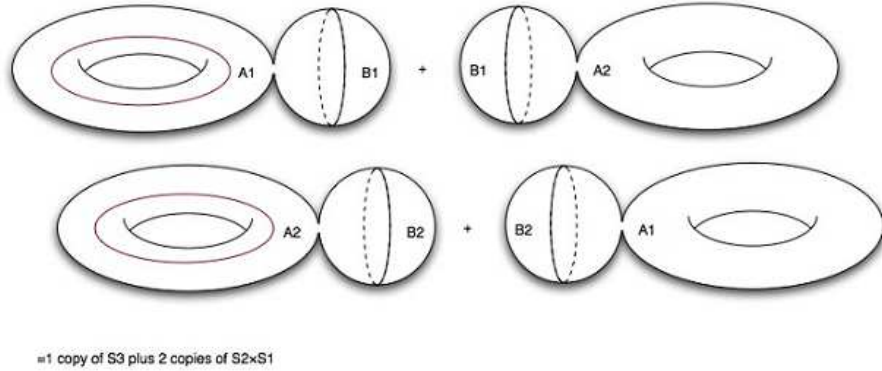


Figure 6.5: The two red circles indicate the two cycles.

the connected sum of an  $S^3$  and  $n S^2 \times S^1$ 's joined along  $n S^2$ 's. It has  $n$  cycles along the  $S^1$  directions of  $n S^2 \times S^1$ . Thus

$$\frac{\text{Tr}\rho_{A(T^2,1)}^n}{(\text{Tr}\rho_{A(T^2,1)})^n} = \frac{\overbrace{1}^{\text{from normalization}}}{Z(S^2 \times S^1)^n} \frac{\overbrace{Z(S^3)Z(S^2 \times S^1)^n}^{\text{from surgery}}}{Z(S^3)^n} = (Z(S^3))^{1-n} = S_{00}^{1-n}. \quad (6.26)$$

We note that this result coincides with the  $S^2$  result. As we shall see, the commonality of these two examples is that the interface is the same; the topology of the A and B regions themselves does not contribute.

It is simple to repeat this construction for other pure states, that is including a Wilson loop in representation  $\rho$  inside the solid torus. In the gluing above, we will now have a  $D_2 \times S^1$  with Wilson loop in representation  $\rho$  glued to a  $D_2 \times S^1$  of opposite orientation with Wilson loop in representation  $\rho^*$  (the

conjugate state). Thus, we have

$$\begin{aligned}
\frac{\text{Tr}\rho_{A(T^2,\rho)}^n}{(\text{Tr}\rho_{A(T^2,\rho)})^n} &= \frac{(Z(S^3)Z(S^2 \times S^1, \rho, \rho^*)^n)}{(Z(S^2 \times S^1, \rho, \rho^*))^n Z(S^3)^n} \\
&= \frac{(Z(S^3)Z(S^2 \times S^1)^n)}{(Z(S^2 \times S^1))^n Z(S^3)^n} \\
&= (Z(S^3))^{1-n} \\
&= S_{00}^{1-n}.
\end{aligned} \tag{6.27}$$

In fact this result can be generalised further, to *any* pure state  $|\psi\rangle = \sum_{\rho} \psi_{\rho} |\rho\rangle$ .

$$\frac{\text{Tr}\rho_{A(T^2,\psi)}^n}{(\text{Tr}\rho_{A(T^2,\psi)})^n} = \frac{\sum_{\{\rho^{(r)}\}} \psi_{\rho^{(1)}} \psi_{\rho^{(2)}}^* \psi_{\rho^{(2)}} \psi_{\rho^{(3)}}^* \dots \psi_{\rho^{(n)}} \psi_{\rho^{(1)}}^* Z(X_n, \rho^{(1)}, \rho^{(1)*}, \dots)}{(\sum_{\rho} |\psi_{\rho}|^2 Z(S^2 \times S^1, \rho, \rho^*))^n}$$

where we have denoted the glued 3-geometry as  $X_n$ ; the Wilson loops  $\rho^{(j)}$  and  $\rho^{(j)*}$  are located along the  $j^{\text{th}}$  cycle. We can now do surgery on each of these cycles, and we obtain

$$\frac{\text{Tr}\rho_{A(T^2,\psi)}^n}{(\text{Tr}\rho_{A(T^2,\psi)})^n} = \frac{\sum_{\{\rho^{(r)}\}} \psi_{\rho^{(1)}} \psi_{\rho^{(2)}}^* \psi_{\rho^{(2)}} \psi_{\rho^{(3)}}^* \dots \psi_{\rho^{(n)}} \psi_{\rho^{(1)}}^* (Z(S^3))^{1-n}}{(\sum_{\rho} |\psi_{\rho}|^2 Z(S^2 \times S^1, \rho, \rho^*))^n} = S_{00}^{1-n}. \tag{6.28}$$

where we have used  $\sum_{\rho} |\psi_{\rho}|^2 = 1$ .

### 6.3.4 Entanglement Entropy on $S^2$ with Two-Component AB Interface

Now let's study the case where A and B meet at an interface with two components. For  $S^2$ , the only choice is to have two disconnected B regions, as in Fig.

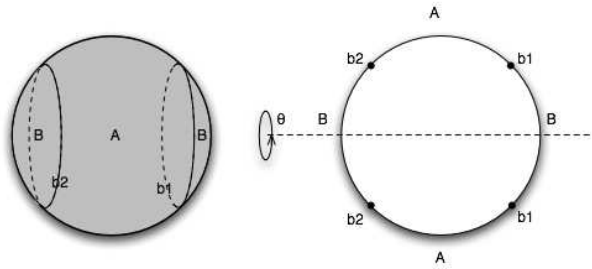


Figure 6.6: Two component interface on spatial sphere. The notation is the same as in Fig. 6.2.

6.6. We glue  $2n$  pieces just as we did in the first example. Fig. 6.7 shows the  $n = 2$  case. In this case the resulting object is a  $T^2$  rotating about the axis passing through the origin of each piece of disks. It has one cycle. For general  $n$ , we will have a surface with  $n - 1$  handles rotating about the axis, which admits

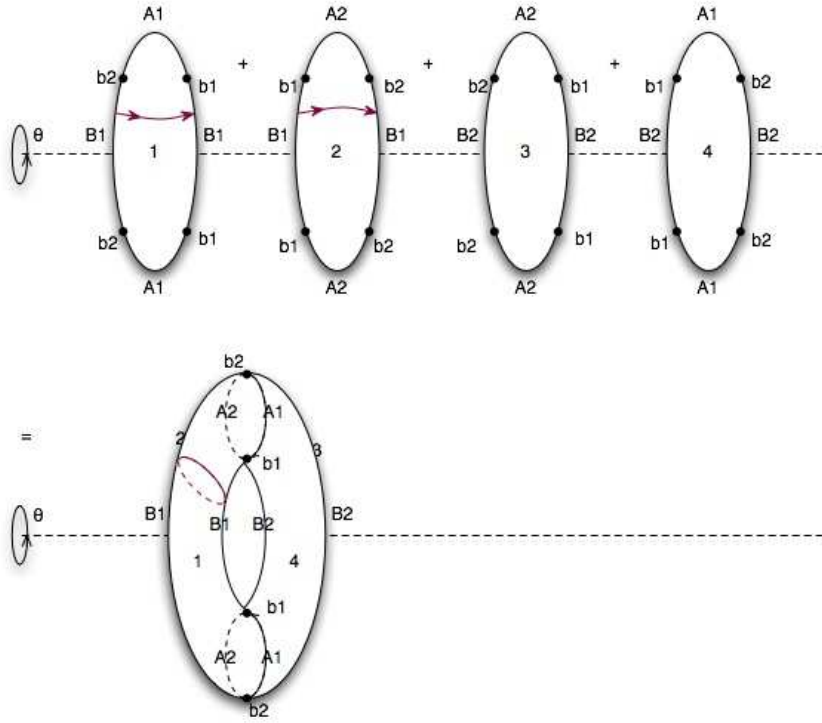


Figure 6.7: The red lines form a cycle.

$n - 1$  cycles. Thus

$$\frac{\text{Tr} \rho_{A(S^2, 2)}^n}{(\text{Tr} \rho_{A(S^2, 2)})^n} = \frac{(Z(S^3))^{1-(n-1)}}{(Z(S^3))^n} = (Z(S^3))^{2(1-n)} = S_{00}^{2(1-n)}.$$

Another way to obtain this result, is to draw the geometry out into two balls

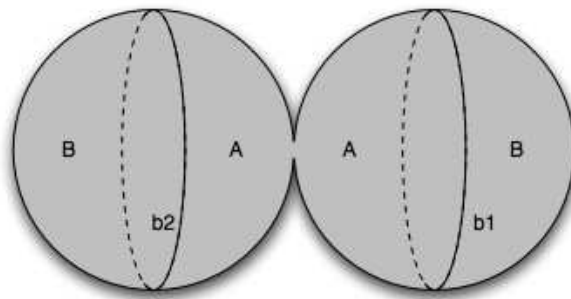


Figure 6.8: Two parts of the A region are connected through a disk, and when we glue  $2n$  copies of A pairwise, they become  $n$  two-spheres.

joined along an  $S^2$ , as shown in Fig. 6.8. When we glue  $2n$  of these together, we obtain two  $S^3$ 's connected through  $n$   $S^2$ 's (Each  $A_i$  region yields one such

connection.).

$$\frac{\text{Tr} \rho_{A(S^2,2)}^n}{(\text{Tr}^n \rho_{A(S^2,2)})^n} = \frac{(Z(S^3))^{-n} (Z(S^3))^2}{(Z(S^3))^n} = (Z(S^3))^{2(1-n)} = S_{00}^{2(1-n)},$$

as before.

It is not difficult to envision the generalization of this result to an  $M$ -component interface, and we find

$$S_A^{(M)} = M \ln S_{00}. \tag{6.29}$$

### 6.3.5 Entanglement Entropy on $T^2$ with Two-Component AB Interface

For  $T^2$  with two interfaces, the topology allows a choice for the way to slice the surfaces. Fig. 6.9 shows the two distinct ways to slice the spatial surface. The first possibility is shown on the left; here, as learned in the last section, when the partitions are simply connected the only effect is to rescale the entropy by the number of interfaces. Indeed, an explicit computation reveals slicing a produces  $S_A = 2 \ln S_{00}$ .

The second possibility, shown on the right in the figure, presents new complications. In this case, it is difficult to draw the resulting manifold, so we will

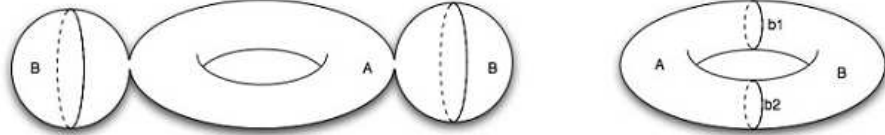


Figure 6.9: Two of the ways to cut torus using two interfaces. The RHS one is a solid torus with the surface cut into two pieces bearing the same topology.

only count the cycles as in 6.3.1. As in Fig. 6.10, where  $n = 2$ , there are 3 cycles in the overall manifold. For general  $n$ , the number of cycles is  $2n - 1$ .

One way to count the number of cycles is by slicing each solid torus into two  $D_2 \times I$  (two disks times an interval). Each power of  $\rho_A$  yields four solid torii, one  $A$  and  $B$  and orientation their reversed copies. When we take overlap of each copy of  $A$  with its orientation reversed image we obtain  $S^2 \times I$  (similarly for each copy of  $B$ ). However, we must take care to glue these together correctly. It is not too hard to see that all of these intervals meet at two  $S^2$ , much like having a  $S^2 \times I$  lying along the seams of a basketball of  $2n$  total seams. At both the north and south poles these geometries are glued along a  $S^2$ . Along a basketball with  $2n$  seams, only  $2n - 1$ , will represent independent cycles.

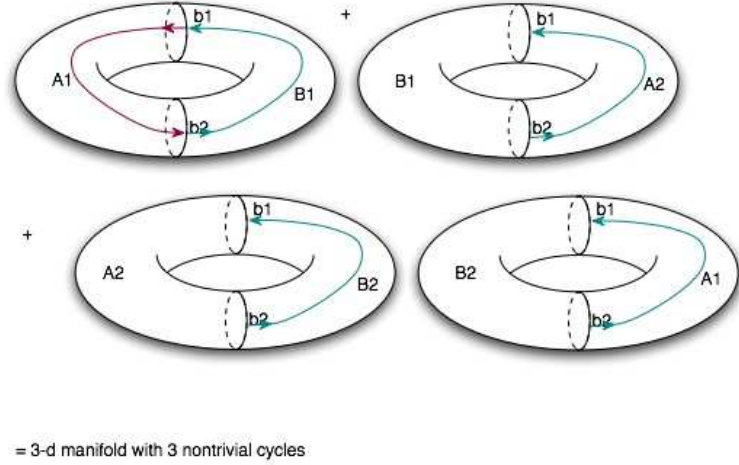


Figure 6.10: The red line forms 3 cycles when connected with the 3 green lines.

$$\frac{\text{Tr} \rho_{A(T^2,2)}^n}{(\text{Tr} \rho_{A(T^2,2)})^n} = \frac{(Z(S^3))^{1-(2n-1)}}{(Z(S^2 \times S^1))^n} = (Z(S^3))^{2(1-n)} = S_{00}^{2(1-n)}. \quad (6.30)$$

Note, this result also matches the previous example.

To check this result, we will also consider a different factorization argument. We squeeze the RHS of Fig. 6.9 into Fig. 6.11. Each of the solid balls, when

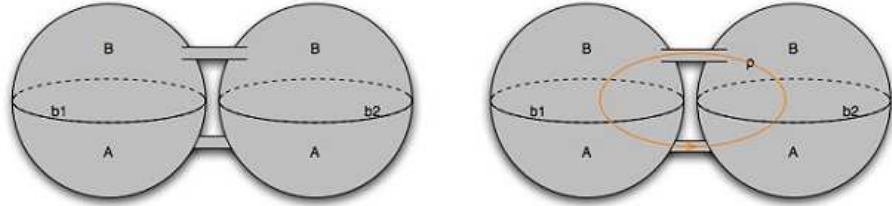


Figure 6.11: Two solid balls connecting each other through two solid cylinders, with or without Wilson loop.

glued with the other  $2n - 1$  pieces, becomes an  $S^3$ . These two  $S^3$ 's are connected through  $2n$   $S^2$ 's (Each  $A_i$  and  $B_i$  contributes one.). Thus we have

$$\frac{\text{Tr} \rho_{A(T^2,2)}^n}{(\text{Tr} \rho_{A(T^2,2)})^n} = \frac{(Z(S^3))^{-2n} (Z(S^3))^2}{(Z(S^2 \times S^1))^n} = (Z(S^3))^{2(1-n)} = S_{00}^{2(1-n)}. \quad (6.31)$$

The complication arises if there are Wilson loops present, that is, if we choose a state other than the trivial one. This is significant here because this Wilson loop threads the interface between the A and B regions. The Wilson loops inside the solid torus will make punctures on the  $S^2$  which connect the two  $S^3$ 's, as in the RHS of Fig. 6.11. Upon gluing the  $2n$  copies, we need to keep track of

the Wilson lines. We have drawn them in Fig. 6.12. The result is that we

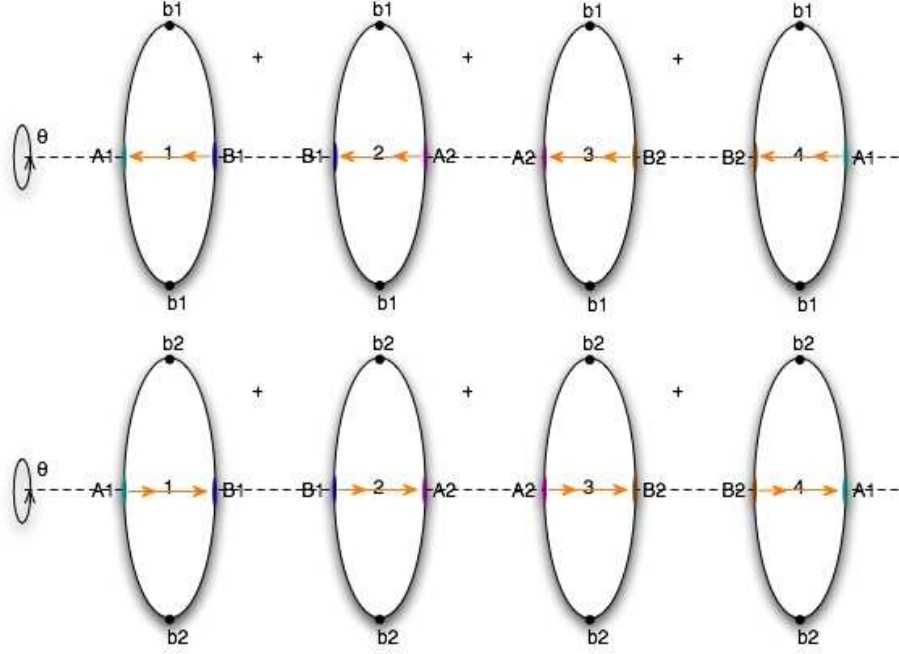


Figure 6.12: The two rows form two  $S^3$  separately. They are connected through the region with the same colors along a  $S^2$  tube.

have two  $S^3$ 's connected by  $2n$  tubes; down each tube, there is a Wilson line in  $\rho$  and a Wilson line in  $\rho^*$ . These Wilson lines are connected to lines in the  $S^3$ 's, the ordering of which is dictated by the gluing prescription. In particular, if we label the orientation reversed image of  $A_i$  ( $B_i$ ) as  $\tilde{A}_i$  ( $\tilde{B}_i$ ), we must glue the Wilson lines with the following weaving

$$\begin{aligned} \rho(A_1) &\rightarrow \rho(\tilde{A}_2)^* \rightarrow \rho(A_3) \rightarrow \rho(B_1) \rightarrow \rho(\tilde{B}_2)^* \rightarrow \rho(B_3) \\ \rho(\tilde{A}_1) &\rightarrow \rho(A_2)^* \rightarrow \rho(\tilde{A}_3) \rightarrow \rho(\tilde{B}_1) \rightarrow \rho(B_2)^* \rightarrow \rho(\tilde{B}_3). \end{aligned} \quad (6.32)$$

This may look complicated, but, because all representations are  $\rho$  or  $\rho^*$ , the weaving just ensures that every  $S^2$  has both types of representations.

The computation of the entropy can be performed by cutting out the tubes and gluing on endcaps possessing Wilson lines (as in 6.3.1). We find

$$\begin{aligned} \frac{\text{Tr}(\rho_{A(T^2,2,\rho)}^n)}{\text{Tr}^n(\rho_{A(T^2,2,\rho)})} &= \frac{(Z(S^3, \rho))^{2n} (Z(S^3, \rho))^2}{(Z(S^2 \times S^1, \rho, \rho^*))^n (Z(S^3, \rho))^{4n}} \\ &= (Z(S^3, \rho))^{2(1-n)} \\ &= S_{0\rho}^{2(1-n)}. \end{aligned} \quad (6.33)$$

In terms of the "basketball" picture, we cap every  $S^2 \times I$  as it approaches both poles, leaving  $2n + 2$   $S^3$ 's (each with a loop in  $\rho$ ), one from each seam and two

from the two poles. The denominator arises because we have performed surgery  $4n$  times.

It is then straightforward to show that for any state  $|\psi\rangle = \sum_{\rho} \psi_{\rho} |\rho\rangle$ ,

$$\frac{\text{Tr} \rho_{A(T^2, 2, \psi)}^n}{(\text{Tr} \rho_{A(T^2, 2, \psi)})^n} = \frac{\sum_{\rho} |\psi_{\rho}|^{2n} S_{0\rho}^{2(1-n)}}{(\sum_{\rho} |\psi_{\rho}|^2)^n}. \quad (6.34)$$

We thus obtain the entropy

$$S_{A(T^2, 2, \psi)} = \sum_{\rho} [2|\psi_{\rho}|^2 \ln S_{0\rho} - |\psi_{\rho}|^2 \ln |\psi_{\rho}|^2] \quad (6.35)$$

Since we can interpret  $|\psi_{\rho}|^2$  as a probability  $p_{\rho}$ , the second term has the familiar form  $-p \ln p$ . More precisely, note that this can be rewritten

$$S_{A(T^2, 2, \psi)} = 2 \ln S_{00} - \sum_{\rho} \mathcal{D}_{\rho}^2 \left[ \frac{|\psi_{\rho}|^2}{\mathcal{D}_{\rho}^2} \ln \frac{|\psi_{\rho}|^2}{\mathcal{D}_{\rho}^2} \right] \quad (6.36)$$

## 6.4 General Case

The example considered in the last subsection is fairly typical of the general case, which we now consider. Suppose we begin with a solid 3-geometry with genus  $g$  boundary. For such a geometry, the space of states is accounted for by placing Wilson loops along a set of independent 1-cycles threading the geometry. The different states (of the chosen basis) then correspond to a choice of representation for each Wilson loop on each cycle.

To define entanglement entropy, we need to choose a pure state, which we will take to be an arbitrary linear combination of these basis states, and we need to make a choice of cutting the genus  $g$  surface into  $A$  and  $B$  regions. These regions may or may not be connected and/or simply connected; the interface between them will generally consist of a number of components. In each such case, we can organize the surface as follows (a representative surface is shown in Fig. 6.13).

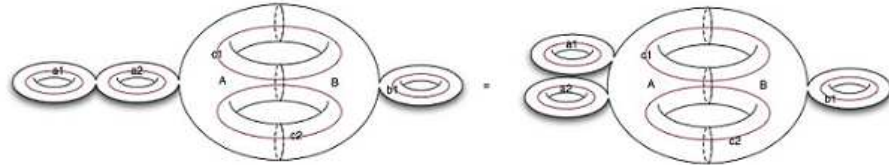


Figure 6.13: A representative example of the general case. Here the  $A$  and  $B$  regions are each connected and are separated by a 3-component interface. In the case shown,  $A$  and  $B$  are connected. Wilson loops are shown in red for a choice of basis 1-cycles.

It behooves us to zoom in on the cycles cut by the interface, a region we

shall label  $C$ . In general there will also be a collection of solid tori connected to  $C$  along disks  $D_2$ , some in  $A$  and some in  $B$ . In Fig. 6.14, we show all of the inequivalent cuttings in the case where the interface consists of three components.

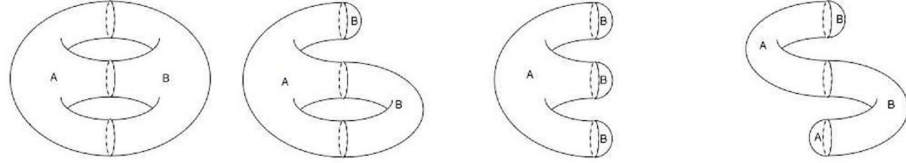


Figure 6.14: Inequivalent choices of cutting into A and B regions when there is a 3-component interface. They have 2, 1, 0, 0 cycles shared by A and B (*i.e.*, in the set  $\{c_k\}$ ).

Next, we segregate the Wilson loops in the chosen basis into three groups:  $m_a$  which only live in the  $A$  region,  $m_b$  which only live in the  $B$  region,  $m_c$  which cross the interface. Similarly, we shall label the collection of representations describing the basis states  $\{\rho_{a_i}, \rho_{b_j}, \rho_{c_k}\}$ . Finally, we shall denote the number of interfaces as  $r$ .<sup>5</sup>

The most convenient way to organize the calculation is to squeeze the  $C$  geometry into balls lying along the interface as in 6.11. These balls will be connected by various tubes. For the surface shown in Fig. 6.14, the result is shown in Fig. 6.15. The  $r$  components of  $C$  (the large spheres) will be denoted

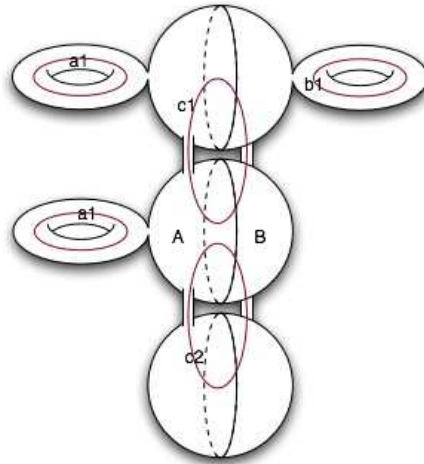


Figure 6.15: The space shown in Fig. 6.14 after 'squeezing'. The components of  $C$  are connected to each other either by a  $D^2$  or  $D^2$  with a puncture.

$d_1, d_2, \dots, d_r$ .

Consider first a pure state which is a basis element  $|\rho_a, \rho_b, \rho_c\rangle$ . For each

<sup>5</sup>Although in Fig. 6.15 it appears that  $m_c = r - 1$ , this is not true in general.

power of  $\rho$  the the cycles wholly contained in regions  $A$  and  $B$  will turn into  $m_a S^2 \times S^1$ 's and  $m_b S^2 \times S^1$ 's all glued to the  $C$  region. We may decouple them from  $C$  using surgery outlined in 6.3.1. From  $A$  we find

$$\begin{aligned} Z(A) &= ((S_0^0)^{m_a-1})^n \\ Z(B) &= ((S_0^0)^{m_b-1})^n. \end{aligned} \quad (6.37)$$

As advertised, these will cancel when computing  $\text{Tr } \rho^n / (\text{Tr } \rho)^n$ .

The remaining topology arises from the interface region  $C$ . To compute  $\text{tr } \rho_A^n$ , we must glue  $2n$  copies of the geometry shown in the figure in the way that we have prescribed earlier; in particular, each of the solid ball components of  $C$  becomes an  $S^3$  after gluing and these are connected by  $2n S^2 \times I$ 's. The simplest example of this is the torus in 6.3.5. When drawn as rotated disks in figure 6.12, each row lead to a different  $S^3$ , connected by  $2n$  tubes. More generally, if drawn as rotated disks, we would have  $r S^3$ 's and  $2n (S^2 \times I)$ 's connecting the  $i^{\text{th}}$   $S^3$  to the  $i+1^{\text{th}}$   $S^3$ .

Having described the the resulting geometry in  $C$ , we may use the surgery results to decompose this into manageable pieces. As in 6.15, the  $1^{\text{st}}$  and  $r^{\text{th}}$   $S^3$  only have one Wilson loop, while all others have two. To pull this geometry apart, we should cap every  $S^2 \times I$  with two balls (with appropriate representations). This leaves us with

$$\begin{aligned} Z_n(C) &= \frac{\overbrace{Z(S^3, \rho_1)Z(S^3, \rho_1, \rho_2)\dots Z(S^3, \rho_{r-2}, \rho_{r-1})Z(S^3, r-1)}^{\text{from } S^3\text{'s}}}{\prod_{i=1}^{r-1} Z(S^3, \rho_i)^{4n}} \\ &\quad \times \underbrace{\prod_{i=1}^{r-1} Z(S^3, \rho_i)Z(S^3, \rho_i^*)}_{\text{from } S^2 \times I\text{'s}} \end{aligned} \quad (6.38)$$

Because "middle" spheres each have two loops, they may be viewed as a connected sum two 3-spheres each with a Wilson loop

$$\begin{aligned} Z_n(C) &= Z(S^3)^{2-r} \prod_{i=1}^{r-1} |Z(S^3, \rho_i)|^{2(1-n)} \\ \frac{Z_n(C)}{Z_1(C)^n} &= \left( Z(S^3)^{2-r} \prod_{i=1}^{r-1} |Z(S^3, \rho_i)|^2 \right)^{1-n} \\ &= \left( (S_0^0)^r \prod_{i=1}^{r-1} |\mathcal{D}_{\rho_i}|^2 \right)^{1-n} \end{aligned} \quad (6.39)$$

The resulting entropy is

$$S_A = r \ln S_{00} + \sum_{k=1}^{m_c} \ln |\mathcal{D}_{\rho_{c_k}}|^2. \quad (6.40)$$

The first piece in eq. (6.4) is the universal term which is proportional to the number of interfaces. The second one depends on the quantum dimensions of the state along each cycle in  $\{c\}$ . In all of the simpler cases studied earlier, this result simplifies to our previous expressions.

In this calculation, we have made the assumption that the splitting into A and B regions is such that the Wilson loops in C are cut into two pieces. More generally, it may happen that they are cut into some even number  $\ell_k$  of pieces. An example of this is shown in Fig. 6.16. In this case, our result is modified to

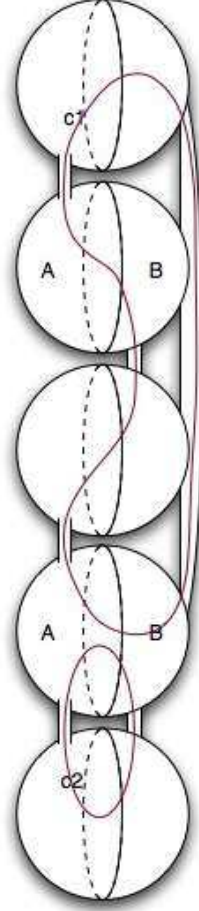


Figure 6.16: A more complicated example, with a Wilson line cut into four pieces.

$$S_A = r \ln S_{00} + \sum_{k=1}^{m_c} \ell_k \ln |\mathcal{D}_{\rho_{c_k}}| \quad (6.41)$$

Consider next a pure state which is a linear combination of the basis states

$$|\psi\rangle = \sum_{\{\rho_a, \rho_b, \rho_c\}} \psi_{\{\rho_a, \rho_b, \rho_c\}} |\{\rho_a, \rho_b, \rho_c\}\rangle.$$

We will assume that the wavefunctions are normalized,  $\sum_{\{\rho_a, \rho_b, \rho_c\}} |\psi_{\{\rho_a, \rho_b, \rho_c\}}|^2 = 1$ . The computation is greatly simplified because of the orthogonality of the basis states. Taking this into account, we arrive at

$$\begin{aligned} & \frac{\text{Tr} \rho_{\{a,b,c\}, \psi}^n}{(\text{Tr} \rho_{\{a,b,c\}, \psi})^n} \\ = & S_{00}^{r(1-n)} \sum_{\{\rho_c\}} \prod_{k=1}^{m_c} |\mathcal{D}_{\rho_{c_k}}|^{\ell_k(1-n)} \\ & \times \sum_{\{\rho_a^{(r)}, \rho_b^{(r)}\}} \psi_{\{\rho_a^{(1)}, \rho_b^{(1)}, \rho_c\}} \psi_{\{\rho_a^{(2)}, \rho_b^{(1)}, \rho_c\}}^* \psi_{\{\rho_a^{(2)}, \rho_b^{(2)}, \rho_c\}} \psi_{\{\rho_a^{(3)}, \rho_b^{(2)}, \rho_c\}}^* \\ & \cdots \psi_{\{\rho_a^{(n)}, \rho_b^{(n)}, \rho_c\}} \psi_{\{\rho_a^{(1)}, \rho_b^{(n)}, \rho_c\}}^*. \end{aligned}$$

Now we define the reduced density matrices

$$[\Psi_{\{\rho_c\}, \{\rho'_c\}}]_{\{\rho_a\}, \{\rho'_a\}} = \sum_{\{\rho_b\}} \psi_{\{\rho_a, \rho_b, \rho_c\}} \psi_{\{\rho'_a, \rho_b, \rho'_c\}}^* \quad (6.42)$$

In fact we will make use of only those which have  $\rho'_c = \rho_c$ . In this notation, the result is

$$\frac{\text{Tr} \rho_{\{a,b,c\}, \psi}^n}{(\text{Tr} \rho_{\{a,b,c\}, \psi})^n} = S_{00}^{r(1-n)} \sum_{\{\rho_c\}} \text{Tr}_{\{\rho_a\}} [\Psi_{\{\rho_c\}, \{\rho_c\}}]^n \prod_{k=1}^{m_c} |\mathcal{D}_{\rho_{c_k}}|^{\ell_k(1-n)}. \quad (6.43)$$

It is not hard to prove that this expression is invariant under unitary transformations of  $\{\rho_a\}$ ,  $\{\rho_b\}$  and  $\{\rho_c\}$ . From the definition of the  $[\Psi_{\{\rho_c\}, \{\rho_c\}}]$  we know that they are hermitian and (semi)positive definite matrices, so they have nonnegative eigenvalues  $\{\lambda_{\{\rho_c\}}\}$  and in terms of these eigenvalues

$$\frac{\text{Tr} \rho_{\{a,b,c\}, \psi}^n}{(\text{Tr} \rho_{\{a,b,c\}, \psi})^n} = S_{00}^{r(1-n)} \sum_{\{\rho_c\}} \sum_{\lambda_{\{\rho_c\}}} \lambda_{\{\rho_c\}}^n \prod_{k=1}^{m_c} |\mathcal{D}_{\rho_{c_k}}|^{\ell_k(1-n)}. \quad (6.44)$$

We thus find

$$S_A = -r \ln \mathcal{D} - \sum_{\{\rho_c\}} \sum_{\lambda_{\{\rho_c\}}} \lambda_{\{\rho_c\}} \ln \frac{\lambda_{\{\rho_c\}}}{\prod_{k=1}^{m_c} |\mathcal{D}_{\rho_{c_k}}|^{\ell_k}}, \quad (6.45)$$

where  $\mathcal{D} = \sqrt{\sum_{\rho} |\mathcal{D}_{\rho}|^2} = S_{00}^{-1}$ . We see that the entanglement entropy consists of two contributions. The first,  $S_1 \equiv -r \ln \mathcal{D}$ , which we have seen repeatedly, is proportional to the number of components of the interface between the A and B regions and is negative. The second contribution may be rewritten

$$S_2 \equiv - \sum_{\{\rho_c\}} \sum_{\lambda_{\{\rho_c\}}} \left( \prod_{k=1}^{m_c} |\mathcal{D}_{\rho_{c_k}}|^{\ell_k} \right) p_{\lambda_{\{\rho_c\}}} \ln p_{\lambda_{\{\rho_c\}}} \quad (6.46)$$

where

$$p_{\lambda_{\{\rho_c\}}} \equiv \frac{\lambda_{\{\rho_c\}}}{\left(\prod_{k=1}^{m_c} |\mathcal{D}_{\rho_{c_k}}|^{\ell_k}\right)} \quad (6.47)$$

This appears to have an interpretation as an entropy for a weighted system: for each  $\{\rho_c\}$ , we effectively have a degeneracy  $\left(\prod_{k=1}^{m_c} |\mathcal{D}_{\rho_{c_k}}|^{\ell_k}\right)$  (or,  $\mathcal{D}_{\rho_{c_k}}$  per cut in the Wilson loop).

These results apply to any Chern-Simons theory. Using explicit forms of matrices described in A.4. In the case of  $U(1)_k$ , we have

$$S_{00} = \frac{1}{\sqrt{\sum_j |\mathcal{D}_j|^2}} = \frac{1}{\sqrt{2k}} \quad (6.48)$$

and hence

$$S_A^{(S^2,1)} = -\ln \sqrt{2k}. \quad (6.49)$$

If we use the  $SU(2)_k$  modular matrix

$$[S_{SU(2)_k}]_{jj'} = \sqrt{\frac{2}{k+1}} \sin\left(\frac{\pi}{k+1}(2j+1)(2j'+1)\right) \quad (6.50)$$

$$S_A(S^1, 1) = \ln\left(\sqrt{\frac{2}{k+1}} \sin\left(\frac{\pi}{k+1}\right)\right). \quad (6.51)$$

This matches the work in [115]

## 6.5 Conclusions

In this chapter we have outlined a general strategy for computing topological entanglement entropies for Chern-Simons Theories. These numbers are expected to characterize the topological phase of many FQH systems. We confirmed, by explicit computation, the entanglement entropie's dependence on information localized near the interface. In addition we were able to extend our results to arbitrary numbers of handles.

This work raises a number of possible extensions. The first extension which immediately presents itself is to include quasiparticles. This chapter only described the degenerate ground states, but the quasiparticle excited states are also expected to exhibit nonlocal, topological characteristics. It would be interesting to be able to compute their entropies as well. It would also be interesting to extend this work to include coset models. This would be of use in describing FQH systems with anyonic character.

Another tantalizing extension would be to use these results to compute entanglement entropies associated with gravitational physics. It well known that  $2+1$  dimensional gravity possesses a Chern-Simons description, albeit with a non-compact gauge group. One might hope that this basic formalism survives to that theory, and one could address information paradoxes associated with

2 + 1 dimensional black holes.

# Appendix A

## Introduction to Conformal Field Theory and Chern-Simons Theory

### A.1 Conformal Field Theory

A conformal field theory is, by definition, a quantum field theory which is invariant under conformal transformations<sup>1</sup>. In general dimensions, we may investigate coordinate transformations,  $x^\mu \rightarrow x^\mu + \epsilon^\mu$  and  $g_{\mu\nu} \rightarrow g_{\mu\nu} - \partial_\mu \epsilon_\nu - \partial_\nu \epsilon_\mu$ , which induce conformal transformations  $g_{\mu\nu} \rightarrow g_{\mu\nu} + f(x)g_{\mu\nu}$ . Equating the two metric variations (focusing on metrics connected to the flat metric) leads to

$$(d-1)\partial^2 f = 0. \tag{A.1}$$

In general, this will only be solved when  $f$  is a quadratic polynomial, leading to the global symmetry group  $SO(2, d+1)$ . However, in two dimensions  $\partial^2 = \partial\bar{\partial}$  in complex coordinates. This implies  $f$  may be any (anti)holomorphic function and a local conformal transformation is generated. The set of local holomorphic function in 2 dimensions is infinite, implying the 2 dimensional local conformal group is infinite dimensional. Our great understanding of 2 dimensional conformal field theories is rooted in this infinite symmetry group, and the infinite set of Ward identities it implies.

### A.2 Basic Structure

#### Stress Tensor

The stress tensor plays a special role in these theories, as it enters into the definition of all conformal group generators. In fact, the identity and stress tensor are the only operators one is guaranteed to have in a conformal field theory.

Because one may make independent holomorphic and anti-holomorphic transformations, is useful to treat the component of the stress tensor separately. We often write, in complex coordinates,

$$T^{zz} \equiv T(z) \quad \text{and} \quad T^{\bar{z}\bar{z}} \equiv \bar{T}(\bar{z}). \tag{A.2}$$

---

<sup>1</sup>All of the material in this section may be found in [62]

The two components of the stress tensor generate holomorphic and anti-holomorphic coordinate transformations respectively.

Part of the data of a classical field theory is behavior of all fields under conformal transformations. The corresponding data for a quantum field theory is encoded in the operator products of the quantum stress tensor with all other fields. A field is termed "primary" if the quantum transformation of a field precisely matches the classical transformations as an operator statement. If the classical transformations only hold for matrix elements the fields are termed "quasi-primary."

A classical holomorphic field of weight  $h$  transforms as  $\phi_{cl}(z) \rightarrow \left(\frac{\partial z'}{\partial z}\right)^h \phi_{cl}(z)$ . For a quasi-primary field we have

$$\langle T(z)\phi(z') \rangle = \left\langle \frac{h\phi(z')}{(z-z')^2} + \frac{\partial'\phi(z')}{(z-z')} \right\rangle. \quad (\text{A.3})$$

If this field is primary, the above result holds as an operator statement. For quasi-primary fields we have

$$T(z)\phi(z') \sim \sum_{n=3}^N \frac{\mathcal{O}_n(z')}{(z-z')^n} + \frac{h\phi(z')}{(z-z')^2} + \frac{\partial'\phi(z')}{(z-z')}. \quad (\text{A.4})$$

The operators  $\mathcal{O}_n$  have zero vacuum expectation value, but become important when considering multiple operator insertions.

New operators occurring in the operator product of  $T$  with a primary field are called conformal descendent fields. In general, quasi-primary fields are conformal descendants. As an example, the Schwinger term computes

$$T(z)T(0) \sim \frac{c/2}{z^4} + \frac{2T(0)}{z^2} + \frac{\partial T(0)}{z}. \quad (\text{A.5})$$

The parameter  $c$  is the central charge indicating a quantum anomaly in the conformal symmetry. Note that nonzero  $c$  indicates that the stress tensor itself is only quasi-primary, appearing as a conformal descendant of the identity,

$$\mathbb{I} \cdot T(z) = T(z). \quad (\text{A.6})$$

We may integrate the anomalous transformation law for infinitesimal conformal variations of the stress tensor,

$$(\partial_z z')^2 T(z') = T(z) - \frac{c}{12} \{z', z\} \quad (\text{A.7})$$

$$\{f, z\} = \frac{2\partial_z^3 f \partial_z f - 3\partial_z^2 f \partial_z^2 f}{2\partial_z f \partial_z f}. \quad (\text{A.8})$$

As a further classification, theories are called rational if they have a finite number of primary fields.

## States

Thus far we have introduced operators, but there are more ingredients in a quantum theory. Most noticeably, one needs states. It is a general feature that, for every local operator in a CFT, we have a corresponding state. The fundamental state is the vacuum vector  $|0\rangle$ , dual to identity operator

$$\mathbb{I} \leftrightarrow |0\rangle \quad (\text{A.9})$$

For a general operator of weight  $h$  one has

$$\mathcal{O}_h(z) \leftrightarrow |h\rangle = \oint dz z^h \mathcal{O}_h(z) |0\rangle \quad (\text{A.10})$$

## Mode Expansions

We may Fourier transform all operators,

$$\mathcal{O}_h(z) = \sum_{n \in \mathbb{Z}} \frac{\alpha_n^{\mathcal{O}_h}}{z^{h+n}} \quad (\text{A.11})$$

$$\alpha_n^{\mathcal{O}_h} = \oint dz z^{h+n-1} \mathcal{O}_h(z). \quad (\text{A.12})$$

We conventionally define  $T(z) = \sum_{n \in \mathbb{Z}} \frac{L_n}{z^{2+n}}$ . As in more standard field theories, one may transfer operator products into commutation relationships. The stress tensor self-multiplication leads to the Virasoro algebra

$$[L_n, L_m] = (n - m)L_{n+m} + n(n^2 - 1) \frac{c}{12} \delta_{n+m,0}, \quad (n, m \in \mathbb{Z}). \quad (\text{A.13})$$

The infinite number of generators in the Virasoro algebra reflects the infinite number of reparametrizations generating local conformal transformations.

## Conformal Blocks

The physical content of a conformal field theory are the operators, the states they generate, and the field's multiplication structure (or fusion). Due to the strong constraints imposed by conformal invariance, one may often solve for a theory's correlation functions, even in the absence of an explicit action. For example, up to normalizations we may immediately write down the two and three point functions (on a sphere),

$$\langle \phi_i(z) \phi_j(0) \rangle = \frac{C_{ij}}{z^{2h_i}} \quad (\text{A.14})$$

$$\langle \phi_i(z_1) \phi_j(z_2) \phi_k(z_3) \rangle = \frac{C_{ijk}}{z_{12}^{h_i+h_j-h_k} z_{23}^{h_j+h_k-h_i} z_{31}^{h_k+h_i-h_j}}, \quad (\text{A.15})$$

where  $z_{ij} \equiv z_i - z_j$ .

The multiplication structure of a CFT, or fusion rules, is encoded in a set

of numbers  $N_{ij}^k$

$$[\phi_i] [\phi_j] \sim \sum_k N_{ij}^k [\phi_k]. \quad (\text{A.16})$$

By  $[\phi_i]$  we denote a conformal family (the primary  $\phi_i$  or any of its conformal descendants). The fusion coefficient  $N_{ij}^k$  represent the number of independent ways  $[\phi_k]$  appears in the product of  $[\phi_i]$  and  $[\phi_j]$ . The  $N_{ijk}$ 's encode the part of the  $C_{ijk}$ 's which are common to all members of a conformal family. As multiplicities the  $N_{ijk}$ 's are important universal integers of a conformal field theory.

In general, conformal invariance alone is not strong enough to determine the higher n-point functions. However, with one additional condition on the correlation functions, we are able to write higher point functions in terms of lower correlation functions. Crossing symmetry requires invariance under the ordering of the external legs. For example, this allows us to unambiguously write the 4-point function as a sum of products of 3-point functions, where we sum over intermediate states.

In the case of a sphere 4 point function, the "sum over intermediate states" corresponds to a sum over conformal blocks. In general, the conformal blocks on a Riemann surface of genus  $g$  with  $k$  marked points are the set of linearly independent functions in terms of which one may write the correlation functions of  $k$  fields on a surface of genus  $g$ . In essence, these are the set of single valued function on a surface respecting all appropriate boundary conditions and symmetries of a field theory.

### Characters

An important example of conformal blocks are the 0-point functions on a torus. Beginning with a Hilbert space defined on a circle, we may write this as a trace of an imaginary time evolution operator,  $Tr e^{2\pi i\tau(L_0 - \frac{c}{24})}$ . The complex parameter  $\tau$  is the torus' modular parameter,

$$T^2 : \begin{cases} z \sim z + 2\pi \\ z \sim z + 2\pi i\tau \end{cases} \quad (\text{A.17})$$

We may decompose the traces into subspaces spanned by primary fields and their descendants. Corresponding to a primary field of weight  $h$  we may define a character

$$\chi_h^{Vir}(q) = \text{tr}_h q^{L_0 - \frac{c}{24}}, \quad (q \equiv e^{2\pi i\tau}). \quad (\text{A.18})$$

The characters provide a basis for the set of conformal blocks on a torus with no insertions.

It is an important feature of the characters that, if we perform a modular

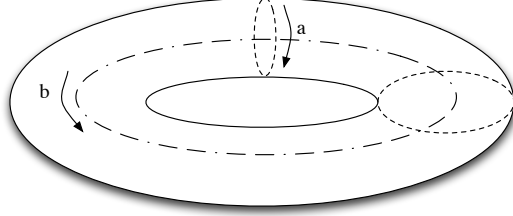


Figure A.1: Cycles on a torus

transformation on the base torus, the set of characters map into itself.

$$\chi_h^{Vir}(\tau + 1) = T_h^{h'} \chi_{h'}^{Vir}(\tau) \quad (\text{A.19})$$

$$\chi_h^{Vir}\left(\frac{1}{\tau}\right) = S_h^{h'} \chi_{h'}^{Vir}(\tau) \quad (\text{A.20})$$

The modular  $S$  matrix is also important for another reason, for rational CFT's, the Verlinde formula relates  $N_{ij}^k$  to the  $S$  matrices:

$$N_{ij}^k = \sum_{\ell} \frac{S_i^{\ell} S_j^{\ell} S_{\ell}^k}{S_0^{\ell}}. \quad (\text{A.21})$$

We shall see this relation again when we discuss boundary conformal field theories and when discussing Chern-Simons theories.

### A.3 Orbifolds

On occasion we may wish to build new conformal field theories from existing theories. One common route is to identify a symmetry group, and declare all states differing by a symmetry transformation to be equivalent. In general such theories are called orbifold field theories. In a path integral language, when we sum over all indistinguishable ways something may occur, we must sum over field configurations differing by boundary conditions related by symmetry transformations.

When deducing the original set of primary fields, one considered boundary conditions on the two dimensional base manifold. In an orbifold theory, one need only demand invariance up to a group transformation, typically leading to additional primary fields. A convenient way to write things is to begin with the original field content and to introduce new "twist" or "spin" fields,  $\sigma$ , which effectively change the original boundary conditions. In twisted sectors, matrix elements are to be taken between twisted vacua,  $|0\rangle_{tw} \sim \lim_{z \rightarrow 0} z^{h_{\sigma}} \sigma(z)|0\rangle$ .

$$\langle \mathcal{O} \rangle_{tw} = \frac{\langle 0 | \mathcal{O} | 0 \rangle_{tw}}{\langle 0 | 0 \rangle_{tw}} \quad (\text{A.22})$$

If we can separately compute the stress tensor 1-point function in a twisted

sector (from an explicit path integral computation, for example), we may then deduce the conformal weights of the twist fields.

$$T(z)\sigma(0) \sim \frac{h_\sigma\sigma(0)}{z^2} + \frac{\partial\sigma(0)}{z} \quad (\text{A.23})$$

$$\langle T(z) \rangle_{tw} = F(z) \quad \text{from a path integral} \quad (\text{A.24})$$

$$\sim \sum_{n=-2}^{\infty} c_{-n} z^n \quad \text{near the origin}$$

$$\langle T(z) \rangle_{tw} = \frac{\langle \sigma^\dagger(\infty)T(z)\sigma(0) \rangle}{\langle 0|0 \rangle_{tw}} \quad (\text{A.25})$$

$$= \frac{h_z \langle 0|0 \rangle_{tw}}{z^2 \langle 0|0 \rangle_{tw}} + \text{less singular.} \quad (\text{A.26})$$

From the explicit computation we know  $c_n$  and we may equate  $c_2 = h_\sigma$ .

## A.4 WZW Models

An important set of conformal field theories are Wess-Zumino-Witten field theories.

$$S = \frac{k}{16\pi} \int_{\Sigma} d^2x \text{tr}' (\partial_\mu g^{-1} \partial^\mu g) - i \frac{k}{24\pi} \int_B d^3y \epsilon^{ijk} \text{tr}' (\tilde{g}^{-1} \partial_i \tilde{g} \tilde{g}^{-1} \partial_j \tilde{g} \tilde{g}^{-1} \partial_k \tilde{g}). \quad (\text{A.27})$$

The manifold  $B$  is defined such that  $\partial B = \Sigma$ . The field  $g$  is a group valued field and  $k$  is level of the theory. The  $\text{tr}'$  is an unusually normalized trace  $\text{tr}' = \frac{1}{x_{rep}} \text{tr}$ , ( $x_{rep}$  is the representation's Dynkin index). The field  $\tilde{g}$  is defined on the 3-geometry  $B$  such that

$$\tilde{g}|_{\partial B = \Sigma} = g. \quad (\text{A.28})$$

This theory has an anomaly free symmetry under  $g \rightarrow f(z)g(z, \bar{z})\bar{f}^{-1}(\bar{z})$ .

While this action is nonlinear, it is not too hard to find the exact quantum stress tensor. If one defines currents,  $T^a J^a(z) = g^{-1} \partial g$ , Ward identities determine

$$J^a(z) J^b(0) \sim \frac{i f^{ab}}{z} J^c(0) + \frac{k \delta^{ij}}{z^2}. \quad (\text{A.29})$$

The classical stress tensor is

$$T_{cl} = \frac{1}{2k} \sum_i (J^i)^2. \quad (\text{A.30})$$

This does not quite satisfy the correct operator products, but a slight modification leads to the Sugawara stress tensor

$$T(z) = \frac{1}{2(k + c_v)} \sum_i : (J^i)^2 : \quad (\text{A.31})$$

where  $c_v$  is the dual coexeter number for the respective Lie algebra. The central charge for this theory is

$$c = c(k, c_v) = \frac{k \dim g}{k + c_v} \quad (\text{A.32})$$

WZW models are quite useful because much of the classical structure is preserved by the quantum theory, although the theory is an interacting quantum field theory. In an operator language, the only modifications upon quantization, is the level  $k$  is shifted in the normalization of the stress tensor to  $k + c_v$  and the primary fields live in the  $k + 1$  smallest group representations. Using the current algebra, the conformal weights may be written in terms of group theoretic data

$$h_\lambda = \frac{C_2(\lambda)}{2(k + c_v)} \quad (C_2 \text{ is the quadratic Casimir}). \quad (\text{A.33})$$

We shall encounter these features later in Chern-Simons theories as well.

An additional property which may be derived from Ward identities is that on  $S^2$ , the 1-point function for any operator, not in the trivial representation, must vanish. This is essentially due to Gauss' law on a compact space. Similarly, one only finds nonzero 2-point functions if the operators live in conjugate representations. For 3-point functions, there are more possibilities, for operators  $\phi_a, \phi_b$  and  $\phi_c$ , one requires  $\phi_a \times \phi_b \rightarrow \phi_c^*$ . There are  $N_{abc}$  independent ways for this to occur.

### Properties of WZW $S$ matrices

The matrix  $S$  satisfies several properties which are used through out this dissertation.

$$S_\rho^\mu = S_{\rho\mu^*} = \overline{S}_{\rho\mu} = S_{\rho\mu}. \quad (\text{A.34})$$

Also we have

$$\sum_\mu S_\rho^\mu S_\mu^\chi = \delta_\rho^\chi. \quad (\text{A.35})$$

Note, as a matter of definition the quantum dimension is

$$\mathcal{D}_\rho \equiv \frac{S_0^\rho}{S_0^0}. \quad (\text{A.36})$$

It is useful to know a few examples. For  $U(1)_k$  the  $S$  matrix is

$$[S_{U(1)_k}]_{\ell m} = \frac{1}{\sqrt{2k}} e^{\frac{\pi i \ell m}{k}}. \quad (\text{A.37})$$

For  $SU(2)_k$  we have

$$[S_{SU(2)_k}]_{jj'} = \sqrt{\frac{2}{k+2}} \sin\left(\frac{\pi}{k+2}(2j+1)(2j'+1)\right). \quad (\text{A.38})$$

Note that these match for  $U(1)_1$  and  $SU(2)_1$ <sup>2</sup>.

### Mode Expansions

If we mode expand the current algebra,  $J(z) = \sum_{n \in \mathbb{Z}} \frac{J_n}{z^{n+1}}$ , we arrive at the affine Kac-Moody algebra

$$[J_n^i, J_m^j] = i f^{ij}_k J_{n+m}^k + \frac{k}{2} n \delta_{n+m,0} \delta^{ij}. \quad (\text{A.39})$$

Because the stress tensor may be written in terms of the WZW currents, We may also write build the Virasoro algebra out of the AKM algebra generators.

$$L_n = \frac{1}{2(k+g)} \sum_i \sum_{m \in \mathbb{Z}} : J_m^i J_{n-m}^i :. \quad (\text{A.40})$$

For convenience, we also write the commutators of the Virasoro generators with the AKM algebra,

$$[L_n, J_m^i] = -m J_{n+m}^i. \quad (\text{A.41})$$

### AKM Characters

As usual in the representation theory of group algebras, it is useful to define characters for AKM algebras.

$$\chi_h(q, \{\lambda\}) = \text{tr} q^{L_0} e^{2\pi i (\lambda^i J_0^i)} \quad (\text{A.42})$$

Note that  $\lambda^i J_0^i$  is an element of the Cartan subalgebra for the simple Lie group. An important example is  $su(2)_{k=1}$ ,

$$\chi(q, \lambda) = \text{tr} q^{L_0} e^{2\pi i \lambda J_0^3} = \frac{1}{\eta(q)} \sum_{j \in \mathbb{Z}} \chi_j^{su(2)}(e^{2\pi i \lambda J_0^3}), \quad (\text{A.43})$$

where  $\chi_j^{su(2)}(g)$  is the standard  $su(2)$  character,  $\text{tr}_j D^{(j)}(g)$ , and  $\eta(q)$  is the Dedikind function,

$$\eta(q) = q^{-1/24} \prod_{n>0} (1 - q^n). \quad (\text{A.44})$$

Incidentally, these characters form a basis for the WZW conformal blocks on a  $T^2$  with no insertions.

## A.5 Boundary Conformal Field Theories

An important extension of the above analysis is to allow the 2 dimensional base manifold to have boundaries. As usual, one must impose boundary conditions,

<sup>2</sup>A  $U(1)_{pp'}$  CFT possesses a description as a free boson, compactified on a circle of radius  $R = \sqrt{\frac{2p}{p'}}$ . Also for  $p = p' = 1$ ,  $U(1)_1$  theory is compactified at the self-dual radius. At this radius, the theory's symmetry group is enlarged to  $SU(2)_1$ . [62]

constraining the allowed field content. Boundary conditions take the form of a relationship between left moving fields and right moving fields, such that  $T = \overline{T}$  on the boundary.

If the boundary of a Euclidean manifold is a closed loop, a time slicing exists such that the spacelike boundary is  $S^1$  whereas if we make a modular transformation, exchanging  $\sigma$  and  $\tau$ , the boundary becomes timelike. The physical content of the theory is independent of such coordinization ambiguities, leading to "open-closed duality". The name refers to the fact that a cylinder in one time slicing may be regarded as an open string propagating in a loop, while in the second slicing, it is a closed string propagating in a line.

Studying conformal field theories on a cylinder allow us to deduce allowed boundary conditions. In the open string channel, the cylinder path integral may be regarded as a simple partition function with fixed boundary conditions  $i$  and  $j$ ,

$$Z_{cyl} = \sum_{\lambda} \mathcal{N}_{ij}^{\lambda} \chi_{\lambda}(q). \quad (\text{A.45})$$

As a partition function, the multiplicities  $\mathcal{N}$  must be integers.

Cardy [] first realized that, if the model is integrable and the boundary conditions are in correspondence with primary fields, one may consistently build open string partition functions by identifying the integers  $\mathcal{N}$  with the fusion coefficients.

We wish to construct boundary states in the closed string channel whose overlap, upon modular transformation, reduces to the open string expressions. By first introducing Ishibashi states labeled by primary fields  $|\lambda\rangle\rangle$ ,

$$\langle\langle \lambda | q^{L_p} \bar{q}^{\bar{L}_0} | \chi \rangle\rangle = \chi_{\lambda}^{Vir}(q) \delta_{\lambda, \chi}. \quad (\text{A.46})$$

we may solve the boundary conditions with:

$$|\ell\rangle = \sum_{\lambda} \frac{S_{\ell}^{\lambda}}{\sqrt{S_0^{\lambda}}} |\lambda\rangle\rangle. \quad (\text{A.47})$$

The overlap of two such boundary states yields

$$\begin{aligned} \langle i | q^{L_0} \bar{q}^{\bar{L}_0} | j \rangle &= \sum_{\lambda} \frac{S_i^{\lambda} S_j^{\lambda}}{S_0^{\lambda}} \chi_{\lambda}(-\frac{1}{\tau}) \\ &= \sum_{\lambda\lambda'} \frac{S_i^{\lambda} S_j^{\lambda} S_{\lambda}^{\lambda'}}{S_0^{\lambda}} \chi_{\lambda'}(\tau) \\ &= \sum_{\lambda'} N_{ij}^{\lambda'} \chi_{\lambda'}(\tau) \quad (\text{using Verlinde's formula}). \end{aligned} \quad (\text{A.48})$$

While this is a consistent partition function, it need not be unique. However, in practice all known integrable boundary conformal field theories are consistent with this construction. For non-integrable models, one may use these states as

a guide, but success is not guaranteed. The main hurdle is that non-integrable models have infinitely many primary fields.

## A.6 Chern-Simons Theory

A topological field theory is one which does not depend upon the local structure of a manifold. There are essentially two ways one may try to achieve topological invariance, either one averages over all metrics or one builds a theory with no metric dependence. The prototypical example of the first approach is general relativity. Chern-Simons is a theory where the metric never enters the action, at least before gauge fixing.

For a compact oriented 3 manifold  $M$ , the Chern-Simons action is

$$S_{CS} = \frac{k}{4\pi} \int_M \text{tr} \left( A \wedge dA + \frac{2}{3} A \wedge A \wedge A \right) \quad (\text{A.50})$$

$$= \frac{k}{8\pi} \int_M \epsilon^{ijk} \text{tr} \left( A_i (\partial_j A_k - \partial_k A_j) + \frac{2}{3} A_i [A_j, A_k] \right). \quad (\text{A.51})$$

The parameter  $k$  is the level. Under variations,  $A \rightarrow A + \delta A$ , the variation of the action is

$$\frac{k}{4\pi} \int_{\partial M} \text{Tr} \delta A A + \frac{k}{2\pi} \int_M \text{Tr} \delta A F, \quad (\text{A.52})$$

where  $F$  is the curvature  $dA + A^2$

It is a not too hard result that under a gauge general gauge transformation,

$$A \rightarrow U A U^{-1} - dU U^{-1}, \quad (\text{A.53})$$

the action is not quite invariant,

$$S_{CS} \rightarrow S_{CS} + \frac{k}{12\pi} \int_M \text{tr} (U^{-1} dU \wedge U^{-1} dU \wedge U^{-1} dU). \quad (\text{A.54})$$

The last integral computes  $\pi_3(G)$  which is both an integer and a topological invariant. Demanding that the path integral's integrand be single valued for all gauge transformations on all 3 manifolds forces the level  $k$  to be an integer.

To construct the quantum theory it is necessary to gauge fix the action and introduce Fadeev-Popov ghosts. For example, in Landau gauge [116]:

$$S_{gf} = \frac{k}{4\pi} \int d^3 x \text{tr} A_\mu^a \partial^\mu B^a \quad (\text{A.55})$$

$$S_{gh} = \int d^3 x \text{tr} \partial_\mu \bar{c}^a (D^\mu c)^a, \quad (\text{A.56})$$

where  $(D_\mu c)^a = \partial_\mu c^a + f^{abc} A_\mu^b c^c$  and  $B$  is a Lagrange multiplier enforcing the gauge condition.

Before gauge fixing, classical action has an obvious independence of the 3

dimensional metric. Any such theory can only depend upon topological data, as it is insensitive to any changes in length scales. However, the introduction of ghost necessarily breaks the metric independence, ghost kinetic terms always require a metric to form Lorentz singlets

## A.7 Summary of Perturbative Renormalization

The perturbative renormalization of Chern-Simons theory is a topic with a long and winding history. It is a subject fraught with regulator subtleties. In this section, I shall not attempt to provide the technical detail, leaving that to the literature [101]. Instead, I shall attempt to give a heuristic summary of the theory's renormalization.

The first point to note is that the Chern-Simons action is only valid in 3 dimensions. The gauge invariance is closely tied to the form nature of the Lagrangian (the presence of the Levi-Civita symbol). This structure means using a common regulator like dimensional regularization is subtle, as is familiar in the analysis of four dimensional anomalies.

A second point is emergence of a supersymmetry in the gauge fixed Lagrangian, in the Landau gauge [116],

$$\begin{aligned}
 \delta A_\mu^a &= \epsilon^\nu \epsilon_{\mu\nu\rho} \partial^\rho c^a \\
 \delta c^a &= 0 \\
 \delta \bar{c}^a &= \frac{k}{4\pi} \epsilon^\mu A_\mu^a \\
 \delta B^a &= \epsilon^\mu (D_\mu c)^a.
 \end{aligned}
 \tag{A.57}$$

These two points allow us to qualitatively understand all renormalizations. By power counting, the gauge propagator corrections are linearly divergent, while the vertex corrections are logarithmic in character. As is all other in gauge theories, the gauge symmetry removes the linear divergence. In addition to gauge invariance, supersymmetry, if valid, implies exact cancelation between gauge and ghost loops. Unfortunately, there is no regulator which simultaneously preserves both supersymmetry and gauge invariance [117, 118]. Enforcing gauge invariance implies a finite, anomalous contributions to supersymmetry variations. It is a non-trivial result that the finite corrections merely shift dependence on the level,  $k$ , to  $k + c_v$ . Note that this was also the behavior of quantized WZW models.

## A.8 Connections with WZW Theories

It is a well known result of Witten [101] that the Hilbert space of Chern-Simons theory on a framed, oriented closed Riemann surface with punctures is in one-one correspondence with the space of a WZW theories conformal blocks defined

upon that surface. The most direct way to show the connection between these two space is to study the wavefunctionals for Chern-Simons theory.

It proves beneficial to work use holomorphic variables for phase space,  $A$  and  $\bar{A}$ . The wavefunctionals of Chern-Simons theory must be functionals of  $\bar{A}$

$$\left( \frac{\delta}{\delta A} + \frac{k}{4\pi} \bar{A} \right) \Psi \quad (\text{A.58})$$

and satisfy Gauss' law constraints

$$\left( D_{\bar{z}} \frac{\delta}{\delta A^a} - \frac{k}{4\pi} F_{a\bar{z}\bar{z}} \right) \Psi. \quad (\text{A.59})$$

Witten [102] found an explicit solution to these equations,

$$\Psi[\bar{A}] = \int [dg] e^{-(S_{wzw}(g) - \frac{k}{4\pi} \int \text{Tr} \bar{A} dg g^{-1} - \frac{k}{4\pi} \int \text{Tr} \bar{A} A)}. \quad (\text{A.60})$$

The overlap of two such states is a WZW path integral on the spatial surface,

$$\int [dA d\bar{A}] \Psi^*[A] \Psi[\bar{A}] = Z_{WZW}. \quad (\text{A.61})$$

This is the simplest relationship between Chern-Simons theory and WZW conformal blocks. This type of relationship may be extended to more complicated states carrying non-trivial group representation data.

A second way to see the relationship between Chern-Simons theories and WZW theories is to consider a 3 geometry which is  $R \times D^2$ . To make the action's variation vanish along the boundary, we must may require  $A^0 \rightarrow 0$  at the boundary. The  $A^0$  field is a Lagrange multiplier forcing the spatial of components  $F^a = 0$  (in the absence of timelike Wilson loops). We may solve the flatness condition by  $A^i = -\partial^i U U^{-1}$ . In terms of this new field,  $U$ , the action may be written

$$S_{CS}[A] \rightarrow \frac{k}{4\pi} \int dt dx \text{Tr} \partial^\mu U^{-1} \partial_\mu U + \frac{k}{12\pi} \int d^3x \text{Tr} (U^{-1} dU)^3. \quad (\text{A.62})$$

Chern-Simons on a finite geometry is equivalent to a chiral WZW theory defined on the boundary. [119]

The main difficulty with using these explicit relationships between Chern-Simons theories and WZW theories is regulator subtleties. Chern-Simons theories are topological, hence, at the end of the day, all length scale dependence must cancel. However, because these wavefunctionals are written in terms of path integrals themselves, it is quite subtle to see that all regulator dependence drops out. Instead, while it is useful to know that such wavefunctional exist, in practice we shall assume the topological invariance which has been repeatedly verified throughout the long literature on Chern-Simons gauge theories.

### Conformal Blocks on $S^2$

On  $S^2$ , with zero or one insertions, there is only one conformal block. Consequently, the Hilbert space of Chern-Simons theory with at most one Wilson loop puncturing  $\Sigma$  is one dimensional. In addition, if  $S^2$  is pierced by two loops, they must live in conjugate representations, or the path integral vanishes. Finally, on  $S^2$  with three punctures living in representations  $i, j$ , and  $k$  the Hilbert space has dimension  $N_{ijk}$ .

## Appendix B

# Tadpole Computations

In this appendix, we will provide the details of complementary calculations using oscillator methods. There are several subtleties that are not regularly seen in the usual backgrounds. We will use the notation where  $\tilde{k}$  is the image of  $k$  under the orbifold.

$$\tilde{k}_o = -k_o \quad (\text{B.1})$$

$$\tilde{k}_u = +k_u \quad (\text{B.2})$$

We want to evaluate

$$T(\tau) = \frac{1}{2} \text{tr}_{U+T} \left[ (1 + \hat{g}) \int d^2 z V(z, \bar{z}) q^{L_o - a} \bar{q}^{\bar{L}_o - \bar{a}} \right] \quad (\text{B.3})$$

It is important to note that in this formalism, obtained by sewing the cylinder into a torus, there are zero modes in the  $U$  sectors of the trace, but not in the twisted  $T$  sectors. The massless vertex operator is of the form

$$V(z, \bar{z}) = \frac{2g_{str}}{\alpha'} : \partial X^\mu \bar{\partial} X^\nu \frac{1}{2} \left( e^{ik \cdot X(z, \bar{z})} + e^{i\tilde{k} \cdot X(z, \bar{z})} \right) : \quad (\text{B.4})$$

The non-zero mode portion of this expression can be evaluated using coherent state methods. For each oscillator  $\alpha_n^\mu$  ( $n > 0$ ) we introduce a coherent-state basis  $|\rho_{n, \mu}\rangle$  and write the trace as a  $\rho$ -integral. If the  $\partial X^\mu$  does not contribute an oscillator, we find (for each  $n > 0$  and  $\mu$ )

$$\int \frac{d^2 \rho}{\pi} e^{-|\rho|^2} e^{\alpha' k_\mu^2 / 4n} (\rho | e^{\sqrt{\alpha'/2} k_\mu \alpha_{-n}^\mu z^n / n} e^{-\sqrt{\alpha'/2} k_\mu \alpha_n^\mu z^{-n} / n} | q^n \rho) \quad (\text{B.5})$$

for the 1-insertion, while for the  $\hat{g}$ -insertion, we get

$$\int \frac{d^2 \rho}{\pi} e^{-|\rho|^2} e^{\alpha' k_\mu^2 / 4n} (\rho | e^{\sqrt{\alpha'/2} \tilde{k}_\mu \alpha_{-n}^\mu z^n / n} e^{-\sqrt{\alpha'/2} \tilde{k}_\mu \alpha_n^\mu z^{-n} / n} | -q^n \rho) \quad (\text{B.6})$$

This is a standard integral whose evaluation can be found in [120]. The result is

$$\frac{1}{1 \mp q^n} e^{\mp \alpha' k_\mu k^\mu \frac{q^n}{2n(1 \mp q^n)}} \quad (\text{B.7})$$

again for each  $n > 0$  and  $\mu$ . For the  $\tilde{\alpha}$  oscillators, we will get the same result,

with  $q$  replaced by  $\bar{q}$ . Now by simple re-ordering of sums and appropriate renormalization, we may compute:

$$\prod_{n \in \mathbb{Z}^+} e^{\frac{1}{n} \frac{q^n}{1+q^n}} = \frac{\theta_2(\tau)}{q^{1/8}}, \quad \prod_{n \in \mathbb{Z}^+ - 1/2} e^{\frac{1}{n} \frac{q^n}{\mp 1 + q^n}} = \theta_{3,4}(\tau) \quad (\text{B.8})$$

On the other hand, the  $\partial X^\mu$  might contribute an oscillator. Then, we have a new matrix element

$$\sum_{m>0} \int \frac{d^2 \rho}{\pi} e^{-|\rho|^2} (\rho | e^{\sqrt{\alpha'}/2 k_\mu \alpha_{-n}^\mu z^n / n} [z^{-m-1} \alpha_m^\mu + z^{m-1} \alpha_{-m}^\mu] \times e^{-\sqrt{\alpha'}/2 k_\mu \alpha_n^\mu z^{-n} / n} | q^n \rho) \quad (\text{B.9})$$

When  $m = n$ , we find, recalling that  $[\alpha_m, e^{a\alpha-m}] = ma e^{a\alpha-m}$  and  $|\rho_n\rangle = e^{\rho \alpha_{-n} / \sqrt{n}} |0\rangle$

$$\frac{\sqrt{m}}{z} \int \frac{d^2 \rho}{\pi} e^{-|\rho|^2} [z^{-m} q^m \rho + z^m \bar{\rho}] (\rho | e^{k_\mu \alpha_{-n}^\mu z^n / n} e^{-k_\mu \alpha_n^\mu z^{-n} / n} | q^n \rho) \quad (\text{B.10})$$

$$= \frac{\sqrt{m}}{z} \int \frac{d^2 \rho}{\pi} e^{-(1-q^m)|\rho|^2} [z^{-m} q^m \rho + z^m \bar{\rho}] e^{k_\mu (z^m \bar{\rho} - z^{-m} q^m \rho) / \sqrt{m}} \quad (\text{B.11})$$

It is straightforward to show that this vanishes. Thus only the zero mode part of the  $\partial X^\mu$  factors contribute. As a corollary then, only the untwisted sector will contribute to the massless tadpole in the Lorentzian orbifold.

It remains to evaluate the zero modes. These are

$$\begin{aligned} U, 1 : & \quad \prod \int \frac{dp}{2\pi} \langle p | \hat{P}^\mu \hat{P}^\nu e^{-\pi \alpha' \tau_2 \hat{P}^2} e^{(\alpha'/2) k \hat{P} \ln |z|^2} | p+k \rangle | z |^{-\alpha' k_o^2 / 2} \\ & = \frac{\eta^{\mu\nu}}{2\pi \alpha' \tau_2} \prod_o \frac{\delta(\sqrt{\alpha'} k_o)}{\sqrt{\tau_2}} \\ U, \hat{g} : & \quad \prod \int \frac{dp}{2\pi} \langle \hat{p} | \hat{P}^\mu \hat{P}^\nu e^{-\pi \alpha' \tau_2 \hat{P}^2} e^{(\alpha'/2) k \hat{P} \ln |z|^2} | p+k \rangle | z |^{-\alpha' k_o^2 / 2} \\ & = \prod_o \frac{e^{-\pi \tau_2 \alpha' k_o^2 / 4}}{2} \times \begin{cases} k_\mu k_\nu / 4 & \mu, \nu \in o \\ \frac{1}{2\pi \alpha' \tau_2} & \mu = \nu \in u \end{cases} \end{aligned}$$

each times a factor  $-\left(\frac{\alpha'}{2}\right)^2 \frac{1}{|z|^2} \prod_u \frac{\delta(\sqrt{\alpha'} k_u)}{\sqrt{\tau_2}}$ . In the first case, this is multiplied by  $X_{1,1} = |\eta(\tau)|^{-24}$ , while in the second, we have  $X_{1,0} = \prod_n |q^{-1}(1-q^n)^{d-23}(1+q^n)^{-(d+1)}|^2$ . Thus, if we go on-shell, we get

$$\begin{aligned} T_0^{\mu\nu} = & - \left( \frac{g_{str} \alpha'}{2} \right) \prod_u \frac{\delta(\sqrt{\alpha'} k_u)}{\sqrt{\tau_2}} \frac{\eta^{\mu\nu}}{2\pi \alpha'} \\ & \times \left( \prod_o \frac{\delta(\sqrt{\alpha'} k_o)}{\sqrt{\tau_2}} X_{1,1} + 2^{-(d+1)} \sum_{(g,h) \neq (1,1)} X_{g,h} \right) \quad (\text{B.12}) \end{aligned}$$

<sup>1</sup>In particular, there is a factor of 2 which must be absorbed by the (implicit) regulator in the first equation. This can be seen, for example, as a requirement of modular invariance.

if  $\mu, \nu$  are in the unorbifolded directions, while if they are in the orbifolded directions

$$T_0^{\mu\nu} = - \left( \frac{g_{str}\alpha'}{2} \right) \prod_u \frac{\delta(\sqrt{\alpha'}k_u)}{\sqrt{\tau_2}} \left( \frac{\eta^{\mu\nu}}{2\pi\alpha'} \prod_o \frac{\delta(\sqrt{\alpha'}k_o)}{\sqrt{\tau_2}} X_{1,1} + \frac{k_\mu k_\nu}{4} 2^{-(d+1)} X_{1,0} \right) \quad (\text{B.13})$$

This result is not modular invariant. However there is an ordering ambiguity<sup>2</sup> in zero modes from the  $(U, \hat{g})$  sector that we have not taken into account. To see the problem, suppose we write the vertex operator as

$$V = \alpha \partial X^\mu \bar{\partial} X^\nu e^{ik \cdot X} + \beta \partial X^\mu e^{ik \cdot X} \bar{\partial} X^\nu + e^{ik \cdot X} \partial X^\mu \bar{\partial} X^\nu \quad (\text{B.14})$$

Then, the  $k_\mu k_\nu / 4$  in eq. (B.13) is multiplied by  $\alpha + 2\beta + \gamma$ . There is a modular invariant choice ( $\alpha + \beta + \gamma = 1$ ,  $\beta = -1$ ) for which the  $kk$  terms cancel. (There is no other effect of this ordering issue.) We then obtain (In the notation of Section 2.4,  $X_{1,1} = \frac{\tau_2^{1/2}}{V_{26}} Z_{o,(1,1)} Z_u$ )

$$T_0^{\mu\nu} = - \left( \frac{g_{str}}{4\pi\tau_2} \right) \eta^{\mu\nu} \frac{\delta^{(26)}(k)}{V_{26}} Z_{o,(1,1)}[\tau] Z_u[\tau] \quad (\text{B.15})$$

(for  $\mu, \nu$  in the orbifold directions). This result agrees with the result in Section 2.4 for the case of the Lorentzian orbifold.

---

<sup>2</sup>This ambiguity does not appear for Euclidean orbifolds.

## Appendix C

# Open String Partition Function Sums

For convenience, we present more details of the  $SU(2)$  module calculations of Sections 3.3 and 3.5.1 here. The multiplicities of the  $j = 0$   $SU(2)$  module can be found in [62], Fig. 15.1. By direct computation, we obtain

$$\text{tr } q^{L_0} = (1 \cdot q^0) + (1 + 1 + 1) \cdot q^1 + (1 + 2 + 1) \cdot q^2 + \dots \quad (\text{C.1})$$

$$= (1 + q + 2q^2 + \dots) + 2q(1 + q + 2q^2 + \dots) + 2q^4(1 + q + \dots) \quad (\text{C.2})$$

$$= \frac{1}{\eta(q)} \sum_{n \in \mathbb{Z}} q^{n^2} . \quad (\text{C.3})$$

In the basis where  $J^1$  is diagonal,  $g$  inverts the sign of ladder operators (or rather,  $g$  anticommutes with  $J^\pm$ ). Thus, inserting  $g$  we obtain  $g = (-1)^m$  and so

$$\text{tr } gq^{L_0} = (1 \cdot q^0) + (-1 + 1 - 1) \cdot q^1 + (-1 + 2 - 1) \cdot q^2 + \dots \quad (\text{C.4})$$

$$= (1 + q + 2q^2 + \dots) + 2q(1 + q + 2q^2 + \dots) + 2q^4(1 + q + \dots) \quad (\text{C.5})$$

$$= \frac{1}{\eta(q)} \sum_{n \in \mathbb{Z}} (-1)^n q^{n^2} . \quad (\text{C.6})$$

With the deformation, the Hamiltonian is shifted to  $L_o = (m + \lambda/2)^2 + (N - m^2) = N + \lambda m + \lambda^2/4$ . The  $j = 0$  contribution is

$$\text{tr } q^{L_0} = q^{\lambda^2/4} \{ (1) \cdot q^0 + (q^\lambda + 1 + q^{-\lambda}) \cdot q^1 + (q^\lambda + 2 + q^{-\lambda}) \cdot q^2 + \dots \} \quad (\text{C.7})$$

$$= \frac{1}{\eta(q)} \sum_{n \in \mathbb{Z}} q^{n^2 + \lambda^2/4} e^{\pi \lambda t n} = \frac{1}{\eta(q)} \sum_{n \in \mathbb{Z}} q^{(n - \lambda/2)^2} . \quad (\text{C.8})$$

With the  $g$  insertion, we get

$$\text{tr } gq^{L_0} = q^{\lambda^2/4} \{ (1) \cdot q^0 + (-q^\lambda + 1 - q^{-\lambda}) \cdot q^1 + (-q^\lambda + 2 - q^{-\lambda}) \cdot q^2 \} \quad (\text{C.9})$$

$$= \frac{1}{\eta(q)} \sum_{n \in \mathbb{Z}} (-1)^n q^{n^2 + \lambda^2/4} e^{\pi \lambda t n} = \frac{1}{\eta(q)} \sum_{n \in \mathbb{Z}} (-1)^n q^{(n - \lambda/2)^2} . \quad (\text{C.10})$$

In the above expressions, we have  $q = e^{-\pi t}$ . Poisson resummation and modular

transformation then gives

$$\mathrm{tr} \, q^{L_0} = \frac{1}{\eta(q)} \sum_{n \in \mathbb{Z}} e^{-\pi t(n-\lambda/2)^2} \quad (\text{C.11})$$

$$= \frac{1}{\sqrt{2}\eta(\tilde{q}^2)} \sum_{m \in \mathbb{Z}} \tilde{q}^{m^2/2} e^{i\pi\lambda m}, \quad (\text{C.12})$$

where  $\tilde{q} = e^{2\pi i\tau}$  and  $\tau = i/t$ . Similarly

$$\mathrm{tr} \, gq^{L_0} = \frac{1}{\eta(q)} \sum_{n \in \mathbb{Z}} (-1)^n q^{(n-\lambda/2)^2} \quad (\text{C.13})$$

$$= \frac{1}{\sqrt{2}\eta(\tilde{q}^2)} \sum_{m \in \mathbb{Z}} \tilde{q}^{(m-1/2)^2/2} e^{i\pi\lambda(m-1/2)}. \quad (\text{C.14})$$

# Appendix D

## Detailed Free Field Theory Entropy Calculations

### D.1 Free Boson

Let's review the calculation of  $\text{tr}\rho_A^n$  for the free scalar. We will compute the partition function  $Z_n$  on an  $n$ -sheeted plane,  $\mathcal{M}_n$ , with branch cut chosen to extend over the negative real axis. More precisely, the Calabrese-Cardy (CC) result is that

$$\text{tr}\rho_A^n = \frac{Z_n}{Z_1^n} \quad (\text{D.1})$$

This geometry is a conformal transformation away from the original geometry in which the entanglement entropy was defined.

We can calculate  $Z_n$  by introducing a mass  $m$  and computing

$$\int dm^2 \frac{\partial}{\partial m^2} \ln Z_n = -\frac{1}{2} \int dm^2 \int d^2r G_n(\vec{r}, \vec{r}) \quad (\text{D.2})$$

This works, because the mass (when the regions' sizes are sent to infinity) is the only parameter on which the partition function may depend. This of course will require regularization. The Green's function  $G_n$  is appropriate to  $\mathcal{M}_n$ , where the monodromy around the cut is

$$\phi(e^{2\pi i} z) = e^{2\pi i k/n} \phi(z) \quad (\text{D.3})$$

To construct the Green's function, we solve the eigenvalue problem

$$(-\nabla^2 + m^2)\phi(r, \theta) = \lambda\phi(r, \theta) \quad (\text{D.4})$$

If we consider solutions of the form  $e^{i\nu\theta} f_\nu(r)$ , we find  $-f_\nu'' - \frac{1}{r}f_\nu' + (m^2 - \lambda + \nu^2/r^2)f_\nu = 0$ . Defining  $\mu^2 = \lambda - m^2$  and rescaling  $x = \mu r$ , we find  $f_\nu''(x) + \frac{1}{x}f_\nu'(x) + (1 - \nu^2/x^2)f_\nu(x) = 0$  and so

$$\phi_{\nu,\lambda} = N_{\nu,\lambda} e^{i\nu\theta} J_{|\nu|}(\mu r) \quad (\text{D.5})$$

According to eq. (D.3), we should take

$$\nu = k/n, \quad k = 0, 1, 2, \dots \quad (\text{D.6})$$

Note that we discard negative indices on the Bessel functions because when  $\nu$  is not an integer,  $J_{-|\nu|}$  is an independent solution which diverges at the origin, while for  $\nu$  an integer,  $J_{-|\nu|}$  is proportional to  $J_{|\nu|}$ ; the linearly independent solution is  $Y_\nu$  and is discarded by regularity. At  $\nu = 0$ , only  $J_0$  is regular at the origin.

The Bessel function is  $\delta$ -function normalizable. Alternatively, we put in a large radial cutoff  $L$  and require the eigenfunctions to vanish at  $r = L$ .

$$2\pi n N_{\nu,\lambda}^2 \int_0^L dr r J_{|\nu|}^2(\mu r) = 1 \quad (\text{D.7})$$

Taking  $\mu_{k,j} = \alpha_{\nu,j}/L$  where  $J_\nu(\alpha_{\nu,j}) = 0$ , we find

$$N_{\nu,\lambda}^2 = \frac{1}{\pi n L^2} \frac{1}{J_{\nu+1}^2(\alpha_{\nu,j})} \quad (\text{D.8})$$

Note that this assumes that  $\alpha_\nu \neq 0$ . For  $\nu \neq 0$ , there are zero zeros and one should treat these separately. However with the given boundary conditions, there do not appear to be solutions—note that these would be solutions of  $\nabla^2 \phi_0 = 0$ .

The required Green's function<sup>1</sup> is constructed from normalized eigenfunctions as

$$\begin{aligned} G_n(\vec{r}, \vec{r}') &= \sum_{k=1}^{\infty} \sum_j \frac{N_{\nu,\lambda}^2}{\lambda_j} \left[ e^{ik(\theta-\theta')/n} + e^{-ik(\theta-\theta')/n} \right] J_{k/n}(\mu_{k,j}r) J_{k/n}(\mu_{k,j}r') \\ &\quad + \sum_j \frac{1}{\lambda_j} J_0(\mu_{0,j}r) J_0(\mu_{0,j}r') \\ &= \sum_{k=0}^{\infty} d_k \sum_j \frac{N_{\nu,\lambda}^2}{\lambda_j} J_{k/n}(\mu_{k,j}r) J_{k/n}(\mu_{k,j}r') \cos(k(\theta-\theta')/n) \end{aligned} \quad (\text{D.9})$$

where  $d_0 = 1$  and  $d_{k>0} = 2$ . This then gives

$$G_n(\vec{r}, \vec{r}') = \sum_{k=0}^{\infty} d_k \sum_j \frac{N_{\nu,j}^2}{\lambda_j} J_\nu^2(\mu_{\nu,j}r) \quad (\text{D.10})$$

Now, the remaining work is a bit tricky, because one has to worry about regulating this expression appropriately. Note that if we assume that we can

---

<sup>1</sup>Use the formula

$$G(x-y) = \sum_n \left[ \frac{1}{\lambda_n} \phi_n(x) \phi_n^*(y) + \frac{1}{\lambda_n^*} \phi_n^*(x) \phi_n(y) \right]$$

where  $\int dx \phi_n^*(x) \phi_m(x) = \delta_{mn}$  and

$$\sum_n [\phi_n(x) \phi_n^*(y) + \phi_n^*(x) \phi_n(y)] = \delta^{(2)}(x-y).$$

interchange the order of sums and integrals, then

$$\int d^2r G_n(\vec{r}, \vec{r}) = \frac{1}{m^2} \sum_{k=0}^{\infty} d_k \sum_{j=1}^{\infty} \frac{1}{1 + \left(\frac{\alpha_{k,j}}{mL}\right)^2} \quad (\text{D.11})$$

This sum can be evaluated precisely. We will return to that after considering the free fermion.

## D.2 Free Fermion

We calculate

$$\frac{\partial}{\partial m} \ln Z_n = + \int d^2r \text{tr} S_n(\vec{r}, \vec{r}) \quad (\text{D.12})$$

up to an infinite (normal-ordering) constant. The trace is over spinor indices. There is a choice of boundary condition that must be made here. In the construction of  $\text{tr} \rho_A^n$ , fermionic fields would satisfy anti-periodic boundary conditions around the imaginary time direction.<sup>2</sup> Thus, we should have

$$\psi(e^{2\pi i} z) = e^{2\pi i(k/n+s)} \psi(z) \quad (\text{D.13})$$

where  $s = -1/2n$  (we will see that this allows  $k = 1, 2, \dots$ ). Other choices of boundary condition could be made, but they will not construct  $\text{tr} \rho_A^n$ .<sup>3</sup> The eigenvalue problem is

$$L_+ \psi(r, \theta) = A \psi(r, \theta) \quad (\text{D.14})$$

where

$$L_+ = \begin{pmatrix} m & 2\partial \\ 2\bar{\partial} & m \end{pmatrix} = \begin{pmatrix} m & e^{-i\theta} \left(\partial_r - \frac{i}{r} \partial_\theta\right) \\ e^{+i\theta} \left(\partial_r + \frac{i}{r} \partial_\theta\right) & m \end{pmatrix} \quad (\text{D.15})$$

We will also take the solutions  $\psi$  to satisfy

$$L_- \psi(r, \theta) = B \psi(r, \theta) \quad (\text{D.16})$$

where

$$L_- = \begin{pmatrix} -m & e^{-i\theta} \left(\partial_r - \frac{i}{r} \partial_\theta\right) \\ e^{+i\theta} \left(\partial_r + \frac{i}{r} \partial_\theta\right) & -m \end{pmatrix} \quad (\text{D.17})$$

and we note that

$$L_+ L_- \psi = AB \psi = -(-\nabla^2 + m^2) \psi = -\lambda \psi \quad (\text{D.18})$$

---

<sup>2</sup>For modes in  $B$ , this means the boundary condition is applied over  $\tau \in [0, \beta]$ , while for modes in  $A$ , it is applied over  $\tau \in [0, n\beta]$  – in particular, the fermionic fields are continuous as we pass from sheet to sheet. As  $\beta \rightarrow \infty$ , the  $n$ -sheeted surface is obtained, so the boundary condition is as stated, with no modifications.

<sup>3</sup>For example, periodic boundary condition presumably computes  $\text{tr}(-1)^F \rho_A^n$ . However, even this is suspect if we use periodic boundary conditions (on  $B$ ) to construct  $\rho_A$ .

and hence  $\lambda = -AB$  where  $\lambda$  are the eigenvalues of  $(-\nabla^2 + m^2)$  found in the previous section. The eigenspinors are

$$\psi_{\nu,\lambda}^{\pm} = \frac{\tilde{N}_{\nu,\lambda}}{\sqrt{2}} \begin{pmatrix} e^{i\nu\theta} J_{\nu}(\mu r) \\ \pm i e^{i(\nu+1)\theta} J_{\nu+1}(\mu r) \end{pmatrix}, \quad (\nu > 0) \quad (\text{D.19})$$

Note that we have the same functions as given in eq. (D.5) (although the values of  $\nu$  will be different). It is important that the  $\mu$  here is common to both functions – this will be somewhat problematic when we put in a spatial cutoff. Indeed the normalization is

$$\tilde{N}_{\nu,\lambda}^2 = \frac{1}{\pi n} \frac{2}{L_{\nu}^2 J_{\nu+1}^2(\alpha_{\nu,j}) + L_{\nu+1}^2 J_{\nu+2}^2(\alpha_{\nu+1,j})} \quad (\text{D.20})$$

Note that we have introduced a spatial cutoff which is  $\nu$ -dependent – precisely, we must have  $\mu_j = \alpha_{\nu,j}/L_{\nu} = \alpha_{\nu+1,j}/L_{\nu+1}$ . This makes little difference in the continuum. The eigenspinors have eigenvalues

$$A = m \pm i\mu, \quad B = -m \pm i\mu \quad (\text{D.21})$$

(and so we confirm  $AB = -m^2 - \mu^2 = -\lambda$ ). To derive these, we have made use of the identities

$$J'_{\nu} = \frac{1}{2} (J_{\nu-1} - J_{\nu+1}) \quad (\text{D.22})$$

$$\frac{\nu J_{\nu}}{x} = \frac{1}{2} (J_{\nu-1} + J_{\nu+1}) \quad (\text{D.23})$$

Now, there should also be solutions for negative  $\nu$ .

$$\psi_{-\nu,\lambda}^{\pm} = \frac{\tilde{N}_{\nu,\lambda}}{\sqrt{2}} \begin{pmatrix} e^{-i(\nu+1)\theta} J_{\nu+1}(\mu r) \\ \pm i e^{-i\nu\theta} J_{\nu}(\mu r) \end{pmatrix}, \quad (\nu > 0) \quad (\text{D.24})$$

These have eigenvalues

$$A = m \mp i\mu, \quad B = -m \mp i\mu \quad (\text{D.25})$$

These four solutions are not all independent; for example  $(\psi_{-\nu,\lambda}^{\pm})^* = \mp i\sigma_1 \psi_{\nu,\lambda}^{\pm}$ . We will take  $\psi_{\nu,\lambda}^{\pm}$  and construct the Green's function,  $tr S_n(\vec{r}, \vec{r}')$

$$\begin{aligned} & \sum_{\nu>0} \sum_j \tilde{N}_{\nu,\lambda}^2 \left[ \frac{1}{A} e^{i\nu(\theta-\theta')} + \frac{1}{A^*} e^{-i\nu(\theta-\theta')} \right] J_{\nu}(\mu_j r) J_{\nu}(\mu_j r') \quad (\text{D.26}) \\ & + \sum_{\nu>0} \sum_j \tilde{N}_{\nu,\lambda}^2 \left[ \frac{1}{A} e^{i(\nu+1)(\theta-\theta')} + \frac{1}{A^*} e^{-i(\nu+1)(\theta-\theta')} \right] J_{\nu+1}(\mu_j r) J_{\nu+1}(\mu_j r') \end{aligned}$$

Assuming  $\nu$  is non-zero, and setting  $\vec{r} = \vec{r}'$ , we get

$$\text{tr} S_n(\vec{r}, \vec{r}) = m \sum_{\nu > 0} \sum_j \frac{\tilde{N}_{\nu, \lambda}^2}{\lambda_j} [J_\nu^2(\mu_j r) + J_{\nu+1}^2(\mu_j r)] \quad (\text{D.27})$$

Integrating over space (and as before interchanging sums and integrals, we find

$$\int d^2 r \text{tr} S_n(\vec{r}, \vec{r}) = 2m \sum_{\nu > 0} \sum_j \frac{1}{\lambda_{\nu, j}} \quad (\text{D.28})$$

### D.3 Evaluation of Sums

Referring back to eq. (D.12), we see that we have obtained

$$\frac{\partial}{\partial m^2} \ln Z_n^{(F)} = +\frac{1}{2} \sum_{k=0}^{\infty} d_k \sum_{j=1}^{\infty} \frac{1}{m^2 + \left(\frac{\alpha_{k/n+s, j}}{L}\right)^2} \quad (\text{D.29})$$

which is to be compared to the bosonic result

$$\frac{\partial}{\partial m^2} \ln Z_n^{(B)} = -\frac{1}{2} \sum_{k=0}^{\infty} d_k \sum_{j=1}^{\infty} \frac{1}{m^2 + \left(\frac{\alpha_{k/n, j}}{L}\right)^2} \quad (\text{D.30})$$

where  $d_0 = 1$ ,  $d_{k \neq 0} = 2$ . Note that we can also write  $d_k = 2 - \delta_{\nu, 0}$ . Note that if we had taken the fermions to have periodic boundary conditions ( $s = 0$ ) on  $\mathcal{M}_n$ , then the fermion and boson would cancel precisely, assuming they have the same mass. Thus the CC result certainly depends on choice of boundary conditions.

Now, using [121] WA550 and eqs. (D.22–D.23), one easily shows

$$\frac{J_{\nu+1}(z)}{J_\nu(z)} = 2z \sum_{j=1}^{\infty} \frac{1}{\alpha_{\nu, j}^2 - z^2} \quad (\text{D.31})$$

and thus we conclude

$$\sum_{j=1}^{\infty} \frac{1}{\alpha_{\nu, j}^2 + z^2} = \frac{1}{2z} \frac{I_{\nu+1}(z)}{I_\nu(z)} \quad (\text{D.32})$$

In our case,  $z = mL$ , so we simply need the asymptotic forms

$$\frac{I_{\nu+1}(z)}{I_\nu(z)} \sim 1 - \frac{\nu + 1/2}{z} + O(1/z^2) \quad (\text{D.33})$$

So we get

$$\sum_{j=1}^{\infty} \frac{1}{m^2 + \left(\frac{\alpha_{\nu,j}}{L}\right)^2} = \frac{L}{2m} \left[ 1 - (2\nu + 1) \frac{1}{2mL} \right] + O(1/L) \quad (\text{D.34})$$

$$= -\frac{1}{2m^2} \left( \nu - mL + \frac{1}{2} \right) + \dots \quad (\text{D.35})$$

Using properties of  $\zeta$  functions,

$$\sum_{k=1}^{\infty} (k + \theta) = \frac{1}{24} - \frac{1}{8}(2\theta + 1)^2 \quad (\text{D.36})$$

Thus, we find

$$\sum_{k=0}^{\infty} d_k \sum_{j=1}^{\infty} \frac{1}{m^2 + \left(\frac{\alpha_{\nu,j}}{L}\right)^2} = \sum_{\nu} (2 - \delta_{\nu,0}) \left[ -\frac{1}{2m^2} \left( \nu - mL + \frac{1}{2} \right) + \dots \right] \quad (\text{D.37})$$

$$= \delta_{\nu,0} \frac{mL - 1/2}{2m^2} - \frac{1}{m^2} \sum_{k=1}^{\infty} \left[ \left( \frac{k}{n} + s + \frac{1}{2} - mL \right) + \dots \right] \quad (\text{D.38})$$

$$= \delta_{\nu,0} \frac{mL - 1/2}{2m^2} - \frac{1}{nm^2} \left[ \frac{1}{24} - \frac{1}{8}(2ns + n - 2nmL + 1)^2 \right] \quad (\text{D.39})$$

$$= (\delta_{\nu,0} - 2ns - 1) \frac{mL - 1/2}{2m^2} - \frac{1}{m^2} \left[ \frac{1}{24n} - \frac{(2ns + 1)^2}{8n} - \frac{n}{2}(mL - 1/2)^2 \right]$$

For the boson, we have  $s = 0$  and  $k = 0, 1, 2, \dots$ , and so we get

$$\frac{\partial}{\partial m^2} \ln Z_n^{(B)} = -\frac{1}{2m^2} \left( \frac{1}{12n} + \frac{n}{2}(mL - 1/2)^2 \right) \quad (\text{D.40})$$

Note that the  $n$ -independent term has cancelled exactly. Constructing  $Z_n/Z_1^n$ , we find just

$$\frac{\partial}{\partial m^2} \ln \left( \frac{Z_n^{(B)}}{Z_1^{(B)n}} \right) = \frac{1}{24m^2} \left( n - \frac{1}{n} \right) \quad (\text{D.41})$$

which is the [83] result. The cancellation of the order  $n$  term in this quantity was noted there as well.

For the fermion  $\nu = s + k/n$  where  $s = -1/2n$  and  $k = 1, 2, \dots$ , so we have

$$\frac{\partial}{\partial m^2} \ln Z_n^{(F)} = -\frac{1}{2m^2} \left( +\frac{1}{24n} - \frac{n}{2}(mL - 1/2)^2 \right) \quad (\text{D.42})$$

and thus

$$\frac{\partial}{\partial m^2} \ln \left( \frac{Z_n^{(F)}}{Z_1^{(F)n}} \right) = \frac{1}{48m^2} \left( n - \frac{1}{n} \right) \quad (\text{D.43})$$

Note that, after integrating with respect to the mass parameter, we arrive at

$$\frac{Z_n}{(Z_1)^n} = \gamma_n m^{\frac{c}{12}(n-\frac{1}{n})}, \quad (\text{D.44})$$

where  $\gamma_n$  is a regulator dependent integration constant (such that  $\gamma_1 = 1$ ) and  $c$  is the central charge of the  $UV$  fixed point (1 for bosons and 1/2 for fermions). The corresponding entanglement entropy becomes

$$S_A = \frac{c}{6} \ln \frac{1}{m}. \quad (\text{D.45})$$

It is an open problem to repeat this calculation for interacting field theories.

# References

- [1] H. Liu, G. Moore, and N. Seiberg, ‘*The Challenging Cosmic Singularity*,’ gr-qc/0301001.
- [2] B. S. DeWitt, ‘*The global approach to quantum field theory. Vol. 1, 2*,’ *Int. Ser. Monogr. Phys.* **114** (2003) 1–1042.
- [3] G. T. Horowitz and A. R. Steif, ‘*Singular String Solutions with Nonsingular Initial Data*,’ *Phys. Lett.* **B258** (1991) 91–96.
- [4] C. R. Nappi and E. Witten, ‘*A Closed, Expanding Universe in String Theory*,’ *Phys. Lett.* **B293** (1992) 309–314, hep-th/9206078.
- [5] C. Kounnas and D. Lust, ‘*Cosmological String Backgrounds from Gauged WZW Models*,’ *Phys. Lett.* **B289** (1992) 56–60, hep-th/9205046.
- [6] E. Kiritsis, ‘*Duality Symmetries and Topology Change in String Theory*,’ hep-th/9309064.
- [7] E. J. Martinec, ‘*Space-like Singularities and String Theory*,’ *Class. Quant. Grav.* **12** (1995) 941–950, hep-th/9412074.
- [8] A. E. Lawrence and E. J. Martinec, ‘*String Field Theory in Curved Spacetime and the Resolution of Spacelike Singularities*,’ *Class. Quant. Grav.* **13** (1996) 63–96, hep-th/9509149.
- [9] J. Khoury, B. A. Ovrut, N. Seiberg, P. J. Steinhardt, and N. Turok, ‘*From Big Crunch to Big Bang*,’ *Phys. Rev.* **D65** (2002) 086007, hep-th/0108187.
- [10] N. Seiberg, ‘*From Big Crunch to Big Bang - Is it Possible?*,’ hep-th/0201039.
- [11] G. Veneziano, ‘*String Cosmology: The Pre-Big Bang Scenario*,’ hep-th/0002094.
- [12] V. Balasubramanian, S. F. Hassan, E. Keski-Vakkuri, and A. Naqvi, ‘*A Space-time Orbifold: A Toy Model for a Cosmological Singularity*,’ *Phys. Rev.* **D67** (2003) 026003, hep-th/0202187.
- [13] N. A. Nekrasov, ‘*Milne Universe, Tachyons, and Quantum Group*,’ *Surveys High Energ. Phys.* **17** (2002) 115–124, hep-th/0203112.
- [14] L. Cornalba and M. S. Costa, ‘*A New Cosmological Scenario in String Theory*,’ *Phys. Rev.* **D66** (2002) 066001, hep-th/0203031.
- [15] J. Simon, ‘*The Geometry of Null Rotation Identifications*,’ *JHEP* **06** (2002) 001, hep-th/0203201.

- [16] H. Liu, G. Moore, and N. Seiberg, ‘*Strings in a Time-Dependent Orbifold,*’ *JHEP* **06** (2002) 045, hep-th/0204168.
- [17] H. Liu, G. Moore, and N. Seiberg, ‘*Strings in Time-Dependent Orbifolds,*’ *JHEP* **10** (2002) 031, hep-th/0206182.
- [18] G. T. Horowitz and J. Polchinski, ‘*Instability of Spacelike and Null Orbifold Singularities,*’ *Phys. Rev.* **D66** (2002) 103512, hep-th/0206228.
- [19] M. Fabinger and J. McGreevy, ‘*On Smooth Time-dependent Orbifolds and Null Singularities,*’ *JHEP* **06** (2003) 042, hep-th/0206196.
- [20] S. Elitzur, A. Giveon, D. Kutasov, and E. Rabinovici, ‘*From Big Bang to Big Crunch and Beyond,*’ *JHEP* **06** (2002) 017, hep-th/0204189.
- [21] B. Craps, D. Kutasov, and G. Rajesh, ‘*String Propagation in the Presence of Cosmological Singularities,*’ *JHEP* **06** (2002) 053, hep-th/0205101.
- [22] J. Simon, ‘*Null Orbifolds in AdS, Time Dependence and Holography,*’ *JHEP* **10** (2002) 036, hep-th/0208165.
- [23] O. Aharony, M. Fabinger, G. T. Horowitz, and E. Silverstein, ‘*Clean Time-Dependent String Backgrounds from Bubble Baths,*’ *JHEP* **07** (2002) 007, hep-th/0204158.
- [24] A. Buchel, P. Langfelder, and J. Walcher, ‘*On Time-dependent Backgrounds in Supergravity and String Theory,*’ *Phys. Rev.* **D67** (2003) 024011, hep-th/0207214.
- [25] M. Alishahiha and S. Parvizi, ‘*Branes in Time-Dependent Backgrounds and AdS/CFT Correspondence,*’ *JHEP* **10** (2002) 047, hep-th/0208187.
- [26] E. Dudas, J. Mourad, and C. Timirgaziu, ‘*Time and Space Dependent Backgrounds from Nonsupersymmetric Strings,*’ *Nucl. Phys.* **B660** (2003) 3–24, hep-th/0209176.
- [27] M. Berkooz, B. Craps, D. Kutasov, and G. Rajesh, ‘*Comments on Cosmological Singularities in String Theory,*’ *JHEP* **03** (2003) 031, hep-th/0212215.
- [28] C. Gordon and N. Turok, ‘*Cosmological Perturbations Through a General Relativistic Bounce,*’ *Phys. Rev.* **D67** (2003) 123508, hep-th/0206138.
- [29] J. Figueroa-O’Farrill and J. Simon, ‘*Supersymmetric Kaluza-Klein Reductions of M2 and M5 Branes,*’ *Adv. Theor. Math. Phys.* **6** (2003) 703–793, hep-th/0208107.
- [30] M. Fabinger and S. Hellerman, ‘*Stringy Resolutions of Null Singularities,*’ hep-th/0212223.
- [31] A. Hashimoto and S. Sethi, ‘*Holography and String Dynamics in Time-Dependent Backgrounds,*’ *Phys. Rev. Lett.* **89** (2002) 261601, hep-th/0208126.
- [32] L. Cornalba and M. S. Costa, ‘*On the Classical Stability of Orientifold Cosmologies,*’ *Class. Quant. Grav.* **20** (2003) 3969–3996, hep-th/0302137.
- [33] A. Lawrence, ‘*On the Instability of 3D Null Singularities,*’ *JHEP* **11** (2002) 019, hep-th/0205288.

- [34] S. W. Hawking, ‘*The Chronology Protection Conjecture,*’ *Phys. Rev.* **D46** (1992) 603–611.
- [35] M. Visser, ‘*The Quantum Physics of Chronology Protection,*’ gr-qc/0204022.
- [36] B. S. Kay, ‘*The Principle of Locality and Quantum Field Theory on (Nonglobally Hyperbolic) Curved Space-Times,*’ *Rev. Math. Phys.* **SI1** (1992) 167–195.
- [37] A. Chamblin and G. W. Gibbons, ‘*A Judgement on Spinors,*’ *Class. Quant. Grav.* **12** (1995) 2243–2248, gr-qc/9504048.
- [38] A. Chamblin and G. W. Gibbons, ‘*Topology and Time Reversal,*’ gr-qc/9510006.
- [39] E. K. Boyda, S. Ganguli, P. Horava, and U. Varadarajan, ‘*Holographic Protection of Chronology in Universes of the Goedel Type,*’ *Phys. Rev.* **D67** (2003) 106003, hep-th/0212087.
- [40] C. A. R. Herdeiro, ‘*Spinning Deformations of the D1-D5 System and a Geometric Resolution of Closed Timelike Curves,*’ *Nucl. Phys.* **B665** (2003) 189–210, hep-th/0212002.
- [41] T. Harmark and T. Takayanagi, ‘*Supersymmetric Goedel Universes in String Theory,*’ *Nucl. Phys.* **B662** (2003) 3–39, hep-th/0301206.
- [42] E. G. Gimon and A. Hashimoto, ‘*Black Holes in Goedel Universes and pp-Waves,*’ *Phys. Rev. Lett.* **91** (2003) 021601, hep-th/0304181.
- [43] L. Dyson, ‘*Chronology Protection in String Theory,*’ *JHEP* **03** (2004) 024, hep-th/0302052.
- [44] C. M. Hull, ‘*Timelike T-Duality, de Sitter Space, Large N Gauge Theories and Topological Field Theory,*’ *JHEP* **07** (1998) 021, hep-th/9806146.
- [45] G. W. Gibbons, ‘*The Elliptic Interpretation of Black Holes and Quantum Mechanics,*’ *Nucl. Phys.* **B271** (1986) 497.
- [46] A. Folacci and N. G. Sanchez, ‘*Quantum Field Theory and the ‘Elliptic Interpretation’ of de Sitter Space-Time,*’ *Nucl. Phys.* **B294** (1987) 1111.
- [47] M. K. Parikh, I. Savonije, and E. Verlinde, ‘*Elliptic de Sitter Space:  $dS/\mathbb{Z}_2$ ,*’ *Phys. Rev.* **D67** (2003) 064005, hep-th/0209120.
- [48] R. Biswas, E. Keski-Vakkuri, R. G. Leigh, S. Nowling, and E. Sharpe, ‘*The Taming of Closed Time-like Curves,*’ *JHEP* **01** (2004) 064, hep-th/0304241.
- [49] N. D. Birrell and P. C. W. Davies, ‘*QUANTUM FIELDS IN CURVED SPACE,*’. Cambridge, UK: Univ. Pr. ( 1982) 340p.
- [50] J. Polchinski, ‘*String theory. Vol. 1: An Introduction to the Bosonic String,*’. Cambridge, UK: Univ. Pr. (1998) 402 p.
- [51] F. Larsen, A. Naqvi, and S. Terashima, ‘*Rolling Tachyons and Decaying Branes,*’ *JHEP* **02** (2003) 039, hep-th/0212248.

- [52] S. D. Mathur, ‘*Is the Polyakov Path Integral Prescription too Restrictive?*,’ hep-th/9306090.
- [53] J. Callan, Curtis G., I. R. Klebanov, A. W. W. Ludwig, and J. M. Maldacena, ‘*Exact Solution of a Boundary Conformal Field Theory*,’ *Nucl. Phys.* **B422** (1994) 417–448, hep-th/9402113.
- [54] J. Polchinski and L. Thorlacius, ‘*Free Fermion Representation of a Boundary Conformal Field Theory*,’ *Phys. Rev.* **D50** (1994) 622–626, hep-th/9404008.
- [55] M. Gutperle and A. Strominger, ‘*Spacelike Branes*,’ *JHEP* **04** (2002) 018, hep-th/0202210.
- [56] A. Sen, ‘*Rolling Tachyon*,’ *JHEP* **04** (2002) 048, hep-th/0203211.
- [57] S. Kawai, E. Keski-Vakkuri, R. G. Leigh, and S. Nowling, ‘*Brane Decay from the Origin of Time*,’ hep-th/0507163.
- [58] S. Kawai, E. Keski-Vakkuri, R. G. Leigh, and S. Nowling, ‘*Fractional S-branes on a Spacetime Orbifold*,’ *Phys. Rev.* **D73** (2006) 106004, hep-th/0602083.
- [59] A. Recknagel and V. Schomerus, ‘*Boundary Deformation Theory and Moduli Spaces of D-Branes*,’ *Nucl. Phys.* **B545** (1999) 233–282, hep-th/9811237.
- [60] I. Affleck, ‘*Conformal Field Theory Approach to the Kondo Effect*,’ *Acta Phys. Polon.* **B26** (1995) 1869–1932, cond-mat/9512099.
- [61] J. L. Cardy and I. Peschel, ‘*Finite-Size Dependence of the Free Energy in Two-Dimensional Critical Systems*,’ *Nucl. Phys. B* **300** [FS22] (1988) 377.
- [62] P. Di Francesco, P. Mathieu, and D. Senechal, ‘*CONFORMAL FIELD THEORY*,’ New York, USA: Springer (1997) 890 p.
- [63] M. R. Gaberdiel and A. Recknagel, ‘*Conformal Boundary States for Free Bosons and Fermions*,’ *JHEP* **11** (2001) 016, hep-th/0108238.
- [64] P. H. Ginsparg, ‘*Curiosities at  $c = 1$* ,’ *Nucl. Phys.* **B295** (1988) 153–170.
- [65] N. Lambert, H. Liu, and J. Maldacena, ‘*Closed Strings from Decaying D-Branes*,’ hep-th/0303139.
- [66] D. Gaiotto, N. Itzhaki, and L. Rastelli, ‘*Closed Strings as Imaginary D-branes*,’ *Nucl. Phys.* **B688** (2004) 70–100, hep-th/0304192.
- [67] J. L. Karczmarek, H. Liu, J. Maldacena, and A. Strominger, ‘*UV Finite Brane Decay*,’ *JHEP* **11** (2003) 042, hep-th/0306132.
- [68] A. Sen, ‘*Rolling Tachyon Boundary State, Conserved Charges and Two Dimensional String Theory*,’ hep-th/0402157.
- [69] K. R. Kristjansson and L. Thorlacius, ‘ *$c = 1$  Boundary Conformal Field Theory Revisited*,’ *Class. Quant. Grav.* **21** (2004) S1359–1366, hep-th/0401003.
- [70] M. R. Gaberdiel, A. Recknagel, and G. M. T. Watts, ‘*The Conformal Boundary States for  $SU(2)$  at Level 1*,’ *Nucl. Phys.* **B626** (2002) 344–362, hep-th/0108102.

- [71] L. Dolan and C. R. Nappi, ‘*Noncommutativity in a Time-dependent Background,*’ *Phys. Lett.* **B551** (2003) 369–377, hep-th/0210030.
- [72] R.-G. Cai, J.-X. Lu, and N. Ohta, ‘*NCOS and D-branes in Time-dependent Backgrounds,*’ *Phys. Lett.* **B551** (2003) 178–186, hep-th/0210206.
- [73] K. Okuyama, ‘*D-Branes on the Null-Brane,*’ *JHEP* **02** (2003) 043, hep-th/0211218.
- [74] Y. Hikida, R. R. Nayak, and K. L. Panigrahi, ‘*D-Branes in a Big Bang / Big Crunch Universe: Nappi-Witten Gauged WZW Model,*’ *JHEP* **05** (2005) 018, hep-th/0503148.
- [75] Y. Hikida, R. R. Nayak, and K. L. Panigrahi, ‘*D-Branes in a Big Bang / Big Crunch Universe: Misner Space,*’ hep-th/0508003.
- [76] Y. Hikida and T.-S. Tai, ‘*D-Instantons and Closed String Tachyons in Misner Space,*’ *JHEP* **01** (2006) 054, hep-th/0510129.
- [77] A. Sen, ‘*Tachyon Matter,*’ *JHEP* **07** (2002) 065, hep-th/0203265.
- [78] A. Sen, ‘*Tachyon Dynamics in Open String Theory,*’ hep-th/0410103.
- [79] M. Oshikawa and I. Affleck, ‘*Boundary Conformal Field Theory Approach to the Critical Two-Dimensional Ising Model with a Defect Line,*’ *Nucl. Phys.* **B495** (1997) 533–582, cond-mat/9612187.
- [80] R. H. Brandenberger and C. Vafa, ‘*Superstrings in the Early Universe,*’ *Nucl. Phys.* **B316** (1989) 391.
- [81] S. Alexander, R. H. Brandenberger, and D. Easson, ‘*Brane Gases in the Early Universe,*’ *Phys. Rev.* **D62** (2000) 103509, hep-th/0005212.
- [82] M. Srednicki, ‘*Entropy and Area,*’ *Phys. Rev. Lett.* **71** (1993) 666.
- [83] P. Calabrese and J. Cardy, ‘*Entanglement Entropy and Quantum Field Theory,*’ *J. Stat. Mech.: Theor. Exp.* **JSTAT06** (2004) P06002.
- [84] G. Vidal, J. I. Latorre, E. Rico, and A. Kitaev, ‘*Entanglement in Quantum Critical Phenomena,*’ *Phys. Rev. Lett.* **90** (2003) 227902.
- [85] F. Verstraete, M. M. Wolf, D. Perez-García, and J. I. Cirac, ‘*Criticality, the Area Law, and the Computational Power of PEPS,*’ *Phys. Rev. Lett.* **96** (2006) 220601.
- [86] G. Refael and J. E. Moore, ‘*Entanglement Entropy of Random Quantum Critical Points in One Dimension,*’ *Phys. Rev. Lett.* **93** (2004) 260602.
- [87] E. Fradkin and J. E. Moore, ‘*Entanglement Entropy of 2D Conformal Quantum Critical Points: Hearing The Shape of a Quantum Drum,*’ *Phys. Rev. Lett.* **97** (2006) 050404.
- [88] A. Kopp and S. Chakravarty, ‘*Non-Analyticity of von Neumann Entropy as a Criterion for Quantum Phase Transitions.,*’ *Ann. Phys. (N. Y.)* **322** (2007) 1466.
- [89] P. Calabrese and J. Cardy, ‘*Entanglement Entropy and Quantum Field Theory: A Non-Technical Introduction,*’ *Int. J. Quant. Inf.* **4** (2006) 429.

- [90] D. V. Fursaev, ‘*Entanglement Entropy in Critical Phenomena and Analog Models of Quantum Gravity*,’ *Phys. Rev. D* **73** (2006) 124025.
- [91] D. V. Fursaev, ‘*Proof of the Holographic Formula for Entanglement Entropy*,’ *J. High Energy Phys.* **JHEP09** (2006) 0618.
- [92] S. Ryu and T. Takayanagi, ‘*Holographic Derivation of Entanglement Entropy from AdS/CFT*,’ *Phys. Rev. Lett.* **96** (2006) 181602.
- [93] S. Ryu and T. Takayanagi, ‘*Aspects of Holographic Entanglement Entropy*,’ *J. High Energy Phys.* **JHEP08** (2006) 045.
- [94] J. M. Maldacena, ‘*The Large N Limit of Superconformal Field Theories and Supergravity*,’ *Adv. Theor. Math. Phys.* **2** (1998) 231.
- [95] S. S. Gubser, I. R. Klebanov, and A. M. Polyakov, ‘*Gauge Theory Correlators from Non-Critical String Theory*,’ *Phys. Lett.* **B428** (1998) 105–114, hep-th/9802109.
- [96] E. Witten, ‘*Anti de Sitter Space and Holography*,’ *Adv. Theor. Math. Phys.* **2** (1998) 253.
- [97] S. Dong, E. Fradkin, R. Leigh, and S. Nowling, ‘*Entanglement Entropy in Chern-Simons Theories*,’ to appear.
- [98] A. Kitaev and J. Preskill, ‘*Topological Entanglement Entropy*,’ *Phys. Rev. Lett.* **96** (2006) 110404.
- [99] M. Levin and X.-G. Wen, ‘*Detecting Topological Order in a Ground State Wave Function*,’ *Phys. Rev. Lett.* **96** (2006) 110405.
- [100] J. Preskill, ‘*Topological quantum computation*,’ Lecture Notes for Physics 219: Quantum Computation, chapter 9; unpublished; Caltech, 2004.
- [101] E. Witten, ‘*Quantum Field Theory and the Jones Polynomial*,’ *Commun. Math. Phys.* **121** (1989) 351.
- [102] E. Witten, ‘*On Holomorphic Factorization of WZW and Coset Models*,’ *Commun. Math. Phys.* **144** (1992) 189.
- [103] J. Leinaas and J. Myerheim, ‘*Theory of Identical Particles*,’ *Nuovo Cimento Soc. Ital. Fis.* **37B** (1977) 1.
- [104] F. Wilczek, ‘*Magnetic Flux, Angular Momentum, and Statistics*,’ *Phys. Rev. Lett.* **48** (1982) 1144.
- [105] A. Y. Kitaev, ‘*Fault-Tolerant Quantum Computation by Anyons*,’ *Annals of Physics* **303** (2003) 2.
- [106] M. H. Freedman, A. Kitaev, M. J. Larsen, and Z. Wang, ‘*Topological Quantum Computation*,’ *Comm. Math. Phys.* **227** (2002) 605. arXiv:quant-ph/0101025.
- [107] S. Das Sarma, M. Freedman, C. Nayak, S. H. Simon, and A. Stern, ‘*Non-Abelian Anyons and Topological Quantum Computation*,’ unpublished; arXiv: 0707.1889, 2007.
- [108] R. B. Laughlin, ‘*Anomalous Quantum Hall Effect: An Incompressible Quantum Fluid with Fractionally Charged Excitations*,’ *Phys. Rev. Lett.* **50** (1983) 1395.

- [109] G. Moore and N. Read, ‘*Non-Abelions in the Fractional Quantum Hall Effect,*’ *Nucl. Phys. B* **360** (1991) 362.
- [110] N. Read and E. Rezayi, ‘*Beyond Paired Quantum Hall States: Parafermions and Incompressible States in the First Excited Landau Level,*’ *Phys. Rev. B* **59** (1999) 8084.
- [111] M. Haque, O. S. Zozulya, and K. Schoutens, ‘*Entanglement Entropy in Fermionic Laughlin States,*’ *Phys. Rev. Lett.* **98** (2007) 060401.
- [112] O. S. Zozulya, M. Haque, K. Schoutens, and E. H. Rezayi, ‘*Bipartite Entanglement Entropy in Fractional Quantum Hall States,*’ *Phys. Rev. B* **76** (2007) 125310.
- [113] S. Furukawa and G. Misguich, ‘*Topological Entanglement Entropy in the Quantum Dimer Model on the Triangular Lattice,*’ *Phys. Rev. B* **75** (2007) 214407.
- [114] C. Holzhey, F. Larsen, and F. Wilczek, ‘*Geometric and Renormalized Entropy in Conformal Field Theory,*’ *Nucl. Phys. B* **424** (1994) 44.
- [115] P. Fendley, Matthew P. A. Fisher, and C. Nayak, ‘*Topological Entanglement Entropy from the Holographic Partition Function,*’ *J. Stat. Phys.* **126** (2007) 1111.
- [116] D. Daniel and N. Dorey, ‘*The Schwinger-Dyson Equations and Nonrenormalization in Chern-Simons Theory,*’ *Phys. Lett.* **B246** (1990) 82–86.
- [117] D. Birmingham, M. Rakowski, and G. Thompson, ‘*Renormalization of Topological Field Theory,*’ *Nuclear Physics B* **329** (Jan., 1990) 83–97.
- [118] N. Dorey, ‘*Ward Identities for Broken Supersymmetry in Chern-Simons Theory,*’ *Phys. Lett.* **B246** (1990) 87–91.
- [119] S. Elitzur, G. W. Moore, A. Schwimmer, and N. Seiberg, ‘*Remarks on the Canonical Quantization of the Chern-Simons-Witten Theory,*’ *Nucl. Phys. B* **326** (1989) 108.
- [120] M. B. Green, J. H. Schwarz, and E. Witten, ‘*SUPERSTRING THEORY. VOL. 1: INTRODUCTION,*’. Cambridge, Uk: Univ. Pr. ( 1987) 469 P. ( Cambridge Monographs On Mathematical Physics).
- [121] I. Gradstein and I. Ryzik, ‘*TABLE OF INTEGRALS, SERIES, AND PRODUCTS,*’. London, Uk: Acad. Pr. ( 1980).

# Author's Biography

Sean Nowling was born in Peru, Indiana, on September 19, 1978. He completed his B.Sc. in physics from Purdue University and his A.M. in physics from the University of Illinois at Urbana-Champaign. While a graduate student at the University of Illinois, he studied theoretical high energy physics under the direction of Robert Leigh.

## Publications

8. *Entanglement Entropy in Chern-Simons Theories*  
(with S. Dong, E. Fradkin, and R. G. Leigh)  
In preparation.
7. *Fractional S-branes on a Spacetime Orbifold*  
(with S. Kawai, E. Keski-Vakkuri, and R. G. Leigh)  
Phys. Rev. D, **73**, 106004 (2006) (hep-th/0602083)
6. *The Rolling Tachyon Boundary Conformal Field Theory on an Orbifold*  
(with S. Kawai, E. Keski-Vakkuri, and R. G. Leigh)  
Phys. Rev. D, **73**, 106003 (2006) (hep-th/0602081)
5. *Brane Decay from the Origin of Time*  
(with S. Kawai, E. Keski-Vakkuri, and R. G. Leigh)  
Phys. Rev. Lett., **96**, 031301 (2006) cover article (hep-th/0507163)
4. *The Taming of Closed Time - like Curves*  
(with R. Biswas, E. Keski-Vakkuri, R. G. Leigh, and E. Sharpe)  
JHEP, **0401**, 064 (2004) (hep-th/0304241)
3. *Nonrelativistic Spin 1/2 Particle in an Arbitrary Non-Abelian Magnetic Field in Two Spatial Dimensions*  
(with T. E. Clark and S. T. Love)  
Mod. Phys. Lett. A, **17**, 95-102 (2002) (hep-ph/0109107)
2. *The Supercharge and Superconformal Symmetry For N= 1 Supersymmetric Quantum Mechanics*  
(with T. E. Clark and S. T. Love)

Nucl. Phys. B, **632**, 3-50 (2002) (hep-th/0108243)

1. *Charged Spin 1/2 Particle in an Arbitrary Magnetic Field in Two Spatial Dimensions: A Supersymmetric Quantum Mechanical System*

(with T. E. Clark and S. T. Love)

Mod. Phys. Lett. A, **17**, 95-102 (2002) (hep-ph/0109107)